Dissertation
Submitted to the
Combined Faculties for the Natural Sciences and for Mathematics
Of the Ruperto-Carola University of Heidelberg, Germany
for the degree of
Doctor of Natural Sciences

Engineering a synthetic p53-Mdm2 network in budding yeast

presented by

Diplom: **Barbara Di Ventura**
Born in: **Latina, Italia**

2006

Dissertation
Submitted to the
Combined Faculties for the Natural Sciences and for Mathematics
Of the Ruperto-Carola University of Heidelberg, Germany
for the degree of
Doctor of Natural Sciences

presented by

Diplom: Barbara Di Ventura
Born in: Latina, Italia

Engineering a synthetic p53-Mdm2 network in budding yeast

Referees: Prof. Dr. Michael Knop
Prof. Dr. Karsten Rippe

A mamma, papa' e Chicca

"Experience is the name everyone gives to their mistake"

Oscar Wilde

Acknowledgments

If I am here, writing the acknowledgements section in my phd thesis, I owe it first of all to my boss, Luis. I am grateful that he wasn't discouraged with the idea of getting an engineer to work in his lab. On the opposite, he often told me that it was an advantage to be naïve and ask the simplest questions. He offered me the opportunity to do my own experiments, to make many mistakes, to develop my own way to do research. Most of all, he has always comforted me in moments of discouragement, assuring me that lack of results or experiments gone wrong are an inevitable feature of research. Luis, your positive attitude, your extreme generosity, your humanity, make of you an example to follow and give me hope that one can be a scientist and lead a happy life at the same time!

Among the many people who have helped me with the basics of molecular biology and that have patiently listened to me talking about the many doubts or troubles related to my project, I first would like to thank Massimiliano. Despite his being totally unrelated to my work, he has always found the time to explain me things, to give me advice, without ever making me feel stupid or incompetent. I will not forget that night when he sat with me for hours and together we went through my contradicting data and finally came out with the idea that my protein could be sumoylated…Thanks Massi, you do know what "sharing knowledge" means!

I am deeply grateful to Kostas, who accepted (despite the short notice!) to read the entire thesis and gave me precious advices for improving it. Kostas, I thanked you at least millions time during our email exchange of revisions of this thesis, but it's never going to be enough to express to you my gratitude!

These four years of endless nights in the lab would have not been the same without my beloved friend, Caro. She is the most amazing person I have ever met. Intelligent, genuine, stubborn and contradictory at times, but always, always willing to help. With her I laughed and fought, cried and played. Caro, if we managed to stay friends after our review-writing period, I am confident that we will be forever ☺

I thank all the people in the lab – past and present – for having created a wonderful atmosphere to work in. Especially Mark and Kostas, with whom I shared the

centrifuge, the fridge, the buffers, but also jokes, scientific discussions and music in the absence of Christina. Remember guys, the time has come to push the button!!

JB, Paulo, Martin, Rob, Markus, Tom, Nga and The Fishpuddings: thanks for the great time spent together playing and singing! Our rehearsals and concerts have been the highlight of my life in Heidelberg indeed.

Fabiana, my dear, you have rescued me many times when I was sinking into the library between introduction and results. Maybe we were drinking too many coffees together, getting a bit distracted…but it was good to keep the mood high ☺

For the constant supply of materials, the yeast strains, the plasmids, the antibodies, all the protocols, I am grateful to the entire Knop lab, especially Christof and Michael. You have been extremely generous, helpful and patient, even when I was coming ten times a day to ask questions…

I thank Charlotta Funaya and Claude Antony for their commitment in the electron microscopy analysis. Thanks to Stefan and Arne who assisted me with the DeltaVision (I still believe this microscope has something against me…), to Vladimir and Tomi who did the microarrays analysis, to Andy for the FACS, to Sigfried Labeit for the human cDNA libraries, to the Böettcher lab for the protease inhibitors.

I am also grateful to the members of my thesis advisory committee, Peer, Karsten, Francois and Michael, who tried many times, for my own good, to persuade me to change project. In the end, I am happy I have persisted ☺

I thank all the wonderful friends with whom I shared these years in EMBL. I would like to mention you all, guys, but it would end up in almost as many pages as the whole thesis!

Last but not least, I'd like to express my gratitude to those who indirectly helped me getting this work done, bringing joy and happiness into my life: mamma, papa', Chicca, my fluffy love-addicted bunny Caffelatte, the most wonderful cat in the whole world Chris, and my living-miracle Robert, who makes every day so worth living.

Contents

Abbreaviations

BSA	bovine serum albumin
bp	base pairs
βME	beta-mercapto-ethanol
°C	degree Celsius
C-terminal	carboxy terminal
Δ	deletion
DMSO	dimethylsulfoxide
DNA	deoxyribonucleotide acid
dNTP	deoxyribonucleotide
DTT	dithiothreitol
E. coli	*Escherichia coli*
ECFP	enhanced cyan fluorescent protein
EDTA	ethylenediamine tetraacetic acid
EtBr	ethidium bromide
EYFP	enhanced yellow fluorescent protein
f.c.	final concentration
GAL promoter	galactose-inducible promoter
HRP	horseradish peroxidase
HU	high urea
LB	Luria Bertoni
Kb	kilobases
kDa	kilodalton
M	molar
Mat	mating type
min	minutes
mM	millimolar
µM, µl	micromolar, microliter
NaPi	sodium phosphate
Ni-NTA	níkel-nitrilotriacetic acid
N-terminal	amino Terminal
OD_{600}	optical density of a cell suspensión at 600 nm wavelength
O.N.	over night
PAGE	polyacrylamide gel electrophoresis
PBS	phosphate buffered saline
PCR	polymerase chain reaction
PEG	polyethylene-glycol
pH	$-\log(H^+)$
PMSF	phenylmethylsulfonyl fluoride
rpm	revolutions per minute
RT	room temperature
sec	seconds
SC	synthetic complete
S. cerevisiae	*Saccharomyces cerevisiae*

SDS	sodium dodecyl sulfate
SORB	sorbitol
TE	tris/EDTA
Tris	Tris(-hydroxymethyl)-aminomethane
v/v	volume per volume
wt	wild type
w/v	weight per volume
YPD	yeast extract peptone dextrose

Summary

p53 is among the most thoroughly studied proteins to date. Its tumour suppressor activity and the consideration that inactivation of the p53 pathway is a common, if not universal, feature of all human cancers, have gained it the interest of a multitude of researches seeking new therapies against this disease. As a consequence, p53 is at the centre of a feverish research and nowadays is reported to be involved in most cellular processes. Despite the vast amount of data published, much is yet to be unravelled about the mechanisms regulating the p53 signalling network. Indeed, the p53 network is extremely intricate and complex, and from a system biology point of view it can be seen as a series of interconnected negative and positive feedback loops, which can give rise to complex dynamics such as oscillations. In the combined effort to understand more of the biological meaning of these oscillations and to study the properties of this network motif from an engineering perspective, a synthetic p53 network has been built in budding yeast with the aim of studying the network *in isolation* while being embedded in living cells. p53 and most proteins in the network are absent from the budding yeast genome. This diminishes the likelihood of interferences on the engineered module from the cellular environment. Surprisingly, despite the evolutionary conservation of the ubiquitin pathway from yeast to humans, p53 ubiquitylation by the E3 ubiquitin ligase Mdm2 - an event central to the oscillatory dynamics of the system - does not appear to take place in budding yeast, even when the human E2 enzyme UbcH5B is exogenously expressed. p53 is instead sumoylated by Mdm2 and sumoylation dictates the co-localization of p53 and Mdm2 to a nuclear body reminiscent of human PML bodies. In conclusion, attempting to rebuild from scratch a simplified version of the intricate p53 network, isolating it from its natural context, has proven to be a very powerful means leading to unexpected findings, testifying the usefulness of the synthetic biology approach.

Zusammenfassung

p53 gehört zu den bislang am häufigsten untersuchten Proteinen. Seine Rolle als Tumorsupressor und die Tatsache, dass der p53 Signalweg in den meisten, wenn nicht gar allen, menschlichen Krebsarten blockiert ist, weckte das Interesse zahlreicher Forscher auf der Suche nach neuen Therapien. Infolge seiner fieberhaften Erforschung findet man dieses Protein inzwischen an den meisten zellulären Vorgängen beteiligt. Trotz dieser enormen Datenmenge ist die Regulation des p53 Signalnetzwerkes aber noch keineswegs verstanden. Tatsächlich ist das p53 Netzwerk extrem verschlungen und komplex. Aus Sicht der Systembiologie stellt es sich als eine Aneinanderreihung miteinander vernetzter positiver und negativer Rückkopplungsschleifen dar, deren komplexe Dynamik zum Beispiel zur Ausbildung von Oszillationen führen kann. Um einerseits die biologische Funktion dieser Oszillationen zu verstehen, sowie andererseits die Eigenschaften des Netzwerkes unter systembiologischen Aspekten zu untersuchen, habe ich ein synthetisches p53 Netzwerk in Sprosshefe eingeführt. Dies erlaubte die Untersuchung des Netzwerkes in lebenden Zellen bei gleichzeitiger Entkopplung von der natürlichen Umgebung; p53 und die meisten der mit ihm verbundenen Proteine fehlen im Genom der Sprosshefe. Dies verringert die Gefahr von Wechselwirkungen zwischen dem synthetischen Modul und der Wirtszelle. Erstaunlicherweise, trotz der evolutionären Erhaltung des Ubiquitin-Signalwegs zwischen Hefe und Menschen, wird p53 in Hefezellen nicht von der E3 Ubiquitin Ligase Mdm2 ubiquitiniert. Diese Reaktion spielt im menschlichen System eine Schlüsselrolle bei der Ausbildung von Oszillationen. In Hefezellen bleibt sie jedoch selbst dann aus, wenn das menschliche E2 Enzym UbcH5B zusätzlich exprimiert wird. Stattdessen wird p53 von Mdm2 sumoyliert, und diese Sumoylierung führt zur Co-Lokalisierung von Mdm2 und p53 in einem Kernkkörper mit Ähnlichkeit zu menschlichen PML-Körpern. Der Versuch, eine vereinfachte Version des p53 Netzwerkes ausserhalb seiner natürlichen Umgebung aufzubauen, erwies sich schliesslich als hervorragender Weg zu neuen Erkenntnissen und bestätigt den Forschungsansatz der synthetische Biologie.

Aim of this study

The aim of this study was to build a synthetic p53-Mdm2 module in isolation from its natural genomic and proteomic environments, ascertain its sufficiency in generating oscillations, determine whether the properties of these oscillations (*e.g.* period, amplitude) would be translated into the preferential activation by p53 of genes involved in apoptosis or cell-cycle arrest and investigate the robustness of the design, since synthetic oscillators are typically noisy as compared to natural ones (Elowitz *et al.*, 2000). Taking advantage of the minimal design of the network, we also aimed at better understanding the relation between p53 and Mdm2 in the absence of other proteins that constitute the intricate p53 regulatory network in human cells.

We chose *Saccharomyces cerevisiae* as a host because it is a eukaryote for which homologues for p53 and Mdm2 have not been identified so far, making it a perfect model organism to study the p53-Mdm2 system "in isolation"; the term "isolation" does not mean that the synthetic module is cut out from any endogenous cellular processes, rather that its communication with the environment comes in a well-defined manner so that in the end the relations among the components of the circuit are only the designed ones (Kobayashi *et al.*, 2004).

Working with p53 in yeast has several advantages. First, one can over-express it in the absence of Mdm2 without incurring in undesirable outcomes such as cell-cycle arrest or apoptosis. For several key regulators in the p53 network (*e.g.* p300, $p14^{ARF}$, promyelocytic leukemia protein (PML)) yeast homologues have not been identified so far, giving us more confidence in interpreting the results in view of p53 and Mdm2 action only. Notably, in human cell lines, even if RNAi is used to selectively eliminate certain proteins from the cell in order to study the effects of a single cellular factor on p53, the observed behaviour could still be due to some other protein(s) present in the network, whose contribution to p53 regulation is yet to be uncovered. Furthermore, yeast has a number of features (beyond rapid growth, ease of handling, *etc.*) which make it particularly suitable for our purposes; mainly the availability of several studies that compare specifically yeast and human cellular processes or machineries (Vijay-Kumar *et al.*, 1987; Yasugi *et al.*, 1996; Huang *et al.*, 2001), easy retrieval of information on yeast homologues of human proteins and finally a highly versatile DNA transformation system

which gives us flexibility in the number of components of the p53 network we wish to include in our circuit.

The idea of expressing p53 and Mdm2 in yeast is not novel. Back in 1993, the Vogelstein laboratory used *S. cerevisiae* to prove that Mdm2 is able to bind the p53 transactivation domain thus blocking p53-dependent transcription (Oliner *et al.*, 1993). Several other laboratories have been exploiting the ability of p53 to interact with the yeast transcription machinery to study aspects of p53 transcriptional activation (Ishioka *et al.*, 1993; Flaman *et al.*, 1995; Pearson *et al.*, 1998; Waddell *et al.*, 2001; Kato *et al.*, 2003).

Mdm2-mediated p53 degradation in yeast, though, was never shown and, if we exclude the pioneering work of the Vogelstein laboratory, no other work was ever published on p53 and Mdm2 dynamic interaction in yeast.

Inspired by the work carried out in the Alon laboratory, where by fluorescence microscopy they studied the p53-Mdm2 oscillations in single human cells (Lahav *et al.*, 2004), we decided upon using the fusion proteins p53-ECFP and Mdm2-EYFP to obtain single-cell data, which would be useful in studying the noise of our synthetic circuit.

Being mathematical modelling an important aspect of a synthetic biology project, we also planned to model the synthetic p53-Mdm2 circuit. To pave the way towards building a sound model, we first wanted to investigate and compare different mathematical formalisms and modelling approaches.

In summary, the aims of this project lied on two different levels: a) the engineering level, which consisted of building a synthetic circuit using both transcription and post-translational modifications to generate oscillations and studying its robustness to noise, while at the same time identifying the most suited mathematical formalism to model the synthetic network; b) the biological-biochemical level, which consisted in taking advantage of an over-simplified interaction network to better understand the p53-Mdm2 regulatory dynamic interactions.

Introduction

Synthetic biology

"Practise what you know, and it will help to make clear what now you do not know"

Rembrandt Harmenszonn van Rijn

Synthetic biology is a striking term: it's the juxtaposition of contradictory words and therefore it grabs people's attention. Synthetic refers to something artificial, something that is being created from scratch often as an imitation of a natural counterpart. Biological is, on the contrary, a synonym for genuine, unaffected. Although this effectual expression isn't new in that it dates back to the 1980's, when it referred to the use of recombinant DNA technology, it is only recently that synthetic biology has gained recognition as a new branch of molecular biology, with its own goals and strategies. The idea of inferring the properties of a system through the analysis of its reaction to perturbations has been used from the beginning of times in biology as in other sciences and the advent of a technology allowing the manipulation of the genetic code has indeed widen the horizons for such perturbation analysis (*e.g.* inserting an additional copy of a certain gene, putting a gene under a different promoter, expressing heterologous genes in a host species). The ascertainment that in any molecular biology enterprise unnatural situations are forced to occur leads many scientists to believe that synthetic biology is nothing more than a term, misused and abused by a group of people (mainly engineers converted to biology) trying to attract public opinion's interest. Several characteristics distinguish, in my opinion, modern synthetic biology from other molecular biology approaches:

1. the will to construct organisms that have never appeared before
2. the will to manipulate organisms to function in a way they never did before
3. the combination of analysis and synthesis to understand biological processes and extract general "design rules" which have emerged from evolution
4. the use of rational design, typical of engineering disciplines, which implies cycling between definition of system specifications, mathematical modelling and simulation, prototype building and testing before reaching the final functional implementation

5. the interdisciplinarity which brings biologists, engineers, physicists, chemists and mathematicians together.

Constructing new organisms fulfilling a set of man-posed requirements sounds very much like science fiction and brings about long philosophical discussions on the timeless desire of human kind to create life, possibly immortal. Despite their falling into the synthetic biology category, I will not discuss these fascinating attempts to make organisms from scratch using minimal genomes (Kobayashi *et al.*, 2003) or totally artificial ones (Smith *et al.*, 2003), or to make synthetic vesicles capable of supporting protein production (Noireaux *et al.*, 2004) and, as final goal, division.

More practical social impact have, instead, those synthetic biology endeavours dealing with the modification of organisms in order to obtain benefits like low-cost drug production (Martin *et al.*, 2003; Herrera, 2005), ecological welfare (Gilbert *et al.*, 2003) and biomedical discoveries (Benner *et al.*, 2003).

Synthetic biology, in this context, is a reverse engineering exercise: there is a product out there, that someone else has built, and you want to understand how it works, with the final aim to change the specifications and implement your own design. What you need to do is dismantle the product, take each part and understand it well, as a single entity first; then, use the parts as building blocks to interconnect in search of a complex function. The advantage of this approach is that, while building your own product using the parts extracted from the pre-existing one, you are very likely to learn much more about this latter than you would if you stopped once reduced the object to pieces. A beautiful example of how synthesis can lead to new discoveries and paradigm shift is offered by the Watson-Crick model of the DNA. The model was so simple that nobody ever doubted that the pairing rules for the nucleobases were the only essential feature of this incredible molecule. Only when attempts to create synthetic self-replicating molecules started, did it become clear that the repeating-charged backbone, thought to be dispensable up to that moment, was in fact an essential characteristic to make DNA the genetic code carrier (Hutter *et al.*, 2002).

Synthesis of unnatural nucleobases also allowed proving that the pairing rules were indeed as simple as predicted by the model and, as a matter of fact, twelve additional base pairs were artificially introduced (Geyer *et al.*, 2003).

For a synthetic biologist, the final product could be the cell for instance, and the building blocks the so-called network motifs. The latter are cross-species recurrent functional modules comprising a stand-alone "body" (*i.e.* genes and proteins, characterized by their own biochemical properties and kinetics, connected according to a certain topology), which performs a specific function (the output) in response to external stimuli, sensed by the module through a well-defined interface (Yeger-Lotem *et al.*, 2004).

The concept of module is well-known in computer science, where it represents a piece of software that groups cohesive subprograms and data structures, can be independently compiled and provides a separation between interface – defining the objects required and supplied by the module – and implementation – the actual working code referring to the objects defined in the interface. Modularity is a highly desirable quality for complex software, because it means the possibility to reuse modules in different contexts (instead of writing dedicated programs each time), to hide information, which makes the software friendlier to anyone approaching it, finally allowing a very efficient tasks distribution among several programmers. Modularity is turning out to be just as good in molecular biology for synthetic purposes (Hartwell *et al.*, 1999). In fact, only thanks to the modularity of biological processes it is now possible to extract such circuits, test their context-free functionality, and then assemble them in new ways which never occurred inside a cell. Until recently, despite the evidence of its existence, modularity wouldn't come out as an emergent property of *in silico* evolved circuits. Only with the introduction of a modularly varying goal (*i.e*. each goal is made of a different combination of sub-goals), did Kashtan and Alon find that networks are selected to be modular (Kashtan *et al.*, 2005); and modularly varying goals seem to be a reasonable assumption requiring that the environment changed so that new functions could be obtained by different combinations of a set of basic biological functions.

The isolation and characterization of biological modules have been the obligatory starting points of the nascent synthetic biology field, since, as previously mentioned, in a reverse engineering approach it is essential to know the behaviour of each individual building block before assembling many blocks in any desired way (Becskei *et al.*, 2000; Gardner *et al.*, 2000; Becskei *et al.*, 2001; Kobayashi *et al.*, 2004; Kramer *et al.*, 2004).

Extracting a network motif, plugging it again inside a cell, isolating it from the other cellular processes, is probably the trickiest part of a synthetic biology project, first of all because the concept of *isolation* is somewhat cryptic. Isolating a module does not mean putting it into an air bubble with no connections to the cellular environment! Indeed, the module becomes "alive" only provided it can successfully interact with endogenous machineries that will transcribe genes, translate mRNAs into proteins, transport them to the right cellular locations, degrade them when needed, *etc*. Communication with the environment has to come in a well-defined manner, though, via specific predictable inputs, so that in the end the relations among the components of the circuit are only the designed ones (Figure 1.1) (Kobayashi *et al.*, 2004).

It should be noted that, although it is in principle possible to connect modules in any desired way, the resulting networks have not been optimized by evolution and it is likely that a considerable amount of work needs to be done in order to obtain a functional circuit out of this assembly. Still, the number of examples of successful construction of complex networks from simpler modules is increasing (Pourquie, 2003; Blatten, 2004; Guido *et al.*, 2006).

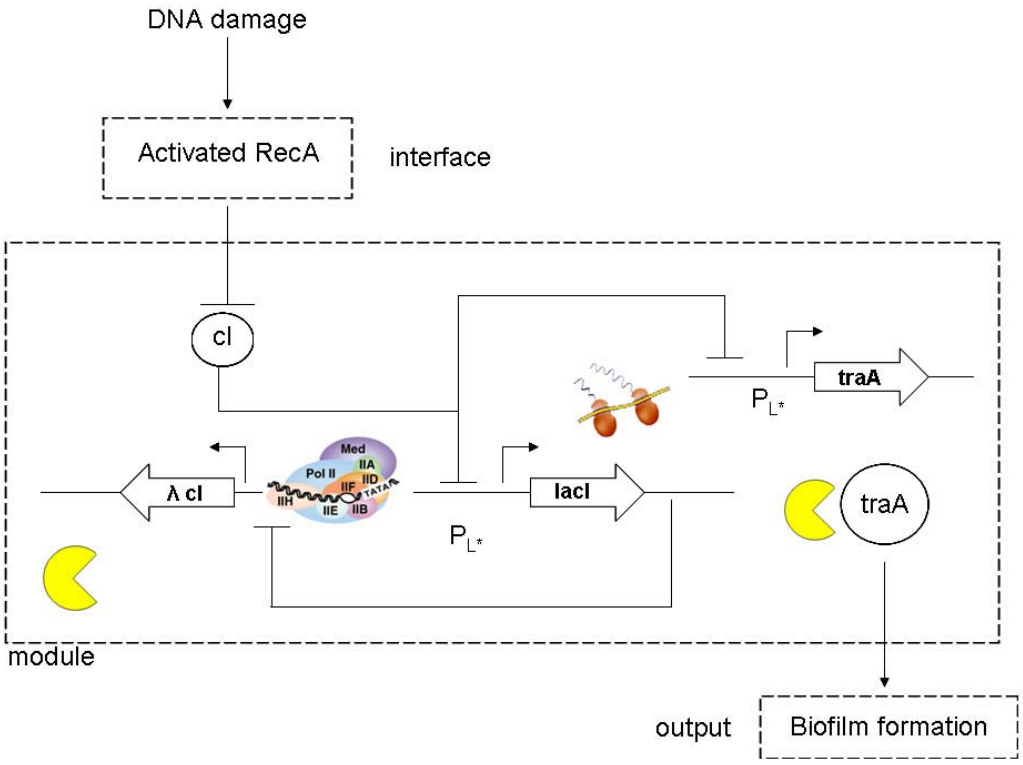

Figure 1.1 | Example of a synthetic module with its interface and output. The interface represents the communication channel between the module itself and the cellular environment acting upon the module, which ensures the isolation of the module from the remaining cellular processes. The separation between these entities (represented by dashed lines) is only for explanatory reasons, because there is no physical separation inside the cell between module and endogenous components. To show some of the interactions which are required for the module to function, I depicted cellular machineries (like the transcriptional, translational and proteolytic - pacman - ones) in colour, while the synthetic network is shown in black and white. DNA damage is the external stimulus to which the circuit responds. Once *RecA* gets activated upon damage, it cleaves cI making it inactive and therefore inhibiting its repressor activity on the P_{L*} promoter. Transcription from this promoter leads to the expression of *lacI*, which represses transcription of cI, and to the expression of *traA*, which induces biofilm formation (output of the network). Adapted from (Kobayashi *et al.*, 2004)

Mathematical modelling and simulation offer to synthetic biologists the opportunity to validate their designs before realizing them, which is common practise in any engineering discipline. Mathematical models can be derived for any biological process, synthetic or not; the advantage of modelling a synthetic network resides in the fact that the network components are chosen among well-characterized ones, and also they are connected in a

predefined way, so that the topology of the network, as well as at least an idea of the parameters ranges, are available (mathematical modelling is discussed in more detail in the paragraph "Mathematical modelling of biological networks").

Mathematical modelling of biochemical networks is not an easy task and there are many pitfalls that could lead to false predictions (see Results Part One). Moreover, noise in biological processes like transcription and translation – due to small numbers of molecules as well as events that fire rarely – makes it more difficult to predict the output of a circuit. In this respect, synthetic networks have been extremely useful in the study of noise properties (*e.g.* noise reduction, amplification, and propagation; distinction between intrinsic and extrinsic noise) (Becskei *et al.*, 2000; Hooshangi *et al.*, 2005; Pedraza *et al.*, 2005; Rosenfeld *et al.*, 2005; Dublanche *et al.*, 2006; Hooshangi *et al.*, 2006), mainly because of the degrees of freedom they offer in respect to endogenous networks.

Despite all their limitations, modelling and simulation offer great benefits to the experimentalists, as beautifully exemplified by several synthetic biology efforts which are proving the symbiosis between theory and bench work possible (Elowitz *et al.*, 2000; Atkinson *et al.*, 2003; Kobayashi *et al.*, 2004; Fung *et al.*, 2005).

Synthetic networks can also be used to study natural circuits. Most of the times, only a simplified version can be obtained (either due to technological limitations - length of DNA that can be inserted into a plasmid, number of plasmids that can be simultaneously introduced in a cell, possibility to separate different wavelengths to follow many proteins at the same time *in vivo*, *etc* - or due to incomplete knowledge), but there are many advantages in using synthetic networks to study natural ones.

First, the synthetic circuit can be more freely modified, thanks to the use of inducible promoters, re-wiring of regulatory proteins for them to act upon uncommon targets, manipulation of proteins' half-life, engineering of receptors to bind unnatural ligands and start signalling cascades upon unnatural inputs, *etc*. The fact that the synthetic network is in principle isolated from the rest of the cell means that the manipulations can be carried out without incurring into downstream side-effects (*e.g.* that an over-expressed transcription factor started several signalling pathways, some of which might lead to cell death).

Also, making slightly different versions of the same circuit can help elucidate the importance of a design detail, for instance the impact of the length of a signalling cascade on noise and timing of response (Hooshangi *et al.*, 2005).

Although studying natural circuits with a synthetic biology approach is indeed very fruitful for the above mentioned reasons, it is clear that this is an application-oriented discipline, its strongest motivation being the desire to build something - from scratch or reassembling what's already out there -, rather than simply contemplating what Mother Nature has done. From the first examples of synthetic circuits, which can be honestly described as beautiful *toys* with little relevance to anything of practical use, but which represent the steps towards acquiring the necessary skills, we are now witnessing a shift towards more and more complex networks that are actually achieving something. For instance, the production of artemisin, the precursor of an anti-malaria drug currently present on the market, through a synthetic pathway engineered in *Escherichia coli* (Martin *et al.*, 2003), or the coordination of cellular behaviour in cell populations using engineered cell-cell communication networks, which would benefit diverse biotechnology applications like fermentation processes, biomaterial production and tissue engineering (Chen *et al.*, 2005).

Just like the advent of recombinant DNA technology raised many doubts and questions about the ethics of pursuing genetic modifications on organisms, with unknown consequences for the society, synthetic biology carries the fear that these engineered organisms (*e.g.* nasty viruses which never existed before and therefore are dreadful more than any other) can escape the laboratories and infect the world. On the contrary of what happened in the past, though, nowadays a good communication between science and society on these delicate issues is being pursued and synthetic biologists are trying to device ways to prevent abuses of these newly acquired skills (Ball, 2004). For example, "control networks" can be used to keep population density of modified organisms under a certain threshold, or to kill the cell once the function it has been designed for is fulfilled. Also, it is noteworthy that most of the modified strains engineered up to now are less fit than the wild type already in the laboratory, so it is not very likely that they could survive in the wild and take over the existing populations. Still, risks are to be taken into account, especially considering that carrying on with synthetic biology can be so rewarding.

Synthetic oscillators

Among the network motifs that are being studied using a synthetic biology approach, oscillators are of particular interest because of their intriguing dynamics and because many cellular processes, such as cell cycle progression (Pomerening *et al.*, 2005), circadian rhythms (Naef, 2005), somite segmentation (Pourquie, 2003), are characterized by oscillatory protein levels. Usually natural oscillators are made of intricate regulatory networks; however, simpler modules have been shown to produce oscillations in different biological contexts (Hoffmann *et al.*, 2002; Lewis, 2003). Studying these simple architectures can help discover common properties of oscillators, as well as determine their contribution to the dynamics of modularly assembled more complex networks.

The first synthetic oscillator to be built was the so-called repressilator, where three repressors are connected in a daisy-chain (Elowitz *et al.*, 2000). The network was built in *E. coli* using components which do not belong to any natural biological clock. The read-out of the system is the fluorescent protein synthesized in each cell. Since the period of the synthetic oscillations is of hours, while *E. coli* divides faster, the state of the system is passed on to the next generation. Notably, the repressilator is rather noisy as compared to the robust performance of natural clocks.

Few years later, a more complex design was shown to generate oscillations, as well as toggle switch behaviour (Atkinson *et al.*, 2003). The beauty of this work consists in the use of a purely theoretical analysis prior to the effective construction of the network.

These two circuits are made only of transcriptional elements, such as transcription factors and genes, but are independent of metabolism. The most recent synthetic oscillator to appear is called the metabolator to stress the fact that metabolism is coupled to transcription to obtain oscillations (Fung *et al.*, 2005). This design uses glycolytic flux to generate oscillations through the signalling metabolite acetyl phosphate. Two enzymes which interconvert two metabolite pools are placed under the (positive and negative) transcriptional control of acetyl phosphate in a way that when glycolytic flux exceeds a critical value the passage between one metabolite pool and the other takes place and so do the oscillations.

Although not coupled with mathematical modelling – which was done separately by other researchers (Takigawa-Imamura *et al.*, 2006) – another beautiful example of how reconstructing a system from scratch can help study modularity and complex dynamical behaviours comes from the *in vitro* cyanobacterium circadian clock (Tomita *et al.*, 2005). The authors show that temperature-compensated, robust circadian cycling can be obtained independently of *de novo* transcription and translation processes. This discovery is very important, since it disproves the general belief that transcription-translation feedback loop is necessary to generate circadian rhythms.

Design able to generate oscillations, as well as the properties of the oscillations, are the focus of intense research, not only experimental, but also theoretical (Lewis, 2003; Blatten, 2004; Guantes *et al.*, 2006; Wong *et al.*, 2006). These theoretical studies can teach us a lot about oscillators and make us long for new exciting synthetic oscillators to be developed.

The p53 natural oscillator

To live or to die, that is the question. Unfortunately existence is not so straightforward. To arrest or to propagate? And so the cell speaks, hiding its secrets in a mass of protoplasm.

Anonymous blogger on the internet

Despite its unassuming name, p53 is an essential protein for the cell and it is evolutionarily conserved from worm to human (Slee et al., 2004). Acting as a sensor of DNA damage, p53 dictates life or death to the cell, dependently on its ability to cope with the damage and repair it. The fundamental role of p53 in ensuring genomic integrity is better reflected in its nickname, "guardian of the genome". This and other epithets, such as "good cop/bad cop" or "heavily dictated dictator", emphasize not only the centrality of p53 in keeping proliferating cells under control, they also suggest that p53 activation can have contradicting effects on the organism (like cancer prevention and aging) and it is therefore itself subject to a tight regulation achieved by a complex network of cellular proteins (Sharpless *et al.*, 2002; Kohn *et al.*, 2005; Lu, 2005). p53 is mainly a sequence-

specific DNA-binding transcription factor which, under normal growth conditions, is kept latent in various ways (see below). When necessity calls, *i.e.* upon some stress signal – such as damages to the DNA, hypoxia, oncogenic expression – p53 is rapidly activated and starts its gene expression program. p53 target genes mediate a plethora of cellular functions, including cell cycle arrest, senescence, apoptosis, differentiation and DNA repair, to name but a few (Liu *et al.*, 2006; Matoba *et al.*, 2006; Roger *et al.*, 2006). Inactivation of the p53 pathway – being it through mutations on the p53 gene itself, mutations on genes encoding key p53 regulators and/or binding partners, or other means – is a common, if not universal, feature of human cancers. p53 is therefore considered the perfect candidate to develop new drugs for this disease. If on the one hand this has considerably boosted research on p53 – so that we now know a lot more about the mechanisms underlying its regulation and functions – on the other hand it has given rise to an explosion in the number of publications involving p53, making it difficult at times to discern reality from artefacts. Artefacts can arise, for instance, from putting together results obtained with different cell lines, under different experimental conditions, in different organisms. At least some of the contradictions found in the field could very probably be explained considering that using a lymphocyte instead of a hepatocyte, or a healthy cell instead of a cancer one can radically affect the results. Through the years, to the processes somehow historically related to p53 (like cell cycle arrest, DNA repair and apoptosis), many more have been added – as diverse as cytokinesis (Scoumanne *et al.*, 2006), mitochondrial respiration (Matoba et al., 2006), Golgi complex integrity (Jung et al., 2006), bone organogenesis (Lengner et al., 2006), exosome secretion (Yu et al., 2006) and cell migration (Roger et al., 2006) – as proofs of the multifaceted role of p53. It is interesting to note that a similar trend is involving another protein in the p53 network, Mdm2. Mdm2 has been first shown to form a complex with p53 and inhibit its transcriptional activity (Momand et al., 1992). Years later, Mdm2 was shown to have ubiquitin ligase activity towards p53, regulating its levels by targeting it for proteasomal degradation (Fuchs *et al.*, 1998). Although Jun-N (amino)-terminal kinase (JNK) was soon after proved to also target p53 for degradation (Fuchs *et al.*, 1998), Mdm2 has monopolized the attention of researchers, and has been considered (wrongly, see below) the one and only p53 negative regulator. As a consequence, much effort has been

invested in discovering Mdm2 functions and mechanisms of action. No wonder if it is now found to be involved in almost as many cellular processes as p53 itself (cell cycle control, differentiation, cell fate determination, DNA repair, basal transcription, and other processes) and to be regulated just as much (Ganguli *et al.*, 2003; Meek *et al.*, 2003).

The p53-Mdm2 feedback loop

A very fascinating aspect of the p53-Mdm2 interaction, from a systems biology perspective, is that it can lead to oscillations. While Mdm2 is negatively acting on p53 (concealing its activation domain and targeting it for degradation), p53 is positively acting on Mdm2, which is in fact a p53 target gene. To use an engineering terminology (which has indeed become of common use in biology as well), p53 and Mdm2 form a negative feedback loop. This motif recurs often in the p53 network. The recently discovered E3 ligases Pirh2 and COP1, in fact, also target p53 for proteasomal degradation while being at the same time transcriptionally activated by p53 (Leng *et al.*, 2003; Corcoran *et al.*, 2004; Dornan *et al.*, 2004). Mathematical analysis of negative feedback loops tells us that oscillations can arise if there is a delay in the production of Mdm2 (Lewis, 2003; Bratsun *et al.*, 2005). This assumption is sufficiently realistic considering that there are several time-consuming steps involved in the production of a functional protein, such as mRNA splicing, translation and protein folding, with nuclear transport playing an important role in the case of nuclear proteins such as Mdm2. Also, it has been shown that, in certain circumstances, Mdm2 transcription is induced later than that of other p53 target genes (Perry *et al.*, 1993; Knippschild *et al.*, 1995). Oscillations in the p53-Mdm2 network have been observed both at the population level (Lahav et al., 2004) and at the single cell level (Lahav *et al.*, 2004; Geva-Zatorsky *et al.*, 2006). In the first case, the oscillations were dumped and the explanation given by the authors was rather logical: p53 levels increase upon stress so that the cell can try to repair the damage to its DNA before committing suicide. After several trials of repair (each corresponding to a peak in p53 levels), p53 goes back to its low basal concentration, either because repair has been successfully accomplished or because the cell undergoes apoptosis. The results coming from single cell studies (Lahav *et al.*, 2004; Geva-Zatorsky *et al.*, 2006), carried on with the fusion proteins p53-ECFP and Mdm2-EYFP for visualization in living

cells, revealed that the oscillations are sustained rather than damped (dampening being the effect of averaging over many cells), with some cells exhibiting oscillations that last several days. This time, the authors do not offer an explanation for this observation and simply conclude that, since oscillations are found also in other systems like the SOS DNA damage response in *E. coli* and the NF-KB system, oscillations likely play a general role in stress or damage response. It would be extremely interesting to find out whether oscillations in the p53 and Mdm2 protein levels occur in normal cells as well as in cancer ones, and whether they do have a physiological relevance or not.

p53 regulation

p53 is subject to a very tight regulation, which ensures that the protein is scarce and dormant when the cell is unstressed. This is achieved in various ways, for instance by keeping p53 in the cytoplasm, by targeting it for proteasomal degradation, or by inhibiting p53 binding to its DNA target sites (Gohler *et al.*, 2002; Liu *et al.*, 2006). When exposed to some source of stress which damages its DNA, the cell invokes p53 to take action. p53 is quickly stabilized and its transcriptional activity is strongly enhanced as a result of the nuclear accumulation of the protein and modifications within both its N- and C-termini. For instance, such modifications allow p53 to recruit more efficiently components of the transcription machinery through its transactivation domains (Figure 1.2) (Espinosa *et al.*, 2003; Liu *et al.*, 2006). Although for many years regulation of p53 at the level of transcription has received little attention, different transcription factors have been found to activate and repress p53 gene expression and the deregulated expression of p53 appears to be a central feature of malignant transformation (Nayak *et al.*, 1999). p53 mRNA levels change during the cell cycle – p53 gene transcription is induced prior to DNA synthesis – and also rise substantially upon serum stimulation and excess of c-Myc (Reisman *et al.*, 1993; Boggs *et al.*, 2006). At first sight, up-regulation of an anti-proliferative gene such as p53 by serum and growth factors might seem contradictory. As a matter of fact, extensively proliferating cells are at a higher risk of acquiring DNA damage and generating cancer-prone progeny than quiescent cells. Therefore, they enter into a state of anticipation characterized by high levels of p53 mRNA which guarantee a rapid and effective response in case of necessity, without

otherwise interfering with normal cellular processes in the absence of DNA damage or other stresses. When the cell is exposed to p53-activating signals, p53 protein levels rise rapidly and, although this is partially due to a higher translational rate of p53 mRNA, the major players in p53 stabilization are post-translational modifications (Figure 1.2). Apart from preventing the association of p53 with its negative regulator Mdm2 and from making it a more potent sequence-specific DNA binding transcription factor, post-translational modifications can influence which downstream pathway is initiated by p53. For instance, p53 phosphorylation at serine 46 has been shown to be required for p53-induced apoptosis, while cell cycle arrest does not depend on this modification (Oda et al., 2000).

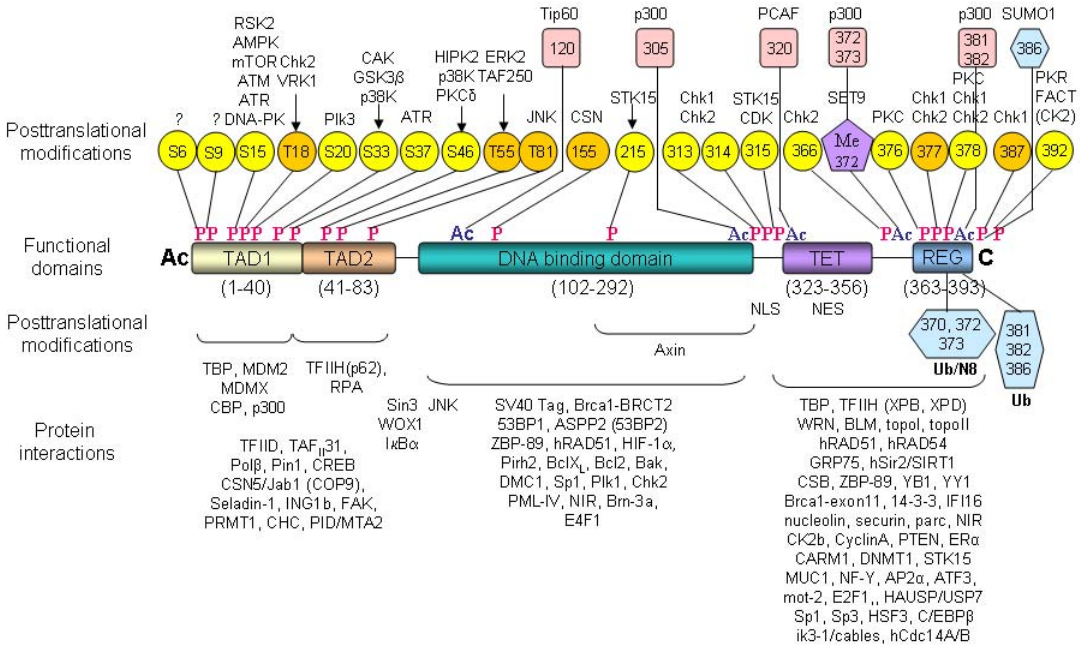

Figure 1.2 | Protein domains, post-translational modification sites, and proteins that interact with human p53. The 393 amino acid human p53 polypeptide is represented schematically with postulated functional regions and domains indicated. Residues ~1-40 (TAD1) and 41-83 (TAD2) comprise independent tandem transactivation domains; residues ~63-97 also is a Src homology 3-like (SH3, not shown) domain that overlaps with a poorly conserved proline and alanine rich segment (33-80); residues ~102-292 contain the central, sequence-specific, DNA binding core region; residues 305-321 contains the primary bi-partite nuclear localization signal (NLS); residues 324-356 comprise the tetramerization domain (TET) which contains a nuclear export signal within residues 339-350; residues 363-393 (REG) negatively regulate DNA binding by the

central core to consensus recognition sites in oligonucleotides and interact in a sequence-independent manner with single- and double-stranded nucleic acids but contribute positively to chromatin binding and transactivation in vivo. Posttranslational modification sites (P, phosphorylation; Ac, acetylation; Me, methylation, N8, neddylation; Ub, ubiquination) are indicated together with enzymes that can accomplish the modifications *in vitro*. Interaction regions for selected proteins are indicated below the polypeptide. The C-terminal six lysines (K370, K372, K373, K381, K382, and K386) can be ubiquinated; K373, K372, and K373 are likely sites of attachment for the ubiquitin-like protein NEDD8; Lys386 may be modified by conjugation with SUMO1, a ubiquitin-like peptide. Adapted from (Appella, 2003)

Mdm2

As mentioned above, Mdm2 is one of p53 main negative regulators, whose critical role in preventing p53 apoptotic function when unnecessary is manifested by the lethality of mice embryos deprived of Mdm2; a phenotype which can be rescued by the simultaneous inactivation of p53 (Jones et al., 1995; Montes de Oca Luna et al., 1995). Mdm2 is, like p53, a multi-domain protein (Figure 1.3). The N-terminus is characterized by the p53 binding domain, which binds on p53 to the N-terminal transactivation domain. In this way, Mdm2 is able to inhibit p53 transcriptional activity independently of its ubiquitin ligase function, which is to be ascribed to the RING-finger domain. This characteristic distinguishes Mdm2 from the other p53 ubiquitin ligases (COP1, Pirh2, ARF-BP1), that can target p53 for proteasomal degradation, but do not conceal its transactivation domain.

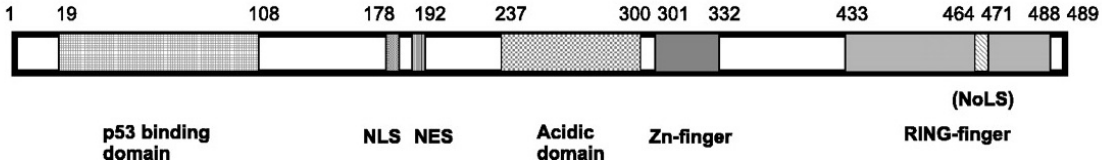

Figure 1.3 | Mdm2 protein motifs. NLS, nuclear localization signal; NES, nuclear export signal; Zn-finger, zinc-finger domain; NoLS, nucleolar localization signal; RING-finger, ring-finger domain. The numbers above the drawing denote amino acid numbers. Adapted from (Iwakuma *et al.*, 2003)

Mdm2 nuclear export signal (NES) was long thought to be essential for Mdm2-mediated p53 degradation, in that Mdm2 would shuttle nuclear p53 out into the cytoplasm, where ubiquitylated p53 would be degraded by cytoplasmic proteasomes (Freedman *et al.*, 1998). It was later discovered that this shuttling does not require the NES on Mdm2, but rather the NES on p53 and an intact RING-finger domain on Mdm2 (Geyer et al., 2000). Furthermore, it has been recently shown that nuclear export is not an obligatory step in p53 degradation, which occurs on cytoplasmic and nuclear proteasomes in the down-phase of a successful stress response, when the cell has repaired its DNA and needs to rapidly eliminate p53 to return to normal homeostasis (Joseph et al., 2003). Also recent is the discovery of a cryptic nucleolar localization signal (NoLS) at the C-terminus of Mdm2, whose biological significance is yet to be clarified (Lohrum et al., 2000). The central acidic domain of Mdm2 is necessary for interaction with the ribosomal protein L5 and with p300, thus contributing to p53 degradation since this requires the chain-elongation enzymatic activity of p300 (see below).

Mono- versus polyubiquitylation

In order to be degraded, p53 – like any other protein – needs to carry a polyubiquitin chain, which is the signal that will recruit the proteasome (see below for more details on ubiquitylation). Monoubiquitylated p53 is exported into the cytoplasm where it can function in a transcription-independent manner (Moll et al., 2005) or where it can be stored in a monomeric form (Li et al., 2003). Mdm2 has been shown to mediate both mono- and polyubiquitylation of p53 depending on its abundance: low levels of Mdm2 result in p53 monoubiquitylation and subsequent nuclear export, while high levels of Mdm2 cause p53 polyubiquitylation and degradation inside the nucleus (Li et al., 2003). These distinct activities of Mdm2 towards p53 are likely exploited under different physiological conditions. For instance, p53 needs to be quickly eliminated when the cell has terminated its response to DNA damage and wants to go back to normal conditions and this correlates well with the fact that Mdm2 levels are found to be higher at this stage. On the other hand, it would be advantageous for an unstressed cell to keep inert forms of p53 into the cytoplasm, so that if necessity calls, these p53 molecules can be rapidly activated (via post-translational modifications) without the need to start from

scratch, and this correlates with the fact that in unstressed cells Mdm2 levels are also kept low – mainly through autoubiquitylation. Despite the ability of Mdm2 to polyubiquitylate p53 when at high levels, additional cellular factors are likely needed to foster p53 degradation in its natural context with endogenous Mdm2. One such protein is p300, whose role in p53 regulation is rather complex. In fact, on the one had, p300 acetylates p53 thus enhancing its transcriptional activity (Liu et al., 1999); on the other, it acts as an E4 in the ubiquitin pathway, *i.e.* it transforms single ubiquitins on p53 into polyubiquitin chains which will recruit the proteasome and lead to p53 destruction (Zhu *et al.*, 2001; Grossman *et al.*, 2003).

Redundancy in the p53 network

The conventional model for p53 regulation sees Mdm2 as the only E3 ubiquitin ligase in charge of p53 destruction. Recent data prove this model wrong, as p53 lacking the major ubiquitylation sites for Mdm2 has a normal half-life and is stabilized and activated upon stress like wild type p53 (Feng et al., 2005; Krummel et al., 2005). This does not come as a surprise, though, since the discovery of other E3 ligases for p53 preceded the work by Feng, Krummel and colleagues (Corcoran et al., 2004). Actually, at least four classes of E3 have been reported to recognize p53 as a target for ubiquitylation, including RING, U-box, HECT (homology to E6AP C-terminal domain), and cullin/ROC1–containing ubiquitin ligase complexes (Figure 1.4) (Dai *et al.*, 2006). The authenticity *in vivo* of some of the newly discovered ligases, though, still needs to be proved.

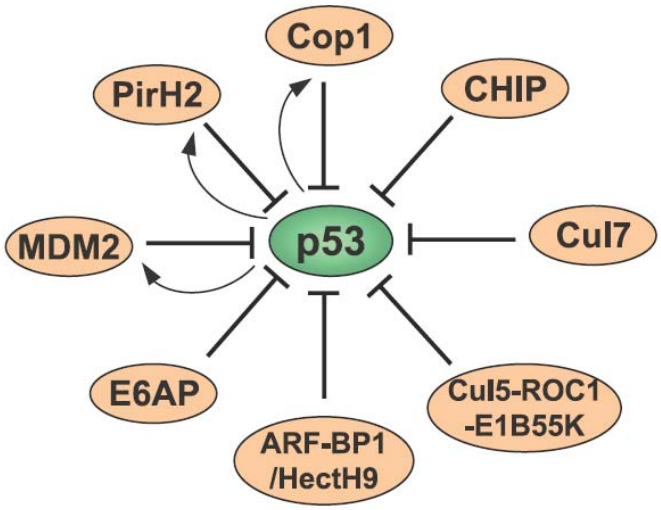

Figure 1.4 | p53 is targeted for degradation by several E3 ubiquitin ligases. In the diagram, bars indicate ubiquitylation and the functional suppression of p53, while arrows indicate the transcriptional activation of the ubiquitin E3 ligase by p53. Adapted from (Dai *et al.*, 2006)

The physiological role of having many ligases for p53 has been elusive, if we exclude a general fail-safe mechanism which relies on redundancy to keep p53 under control were the function of one or more ligases impaired at any given time. Some differences between these ligases could also turn out to be important under different conditions. For instance, Pirh2 inhibits p53 transcriptional activity by binding to p53 central sequence-specific DNA-binding domain, instead of binding to its transactivation domains like Mdm2 (Leng et al., 2003).Recently, yet another ubiquitin ligase for p53 has been discovered, the HECT-domain ligase ARF-BP which, differently from Mdm2, COP1 and Pirh2, is not a p53 transcriptional target (Chen et al., 2005). This detail led Christopher L. Brooks and Wei Gu to propose a new model for p53 regulation, with Mdm2, COP1 and Pirh2 in charge of p53 destruction in response to stress, and ARF-BP1 in charge of keeping p53 levels low during normal cellular growth (Figure 1.5) (Brooks *et al.*, 2006). In fact, being ARF-BP1 independent of p53 transcriptional activity, it can degrade equally well wild type and mutant p53, accounting for the observed instability of mutant p53 in tumor cells – which are generally under stress, for instance due to oncogene activation. One could

think that this model is in contradiction with the observed embryonic lethality of mice caused by Mdm2 depletion. On the other hand, the embryos survive until day E5.5 of development so, were Mdm2 the primary source of p53 degradation in unstressed cells, we would expect the Mdm2 null embryonic cells to undergo some sort of growth arrest much before, due to p53 unconstrained activity. It is possible, therefore, that these embryos die because p53 is activated by an undefined stage-specific developmental stress, and its proapoptotic functions do not find any opposition in the absence of Mdm2, although it is unclear why the other E3 ligases (COP1, Pirh2) do not suffice to make up for Mdm2's absence.

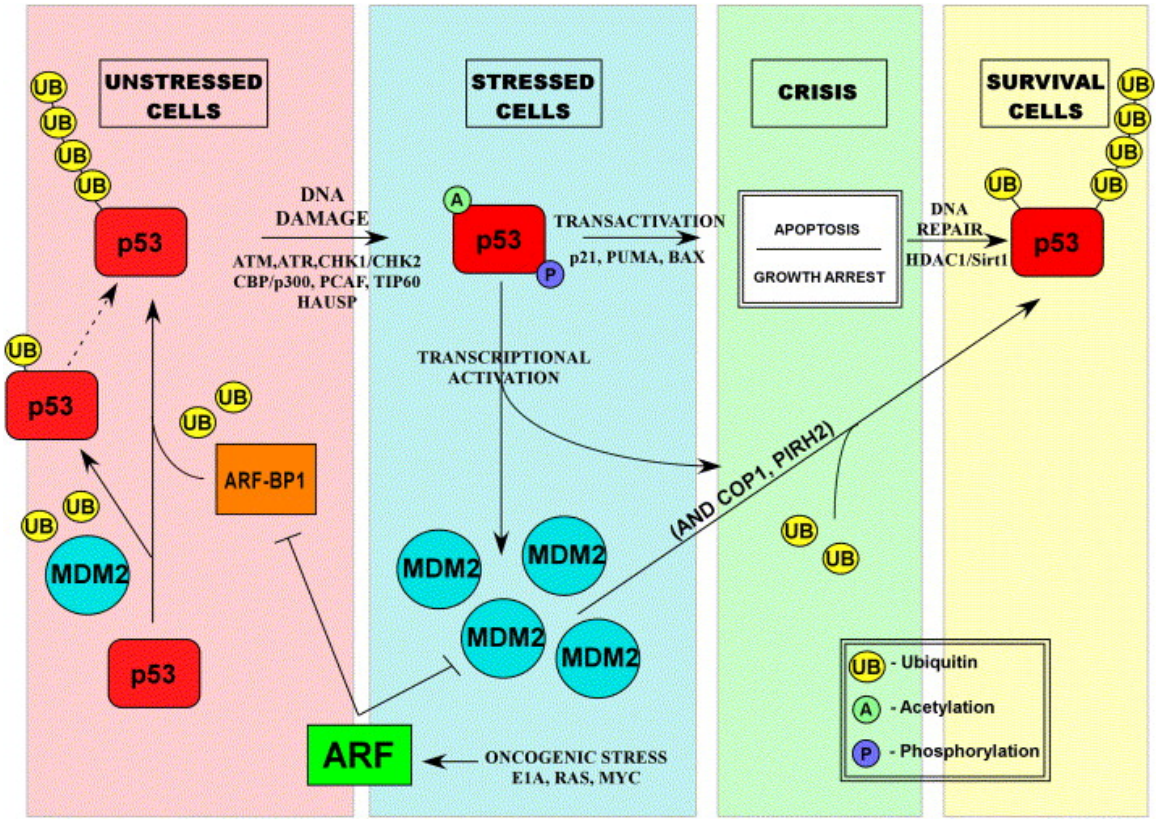

Figure 1.5 | A new model for p53 regulation under stressed and unstressed conditions. In unstressed cells, ARF-BP1 might be the major ligase responsible for p53 ubiquitylation and degradation, with Mdm2, present at low levels in the cell, only triggering p53 monoubiquitylation. In response to stress, p53 is rapidly stabilized and activated, and as a consequence of its transcriptional activity, the levels of Mdm2, COP1 and Pirh2 increase and engage in p53 degradation. Adapted from (Brooks *et al.*, 2006)

Indeed, it seems that only lower organisms such as *Caenorhabditis elegans* and *Drosophila melanogaster* can cope with having a fully functional p53 gene and no Mdm2. Considering that ARF-BP1 gene is instead conserved in both *C. elegans* and *D. melanogaster*, one could speculate that ARF-BP1 is present in all species encoding p53 and that the other ligases (*e.g.* Mdm2, COP1, Pirh2) emerged in evolution to regulate p53 under different cellular conditions (Brooks *et al.*, 2006). It is interesting to note that p53 function itself evolved, since in *C. elegans* and *D. melanogaster* cells p53 can only trigger apoptosis, with growth arrest entering into play only in mammals. It is possible, then, that Mdm2 and the other ubiquitin ligases evolved to give stressed cells the opportunity to undergo a transient growth arrest before committing to a death response (Brooks *et al.*, 2006).

Other players in p53 regulation: HAUSP, MdmX, p14^{ARF} and nucleolar proteins

One of the defining characteristics of post-translational modifications is that they are very dynamic (see below). p53 is no exception and much of the regulation of its degradation is exerted through the fine-tuning of ubiquitylation and deubiquitylation reactions. In particular, the ubiquitin hydrolase HAUSP seems to play a critical role in the control of the stabilities of both p53 and Mdm2 (Li et al., 2004). On the one hand, HAUSP over-expression leads to the activation of p53-dependent transcription and growth arrest, while partial reduction of HAUSP levels by RNAi induces p53 destabilization. On the other hand, complete ablation of HAUSP causes indirectly p53 activation because Mdm2 autoubiquitylation is not counterbalanced anymore and Mdm2 is too unstable to degrade p53. The regulation of the p53-Mdm2 feedback network involves also many other players, among which MdmX and p14^{ARF} are of note. MdmX is, like Mdm2, a RING-finger protein, whose N-terminus contains a p53 binding domain which makes of MdmX a perfect candidate for being a ubiquitin ligase for p53 (Shvarts et al., 1996). Until recently, though, MdmX was believed to be unable to ubiquitylate p53 and to not affect Mdm2-mediated p53 ubiquitylation. At the same time, MdmX was shown to stabilize both p53 and Mdm2, the first by preventing its nuclear export and subsequent degradation, the second by heterodimerization of the respective RING fingers and inhibition of Mdm2 autoubiquitylation (Stad et al., 2001). Since Badciong and Haas

reported that MdmX has *in vitro* E3 ligase activity and that it can ubiquitylate itself and p53 synergistically with Mdm2 (Badciong *et al.*, 2002), there is the urge for further experiments that can better delineate MdmX role in the p53 network. $p14^{ARF}$ is a tumor suppressor which inhibits cell proliferation by activating p53 and the retinoblastoma protein Rb. Lately, $p14^{ARF}$ is gaining the interest of the scientific community for its p53-independent activities which seem to correlate with the sumoylation, and subsequent inactivation, of several transcription factors by $p14^{ARF}$ (Sherr et al., 2005). $p14^{ARF}$ has been shown to promote Mdm2 rapid degradation, regardless the presence of p53 (Zhang et al., 1998) and to block Mdm2-dependent p53 degradation by anchoring Mdm2 into the nucleolus thus keeping Mdm2 from shuttling p53 out of the nucleus into the cytoplasm where it can be degraded (Tao *et al.*, 1999). Similarly to blocking Mdm2, $p14^{ARF}$ also suppresses ARF-BP1-mediated p53 degradation (Chen et al., 2005). Interestingly, p53 down-regulates expression of its positive regulator $p14^{ARF}$, giving rise to another feedback loop in the p53 network (Stott et al., 1998).

Finally, nucleolar proteins, such as the ribosomal proteins L11, L23 and L5, have also been implied in p53 regulation, for their ability to inhibit the action of Mdm2 on the tumour suppressor (Dai *et al.*, 2004; Dai *et al.*, 2004; Dai *et al.*, 2006). These proteins act as sensors of ribosomal stress (*i.e.* any situation in which rRNA synthesis, rRNA processing and ribosome assembly is impaired) upon which they are released from the nucleolus into the nucleoplasm where they can directly associate with Mdm2 and block p53 degradation. The precise mechanism underlying such regulation is not clear. It has been suggested that these proteins bind to Mdm2 in its central acidic region, which has been implicated in p53 ubiquitylation (Argentini *et al.*, 2001; Kawai *et al.*, 2003; Meulmeester *et al.*, 2003; Zhang *et al.*, 2003; Dai *et al.*, 2004; Dai *et al.*, 2004; Dai *et al.*, 2006). Also, different ribosomal proteins seem to use different mechanisms, in that L26 was found to bind the 5'UTR of the p53 mRNA and enhance its translation (Takagi et al., 2005).

p53 sumoylation

To the long list of post-translational modifications influencing in a way or another p53 activity, sumoylation has been lately added (Gostissa et al., 1999; Rodriguez et al., 1999) (see below for more details on protein sumoylation). The initial suggested

enhancement of p53 transcriptional activity by such modification has been questioned though, so much that at the moment the biological function of sumoylated p53 is rather contradictory (Watson *et al.*, 2006). Also under debate is the effect of sumoylation on p53 localization, since on the one hand it has been reported that the p53 mutant protein that cannot be sumoylated (p53K386R) shows unchanged cellular distribution as compared to wild type p53 (Fogal et al., 2000; Kwek et al., 2001); on the other hand, p53 sumoylation seems to be related to the association of the protein with nuclear organelles such as the nucleolus (Muller *et al.*, 2001; Chen *et al.*, 2003). The speculation that p53 association with nuclear bodies is a prerequisite for p53 sumoylation comes rather naturally when putting together the following observations: a) p53 recruitment to the PML bodies triggers activating modifications on p53 (Gostissa et al., 2003); b) nuclear bodies seem to stimulate SUMO conjugation and proteins that bind transiently to nuclear bodies are often SUMO targets (Jackson, 2001; Seeler *et al.*, 2001); c) p53 is itself a SUMO target and the major site for sumoylation lies into the C-terminus of p53, which is known to regulate p53 transcriptional activity (Gostissa et al., 1999); d) p73, another member of the p53 protein family, is also sumoylated and its sumoylation might be involved in the re-localization of p73 into nuclear bodies (Minty et al., 2000).

Indeed, sumoylation affects p53 directly or indirectly, because several of its regulators – Mdm2, MdmX, and PML for instance – are found to be modified by SUMO. Nonetheless, the current data available on the SUMO system in the p53 pathway still fail to give a unified model and more work is needed to uncover the network of protein-protein interactions and the interplay of post-translational modifications that may play a role in the SUMO-mediated regulation of p53.

Regulation of protein function through post-translational modifications

A cell is a very dynamic entity: in order to survive, it has to continuously interact with its environment and be able to rapidly respond to external changes with internal ones. To do this, cells can count, among other things, on an army of modifications which proteins undergo depending on the circumstances. An important characteristic of these modifications is their reversibility (not all modifications are reversible, but those involved

in signalling mostly are) and their possible coexistence, which dramatically increases the number of functions that very cell can perform with a limited number of proteins encoded by a limited number of amino acids. These modifications are called post-translational modifications (PTMs) because they occur after protein synthesis; this, together with the fact that a modified protein can be brought back to its original unmodified status, make PTMs a fast, efficient way for the cell to regulate its functional units without the need to re-synthesize proteins from scratch. The way in which PTMs work is sometimes by inducing a new conformational state of the protein, which brings an altered function about. Alternatively these modifications constitute anchoring points for other proteins resulting in complex formation and therefore new functionalities. Recently, a very elegant, evolutionary sound model has been proposed. The task of decoding the status of the proteins inside the cell is assigned to the modular protein interaction domains that proteins are made of. These domains are dedicated to the recognition of specific modifications and combinations of them in a way that is general and does not require molecular interactions tailor-made to a particular polypeptide (Seet et al., 2006) . Despite their being all fascinating, in the following sections only two of these modifications will be discussed: ubiquitylation and sumoylation.

Eukaryotic protein degradation and the ubiquitin pathway

Proteins exist as a chain of amino acids which can degrade over time being this reaction thermodynamically favourable in aqueous solution. Protein turnover (*i.e.* degradation), together with protein synthesis, determine the concentration of each protein inside the cell. The great majority of proteins are long-lived, abnormal proteins and key regulatory proteins representing an exception with their very short half-lives. Rapid and specific degradation of regulatory proteins in charge of the activation of one or more pathways is indeed an essential feature for cells, because it means blocking these pathways (when needed!) without hesitation or mistake. Mistakes could arise, in fact, were the regulatory protein simply inhibited in its function - via a conformational change, for instance -, since such inhibition could be accidentally removed (being a reversible process).

Degrading regulatory proteins instead of inhibiting them is therefore a much safer option which, despite its high cost (proteins need to be synthesized from scratch!), ensures that processes, potentially lethal to the cell if executed in the wrong circumstances, are kept strictly under control. Starting from a rather dark past, when it received little attention compared for instance to protein synthesis, protein degradation slowly gained ground, finally granting Aaron Ciechanover, Avram Hershko and Irwin Rose the Nobel Prize in Chemistry in 2004 for their major contributions to the elucidation of the mechanisms regulating the highly specific breakdown of intracellular proteins through the ubiquitin pathway. Together with lysosomal proteolysis, the ubiquitin-proteasome pathway represents the major pathway mediating protein degradation in eukaryotic cells. Lysosomes (membrane-enclosed organelles that contain an array of digestive enzymes) are used by the cell to dispose of extracellular proteins - taken up by endocytosis - as well as cytoplasmic organelles and cytosolic proteins. Alternatively, in order to quickly degrade cytosolic and nuclear proteins, cells adopt a tightly regulated process which requires to first put a tag on those proteins which need to be eliminated, and then proceed to their destruction. The tagging process is called ubiquitylation (ubiquitination in earlier publications) from the name of the protein (ubiquitin, precisely) which is covalently attached to a substrate to signal that its time has come. The destruction is carried out by the multisubunit ATP-dependent protease called proteasome. Ubiquitylation is actually more complex than what emerges from this description, as one might guess considering its being involved in many cellular processes, as diverse as cell cycle progression (Krek, 1998) and immune response (Liu, 2004). It requires, in fact, the coordinated action of at least two, but most of the times three, different enzymes (many more if we consider the newly described chain elongation factor E4 and the de-ubiquitylating enzymes DUBs): the E1, ubiquitin-activating enzyme, an active cysteine residue of whom forms a thioester bond with ubiquitin C-terminus, thus activating it for the next step in the cascade; an E2, ubiquitin-conjugating enzyme, onto which ubiquitin is passed from the E1, again through the formation of a thioester bond between a cysteine on the E2 and ubiquitin C-terminus.

The E2 can either directly catalyse the conjugation of ubiquitin to the substrate or cooperate with one of the so-called ubiquitin-ligase E3 enzymes, which recognize the substrate and, by binding simultaneously to it and to the E2, facilitate the passage of ubiquitin from this latter to the substrate. Sometimes there is no other substrate than the E3 itself, which can mediate its own degradation through a mechanism called autoubiquitylation, term that does not distinguish between inter or intramolecular *modus operandi* (this latter is being demonstrated in some cases (Banerjee et al., 1993). This three-step mechanism initiates all known ubiquitylation reactions, independently of whether the substrate-bound ubiquitins will signal proteosomal degradation or some other fate. Contrary to what was believed until recently, in fact, ubiquitylation regulates other cellular functions than protein degradation, like protein localization (d'Azzo et al., 2005), transcription (Dhananjayan et al., 2005), endocytosis (Rotin et al., 2000), ribosomal function (Panasenko et al., 2006), postreplicational DNA repair (Baarends et al., 2000) and budding of retroviruses from the plasma membrane (Kikonyogo et al., 2001). Whether or not an ubiquitylated protein will be degraded depends on the number of ubiquitin molecules it carries and, when many, on the type of linkage between them; degradation being triggered only by the presence of a long polyubiquitin chain, attached at a single site on the substrate, where at least four molecules are linked pair-wise via an isopeptide bond between the ε-amino group of a lysine of one ubiquitin and the C-terminal carboxyl group of the next ubiquitin in the chain (Thrower et al., 2000). Monoubiquitylation, multiubiquitylation characterized by single ubiquitins attached at different sites on the same protein, or a polyubiquitin chain with a different type of linkage between ubiquitins, are instead the signal recognized by the array of cellular processes regulated by ubiquitin in a proteasome-independent way (Figure 1.6).

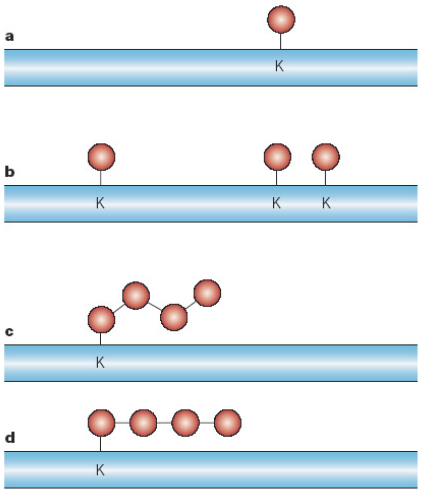

Figure 1.6 | Schematic representation of the difference between mono and multiubiquitylation. **a**, monoubiquitylation is characterized by a single ubiquitin covalently attached to a lysine residue on a target protein. **b**, Multiubiquitylation characterized by several single ubiquitin attached at different lysines on the protein. **c**, Multiubiquitylation characterized by a chain of ubiquitins where the C-terminal glycine 76 of one ubiquitin is linked to lysine 48 of the next ubiquitin. This chain signals the destruction of the protein by the proteasome. **d**, Multiubiquitylated proteins can also have a different type of chain, the best known being characterized by a bond between lysine 63 of one ubiquitin with the C-terminus of another ubiquitin. Adapted from (Haglund *et al.*, 2005)

The mechanism(s) of ubiquitin-chain assembly is still somewhat controversial. The textbook version holds that ubiquitin molecules are added on at a time, first to the substrate and then to the most distal ubiquitin of the growing chain (Figure 1.7). This model, called the "sequential addition model", is a natural extension of a monoubiquitylation reaction, in which the most distal ubiquitin in the chain provides the lysine residue to which the next molecule can be attached.

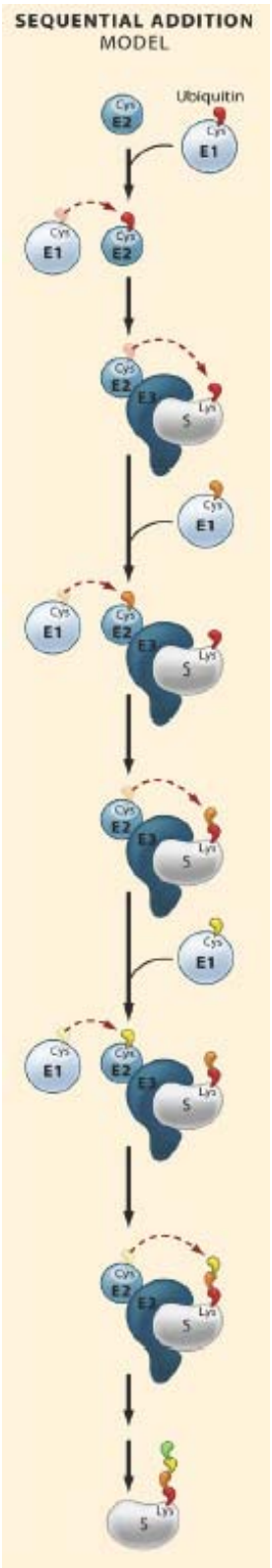

Figure 1.7 | Schematic representation of the sequential addition model. In this model, the most distal ubiquitin in the chain provides the lysine residue to which the next molecule can be attached. Adapted from (Hochstrasser, 2006)

This model becomes less intuitively appealing when we consider that a polyubiquitin chain can be very long and therefore the free end of it becomes structurally remote from the original substrate. A way to justify this would be to consider that the chain is looped out between the substrate and the E2 binding sites on the E3. Given the discovery that E1 and E3 binding sites on the E2 overlap and their binding to E2 is mutually exclusive (Eletr et al., 2005), if the chain is assembled on the substrate by a sequential addition mechanism, then multiple cycles of E2-E3 binding and release are necessary if continuous E3-substrate binding is required for processive ubiquitylation (Reiss *et al.*, 1989; Rape *et al.*, 2006). An intriguing possibility in this respect would be that the E2 dimerizes and the E1 and the E3 would each bind to one monomer in the dimer, thus avoiding the full release of the E3 from the E2 (Pickart, 2001). Yet another possibility is that unanchored ubiquitin chains are assembled in solution, prior to attachment to a substrate, which would occur once the E1 fishes the chain and activates the C-terminal carboxyl group at its base of the chain, This idea is supported by the observation that many cell types have a significant amount of what appears to be "free" ubiquitin chains (van Nocker *et al.*, 1993) which are competent intermediates in the ubiquitylation pathway. While degradation is irreversible, ubiquitylation is a reversible process; the cell can in fact call upon a class of thiol proteases, called deubiquitylating enzymes (DUBs), to hydrolyze the amide bond between glycine 76 of ubiquitin and the substrate protein (or another ubiquitin), thus adding another layer of regulation on the amount and identity of ubiquitylated proteins.

Ubiquitin

Ubiquitin is a heat-stable small protein, comprising 76 amino acids, which can exist either in free form or as part of a complex with other proteins. Figure 1.8 shows ubiquitin three-dimensional structure, at 1.8 Å resolution, with its characteristic β-grasp fold, which is shared by other proteins as well, also referred to as the ubiquitin-like fold due to ubiquitin popularity. Its name eloquently signifies its ubiquitous presence all over the cell and throughout all eukaryotes, from yeast to humans.

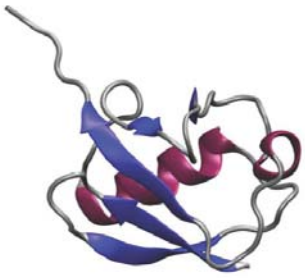

Figure 1.8 | Three-dimensional structure of ubiquitin Adapted from (Gumbart, 2006)

The conservation of the amino acid sequence of ubiquitin becomes obvious when comparing plants and animals, for there is just a two amino acid difference between ubiquitin of the two groups (Figure 1.9). This high degree of conservation strongly suggests that each amino acid is extremely important for ubiquitin's proper functioning, which, being essential to the survival of any eukaryotic cell, pressed for its fine-tuning before the appearance of multi-cellular organisms.

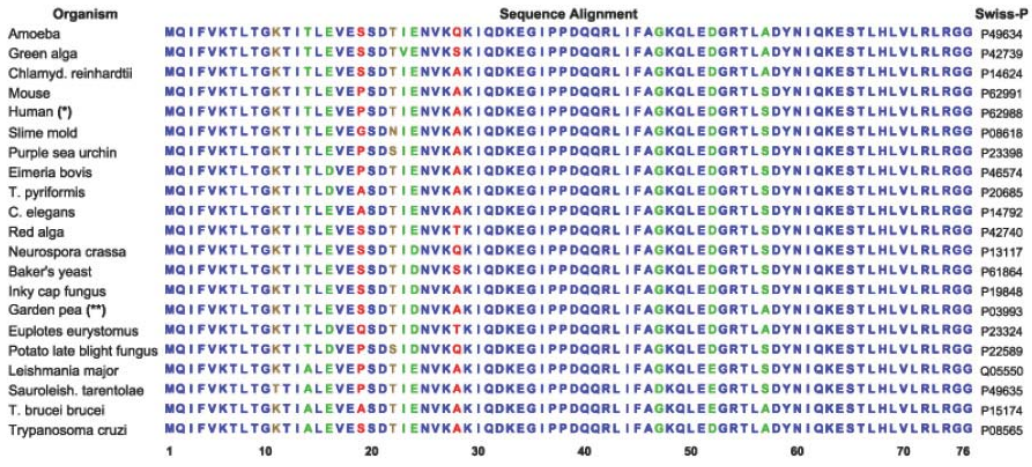

Figure 1.9 | Sequence alignment of ubiquitin from different organisms. The colours represent different degrees of amino acid conservation. In blue are identical residues, in green are conserved substitutions, in light brown are semi-conserved substitutions. Red means no conservation among residues. In the far-right column, protein accession numbers to the NCBI database are given. Adapted from (Gumbart, 2006)

E1, the ubiquitin-activating enzyme

All E1s known so far share a common homology domain, which contains a nicotinamide adenine dinucleotide (NAD) binding site. This domain assumes a fold found in many NAD binding proteins and can be traced back to bacteria (Begley et al., 1999; Unkles et al., 1999). Interestingly, E1s harbouring two NAD domains like yeast Uba1 and human UBE1 act as monomers, while those with a single copy need to be in complex with a protein containing a second NAD-binding domain (Huang et al., 2004). Figure 1.10 shows a comparison between the E1 enzymes of budding yeast and humans. Although the E1 concentration is usually less than the total E2 concentration, E1 is a very efficient enzyme producing enough activated ubiquitin for all downstream conjugation reactions. While the connection between structure and function remains to be elucidated, the mechanism of ubiquitin activation is known in great detail. The reaction starts with the binding of MgATP followed by the binding of ubiquitin; a ubiquitin adenylate intermediate is thus formed which serves as the donor od ubiquitin to a cysteine in the E1 active site. A fully loaded E1 carries two ubiquitins, one as a thiol ester, which is further transferred onto the next enzyme in the cascade, and one as an adenylate. E1 has a rather weak binding affinity for ubiquitin prior to ATP binding, suggesting an ATP-dependent conformational change that helps increase the accessibility of a ubiquitin binding site.

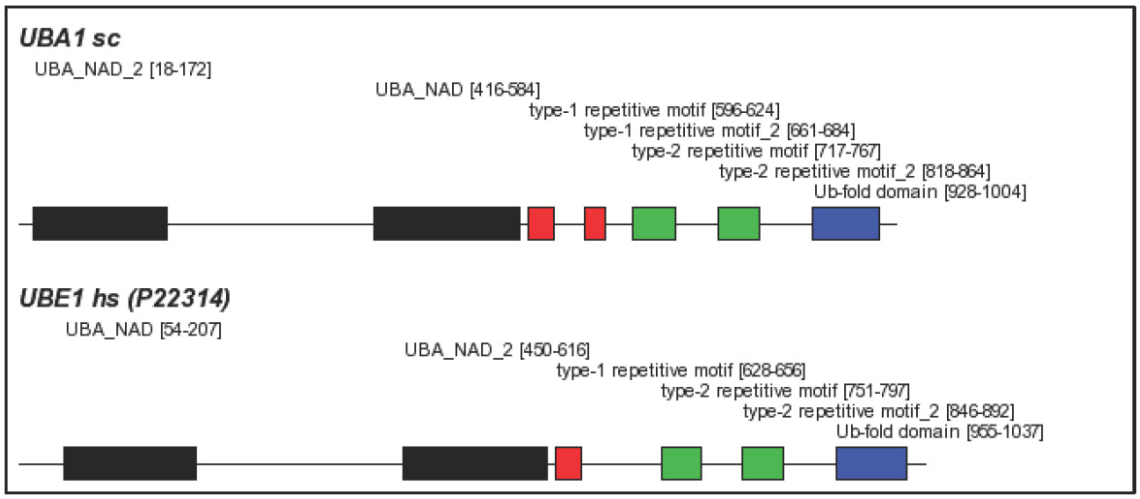

Figure 1.10 | Domain structure of budding yeast (UBA1 sc) and human (UBE1 hs) ubiquitin activating enzymes. The name of each domain is written on top of the box representing the domain. Type-I repetitive domain following a UBA_NAD domain contains the active cysteine. Adapted from (Scheel, 2005)

Currently, there is no solved crystal structure for the ubiquitin-activating E1, but inferences can be made using the crystal structures for the E1 enzymes that catalyze the attachment on substrate proteins of so-called ubiquitin like proteins (Ubls), among which the most studied are SUMO (*s*mall *u*biquitin like *mo*difier) and NEDD8.

Based on weak sequence similarity to these proteins, the structure of ubiquitin-E1 is thought to consist primarily of the adenylation domain and the catalytic cysteine domain, plus a ubiquitin-like domain at the C terminus of the protein (Figure 1.11).

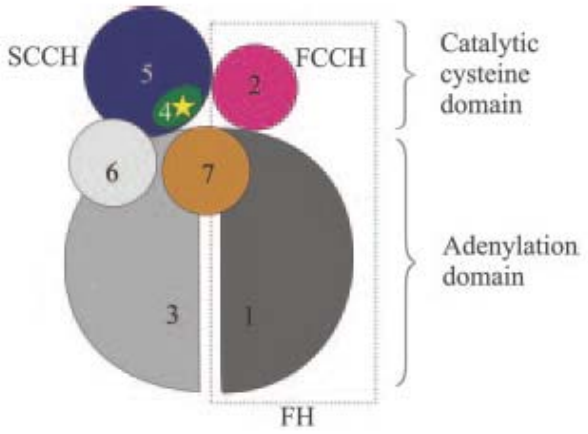

Figure 1.11 | Schematic diagram of the likely domain structure of the E1 (1-6) in complex with ubiquitin (7). The fragments of ubiquitin-E1 are (**1**) first adenylation half-domain, (**2**) first catalytic cysteine half-domain (FCCH), (**3**) second adenylation half-domain, (**4**) second catalytic cysteine half-domain (SCCH), (**5**) SCCH poorly conserved region and (**6**) Ubl-domain. The *dotted rectangle* marks the extent of the first half-domain (FH), which consists of the first adenylation half-domain and the FCCH. The *yellow star* marks the location of the catalytic cysteine residue. Adapted from (Szczepanowski *et al.*, 2005)

Sequence conservation among Ubl-E1s is highest for the adenylation half-domains, which are also homologous to each other. Therefore, it is very likely that the adenylation domain of ubiquitin-E1 resembles the pseudodimeric adenylation domains of the NEDD8-E1 and SUMO-E1.

In contrast, no confident homology model can be built for the catalytic cysteine half-domains. Both half-domains differ significantly between E1s for different ubiquitin-like modifiers (Figure 1.12).

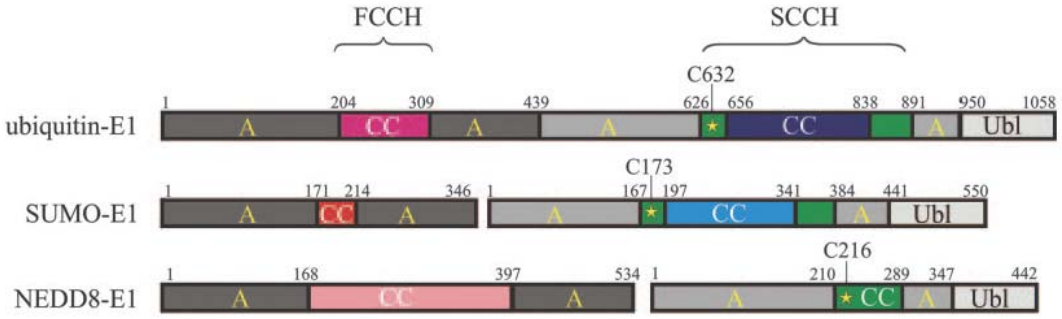

Figure 1.12 | Domain organization mapped to linear sequence for the ubiquitin-E1 (*top*), SUMO-E1 (*middle*), and NEDD8-E1 (*bottom*). The adenylation half-domains are shown in *dark* and *light gray*, the FCCH in different *shades* of *red*, the SCCH in *green* and *blue* (representing the well conserved and poorly conserved parts, respectively), and the Ubl domain in *very light gray*. *A*, adenylation domain; *CC*, cysteine catalytic domain. The catalytic cysteine residue is marked by a *yellow star*. Adapted from (Szczepanowski *et al.*, 2005)

E2, the ubiquitin-conjugating enzyme

Any member of the E2 protein family is characterized by the presence of a cysteine into a conserved domain; it is this cysteine to form the thioester bond with the ubiquitin coming from the E1, thus conferring the enzyme its catalytic function, which is abrogated by substitution of the cysteine residue (VanDemark *et al.*, 2002). Opposite the active site poorly conserved residues are found which might have diverged due to low selective pressure, but it is likely that they mediate interactions important for the specific function of each individual E2. In fact, despite their similarity to one another (similarity that holds even between E2s dedicated to ubiquitin and ubiquitin like proteins, as shown by the crystal structure of the SUMO-specific yeast E2, Ubc9), different E2s have distinct biological functions, probably consequence of their highly specific interaction with E3s.

Although it would seem plausible that the binding of an E3 would reposition residues in the E2 active site, the currently available crystal structure of E2-E3 complexes do not show any alteration in the E2 conformation.

This suggests that the residues responsible for the passage of ubiquitin from the E1 onto the E2 mainly sit in the E1 active site, while those responsible for conjugation of ubiquitin to a substrate mainly sit in the E3 active site.

Free E2s bind tightly to the loaded E1 molecule as well as to their cognate E3s, but weakly to free ubiquitin and free E1. Like ubiquitin activation by E1, ubiquitin transfer to E2s is rapid relative to downstream reactions of substrate ubiquitination. There are eleven E2 enzymes in the budding yeast genome (Pickart, 2001) and approximately fifty in the human genome (Jiang *et al.*, 2004).

A comparison between yeast Ubc4 and human UbcH5B is shown in Figure 1.13. When one considers that the molecular character of the E2-E3 interaction is well conserved across several E2-E3 pairs, it is natural to wonder what the need to have many E2s for each E3 might be. Plausibly, having various E2s ensure that the pool of activated ubiquitin is appropriately distributed among different E3s, although the discovery of new interacting E2 partners could shed some light on the reasons behind the need of specialized E2s.

a

```
UbcH5B:   2 ALKRIHKELNDLARD  ---  58 TDYPFKPPK  ---  93 WSPALTI  ---
yUBC4:    3 SSKRIAKELSDLERD  ---  59 TDYPFKPPK  ---  94 WSPALTL  ---
```

b

Figure 1.13 | Comparison between the yeast E2 enzyme Ubc4 and the human E2 enzyme UbcH5B. **a**, Sequence alignment of human UbcH5B and yeast UBC4 encompassing the _α1 helix and the L1 and L2 loops. Conserved residues are displayed in bold. **b**, X-ray structure of Ubc4 and ensemble of UbcH5B models as predicted by (Dominguez et al., 2004). These enzymes have been chosen since UbcH5B is the E2 responsible for p53 ubiquitylation together with the E3 enzyme Mdm2 (Saville et al., 2004). Adapted from (Dominguez *et al.*, 2004)

E3, the ubiquitin ligase

Ubiquitin ligases are divided into three families: the HECT, the RING-finger (Figure 1.14) and the U-Box families. Contrary to what the name suggests, RING-finger and U-Box E3s do not catalyse the ligation of ubiquitin onto the substrate, rather they act as scaffolds to bring the E2 and the protein to be modified together (Figure 1.15). The HECT E3s, instead, do perform the ligation step, since ubiquitin is first temporarily transferred to a cysteine of the E3 and then attached to the substrate (Figure 1.15). U-Box E3s have been identified recently, therefore details about their catalytic action are not known.

As previously mentioned, often proteins do not acquire a single ubiquitin but a chain of them. It is still not clear how an E3 distinguishes between attaching a ubiquitin to another ubiquitin already present on the substrate (thus starting or elongating a chain) or to another lysine on the substrate.

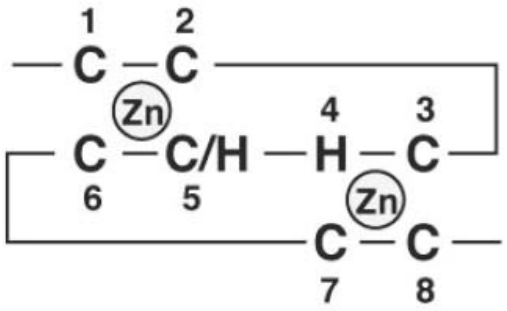

Figure 1.14 | RING domain This domain is characterized by a series of histidine and cysteine residues with a characteristic spacing allowing the coordination of zinc ions. The spacing, rather then any primary sequence, is conserved in the RING finger family. The zinc ions and their ligands are catalytically inert, suggesting for the E3s a role as molecular scaffolds to bring different proteins together. Adapted from (Pickart, 2001)

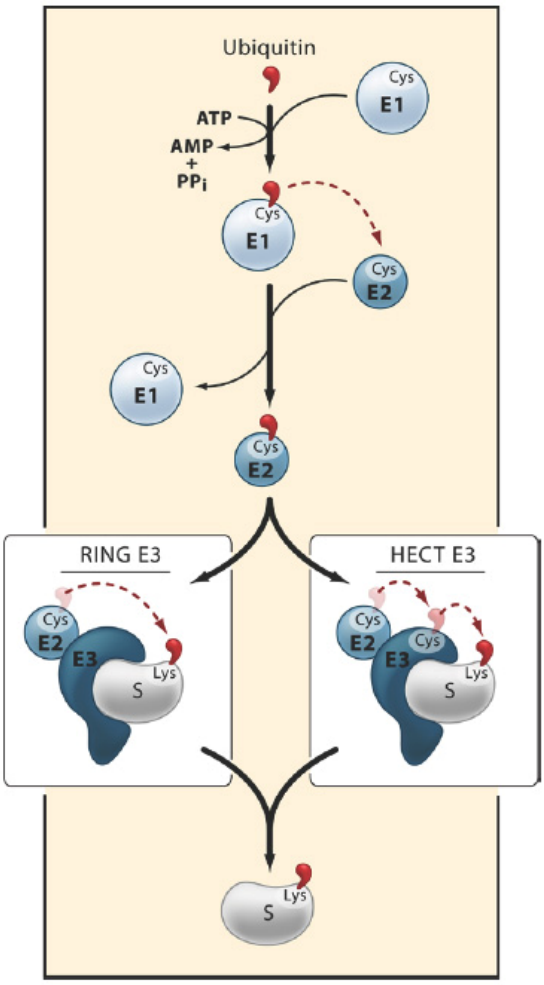

Figure 1.15 | Outline of the ubiquitin-conjugation payhway. Activation of the ubiquitin C terminus by E1 proceeds in two steps: adenylation (not shown) followed by attack by a cysteine side chain to form a thioester bond between the E1 and ubiquitin. Ubiquitin is then passed to a cysteine of an E2. Ligation of the ubiquitin to a substrate (S), usually to a lysine side chain, follows either directly with the aid of a RING-bearing E3 or after an intermediate transthiolation to a cysteine side chain of a HECT-domain E3. Both types of E3 interact with their substrates, many of which acquire a polyubiquitin chain rather than just a single ubiquitin. Note: The dashed red arrows represent the direction of movement of ubiquitin, not the direction of nucleophilic attack. Adapted from (Hochstrasser, 2006)

The kinetic of the first process could be faster than that of the second, for instance, or perhaps conjugation of the first ubiquitin inhibits attachment of other ubiquitins on different lysine residues on the same substrate, leaving the door open for chain elongation.

This model is attractive in that it agrees with the evidence that monoubiquitylated proteins predominate when ubiquitin self-conjugation is abrogated. It also remains to be elucidated whether the E2-E3 pair that executes the first ubiquitin ligation is the same that elongates the chain or if there are other pairs dedicated to this (allowing for further regulation of polyubiquitylation). Recently, a new class of enzymes has been identified in the ubiquitin pathway - referred to as E4 enzymes or chain elongation factors - which mediates the passage from mono- or oligoubiquitylated (*i.e.* few ubiquitins) protein to a polyubiquitylated one (Hoppe, 2005). E3s appear not to discriminate among the different lysines on a substrate, although experimental validation of this is yet to come. Finally, it is important to note that productive ubiquitylation depends upon successful interaction of the E3 with both the E2 and the substrate, paving the way for regulation of ubiquitylation at the level of protein-protein interactions; for instance, the E3 might need to be covalently modified before being in the right conformation to bind the E2 or the substrate; this latter might also need some modification (often phosphorylation) in order to be recognized by the E3; finally, the E2 levels might be a function of time.

Sumoylation

Despite its name, SUMO is a small protein which is attached to other proteins in a very dynamic, reversible covalent way. Indeed, together with ubiquitin, it represents one of the biggest tags that a protein can acquire (SUMO and ubiquitin being proteins of about ten kilo Daltons). Even if the sequence similarity between SUMO and ubiquitin is rather poor, SUMO shares (like the other ubiquitin-like modifiers) with ubiquitin its typical fold, to which a C-terminal loop is added, probably conferring to SUMO the specificity that distinguishes it from ubiquitylation notwithstanding their surprising similarity (Figure 1.16).

Figure 1.16 | Comparison between ubiquitin and SUMO three-dimensional structures. Adapted from <www.roberts-publishers.com/walsh/chapter9.pdf >

The mechanism of SUMO conjugation is the same as for ubiquitin and the enzymes in this cascade are also referred to as E1, E2 and E3 (Figure 1.19). First SUMO needs to get into its mature form through the action of a SUMO protease that exposes a carboxy-terminal glycine residue on the protein; then SUMO is activated by temporary attachment to the E1 via the formation of a thioester bond between the C-terminal glycine of SUMO and a cysteine on the E1. Contrary to the ubiquitin E1, which is a single protein, SUMO

E1 is a heterodimer whose subunits are respectively in charge of the adenylation and thioesterification reactions (Figure 1.17).

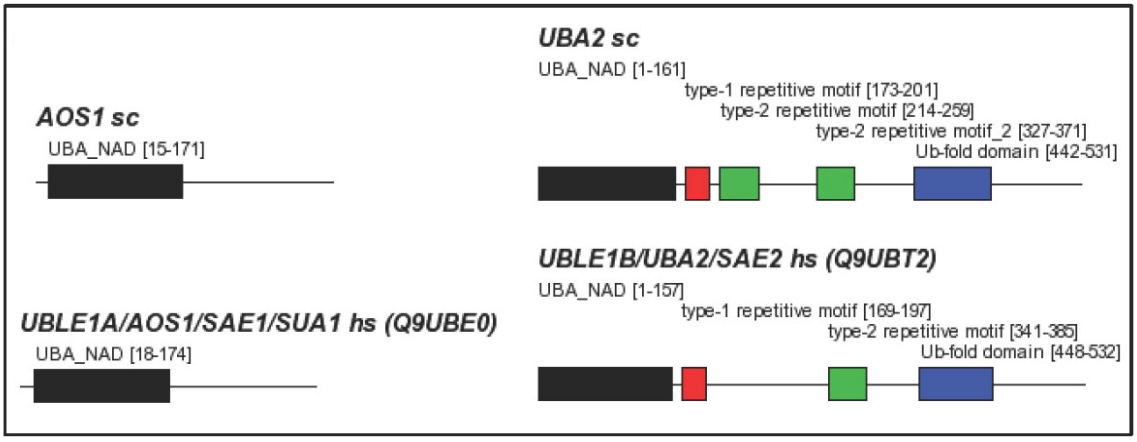

Figure 1.17 | Domain structure of budding yeast (AOS1/UBA2 sc) and human (UBLE1A/AOS1/SAE1/SUA1/UBLE1B/UBA2/SAE2 hs) SUMO activating enzymes. The name of each domain is written on top of the box representing the domain. The subunits of the heterodimeric E1s are shown as separate proteins in the same row. Adapted from (Scheel, 2005)

The structural analogy with the ubiquitin E1 is nonetheless preserved, since the two subunits of the heterodimer correspond to its amino and carboxy termini, this solution being in addition more suitable for regulation. SUMO then passes onto the E2, again through the formation of a thioester bond between a cysteine on the E2 and a C-terminal glycine on SUMO. Notably, there exists only one E2 (Ubc9) for SUMO conjugation compared to the many E2s in the ubiquitylation pathway (see Figure 1.18 for a comparison between the human and the yeast SUMO E2s). Ubc9 can interact directly with the substrate leading to its sumoylation; the fact that the target protein carries all the necessary information to specify its own sumoylation led to discard the hypothesis of the existence of E3 SUMO ligases. Recently, this belief has been shelved since different E3 ligase types have been identified (Hochstrasser, 2001). This discovery reveals another layer of regulation in the sumoylation pathway which adds itself to other regulatory mechanisms, like, for instance, the desumoylation responsible of cleaving SUMO off target proteins.

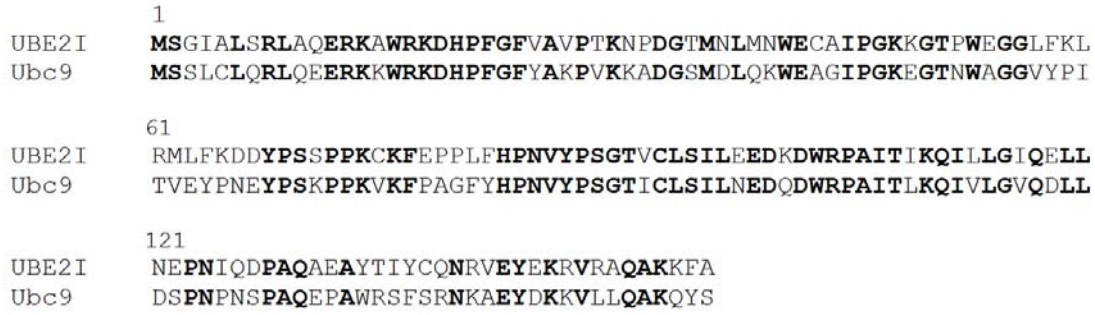

Figure 1.18 | Sequence alignment of the human SUMO E2 UBE2I and the budding yeast SUMO E2 Ubc9. Conserved residues are shown in bold. The numbers indicate the position of the respective amino acid.

Sumoylated proteins are not targeted for proteasomal degradation. Sumoylation signals the re-localization of proteins, as well as regulates nucleocytoplasmic shuttling, genome integrity and transcription. The vast majority of sumoylated targets are in fact transcription factors, but the effects of sumoylation on such proteins has proven to be subtle, bringing some doubts over the role of this modification in the transcriptional process.

Currently, there are two models (which could also be both correct, since they do not contradict one another) for the role of SUMO in the regulation of transcription factors activity. The most experimentally validated is the "sequestration" model, for which sumoylation signals the re-localization of transcription factors to specific cellular compartments, often nuclear speckles or bodies (*e.g.* the PML bodies) (Muller et al., 2001). The other model, still awaiting clear experimental evidence, is the "promoter" one, for which sumoylated transcription factors, as well as components of the sumoylation machinery, are bound directly to the chromatin. Supporting this model is the fact that sumoylation most often leads to the attenuation or repression of transcriptional activity (Seeler *et al.*, 2003).

Sumoylation appears to be mainly directed towards nuclear proteins, although some cytoplasmic targets have been also identified.

Like any other post-translational modifications, sumoylation can be influenced by other modifications and in fact it is not rare the finding that the same residue on a certain protein can be ubiquitylated, sumoylated or acetylated. Therefore, although sumoylation is not directly involved in the degradation of proteins, it can indeed indirectly influence their half lives, competing with ubiquitylation for the same lysine residue(s) and therefore protecting it from proteasomal targeting. The most striking characteristic of sumoylation is its relation with subnuclear structures. All three types of E3 SUMO ligases that have been identified up to now are bound to specific subnuclear structures, like PML or other nuclear bodies, the nuclear pore complex and so-called Polycomb group bodies (Seeler *et al.*, 2003). Regardless of how attractive this can be, it is difficult to assign to sumoylated proteins some clear-cut, specific characteristics that distinguish them from their non-modified counterparts. Apart from few striking cases (Muller *et al.*, 1998; Johnson *et al.*, 1999), most of the times only subtle effects have been attributed to sumoylation. This is fastly changing though and in the literature more and more examples of proteins whose function is modulated by SUMO are found. Also, it is likely that SUMO effects are going to reveal themselves the closer experimental setups will get to physiological conditions. Moreover, from the available data, it is evident that sumoylation often affects many components of the same complex (Seeler *et al.*, 2001). This raises the possibility that what really matters is the dynamic equilibrium among modified and unmodified components, which would explain why mutations of the sumoylation acceptor residues on a protein show only subtle effects. There is still room for great discoveries about the mechanisms underlying this new exciting post-translational modification, one of which is indeed the role *in vivo* of poly-SUMO chains, which have appeared only recently on the scene, having been thought not to exist before.

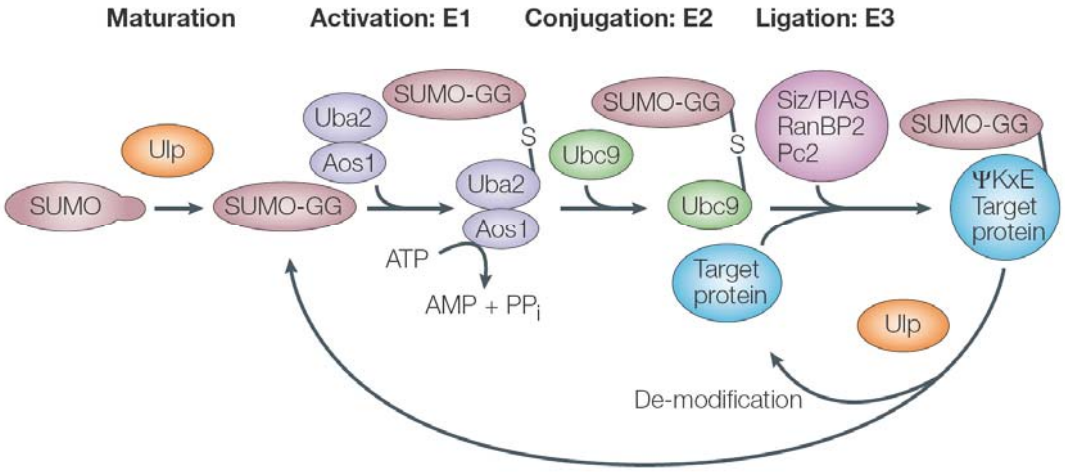

Figure 1.19 | Different steps in the sumoylation cycle. Before being attached to protein substrates, SUMO needs to get into its mature form. This is achieved through cleavage by a SUMO protease (Ulp in the scheme). The three following steps, namely activation, conjugation and ligation, are similar to those int the ubiquitin pathway (see text for details). On the target protein, the short consensus sequence ΨKxE – where Ψ is an aliphatic residue – surrounding the acceptor lysine residue is shown. Adapted from (Seeler *et al.*, 2003)

Mathematical modelling of biological networks

Biologists are very familiar with the term 'model'. They use it repeatedly to designate a verbal or graphical description of a mechanism underlying a certain cellular process. Less often do they use it to refer to a set of equations expressing in a formal manner relations among variables that characterize the state of a biological system. Yet these mathematical models, more rigorous and more potent than the former ones, are entering biology at an increasingly rapid pace, pressing biologists to make themselves familiar with them. In many cases, concepts derived from engineering can be applied directly to graphical models. Thus, a negative feedback loop is expected to diminish the noise (Becskei *et al.*, 2000), while a positive feedback loop could produce a switch behaviour (Becskei et al., 2001). Although topological models, with their comprehensive list of connected parts, can give important insights into the process they represent, predicting the behavior of a system just based on its topology is risky (Guet et al., 2002). A biological network is in fact a dynamical system and the values of the kinetic parameters of the reactions taking place in the network define what the outcome will be

(Ronen et al., 2002). Bridging the gap between an oversimplified model of a biological process, and a sufficiently detailed one to be useful is not trivial. Equations don't get along well with fuzziness, so having a clear mind about the way things go in the system, and by that, knowing what to include in the model and what type of downstream analysis to do on the results, is a great benefit if one wishes to write down equations that are to be meaningful. Despite the satisfaction that can derive from writing such equations, for a mathematical model of a biological system to be useful, more than formally correct equations are needed. A successful model should allow predicting the system's behaviour under conditions that were never tested before and that, therefore, were not used during the model building process. Ideally, in order to model a biological system one would like to make a replica of it *in silico*, what we could call the "molecular dynamics" of modeling. Thus spatial distribution, diffusion parameters, excluded volumes, concentrations and rates could be fed into a maximally detailed model to get an accurate reproduction of the biological process' dynamics. Unfortunately, even for the best-studied fields of research, for which daunting amounts of knowledge have accumulated and continue to do so, the variety of elementary processes such as posttranslational modification, degradation, or complex formation, as well as spatial information and timing of events in relation to the cell cycle are, at best, partially known and, even then, rarely in numbers. Nonetheless, insights can often be obtained in the absence of any precise quantitative knowledge of the system, using modelling tools unconcerned with precisely specified parameter values, but that are instead well suited to incorporate data of the type which is by far more readily available at present, *i.e.* qualitative.

Qualitative Modelling

Qualitative models are simplified models obtained by sacrificing details. In order for qualitative models to be useful in gaining an understanding of a biological system, a wiring diagram of the network – representing causality relationships between events linked to model components – or logical statements need to be given. As is still most often the case due to techniques routinely used in labs, the analysis of experimental data leads to knowledge of qualitative nature, which integrated with other data allows the formulation of statements translated more or less accurately by diagrams. While logical

inferences are manageable when the amount of information is small, the fields of model-checking and model validation within qualitative reasoning have proven invaluable to accomplish the same task on much larger amounts of accumulated knowledge, for instance by highlighting inconsistencies (Batt et al., 2005).

Closer to the goals of systems biology, a qualitative modelling approach may be more effective in gaining higher-level understanding of the organizational principles of a family of processes, through the theoretical study of generic systems. Such mathematical investigations lead to conclusions that are valid for the family of systems matching the description, stating for instance under which conditions certain behaviours such as oscillations can be expected. For modelling gene networks, as step functions are in fact a good approximation of gene activity, such qualitative models using Boolean formalism are particularly well suited. However, even a rough exploration of parameter space can become intractable as the size of the system increases, and therefore methods to accelerate the search and access to increasingly powerful computer resources are critical. For example, in the sister field of network identification, a task seeking to make out the set of reactions carried out during glycolysis (10 reactions and 15 metabolites) took several months on a 65 node Beowulf cluster to compute (King et al., 2005).

Qualitative models can be quite useful when aiming at a quick general description of the possible behaviour of a system, but has the risk of leading the user to false conclusions (see Results Part One).

Quantitative modelling

Compared with qualitative models, quantitative ones have a natural appeal in that they offer greater detail in mimicking reality. Moreover, rich qualitative insights on the system are possible using theoretical tools such as bifurcation and stability analysis (Fall et al., 2002), which, for example, indicate the precise boundaries of parameter ranges to which steady states or sustained oscillations correspond, or reveal the stability of the solutions before actually solving the dynamical equations representing the system. Quantitative models can be either deterministic or stochastic. The most popular is the deterministic formalism of ordinary differential equations (ODEs) which when extended to include spatial information is referred to as partial differential equations (PDEs). Each

equation in a set typically represents the rate of change of a species' continuous concentration as a sum or product of, more or less, empirical terms (typically law of mass action terms, Michaelis–Menten functions, power laws and so on), accounting for the effect of biological events on such concentrations. By definition, the initial state of the system in a deterministic model uniquely sets all future states. As analytical solutions seldom exist, numerical solutions need then to be computed (once for each set of parameter values and initial conditions explored). A word of caution: although this step is simple in principle, wrong solutions can arise. For instance, the chosen step-length for the integration of the ODEs can be sufficiently large to cause divergence of the numerical solution from the correct one (numerical instability), making a minimum of experience with related issues a strong asset for the user. In general, ODEs are best suited to capturing the behaviour of systems where species are abundant and reaction events frequent (as is often the case for metabolic pathways, for example), because species concentrations are then acceptably approximated as varying continuously and predictably.

Molecular interactions are intrinsically random and cellular behaviour itself sometimes seems to reflect this randomness (Liu *et al.*, 2004). Indeed, occurrences of noise have been found to be exploited by cells – for instance, to survive a variety of environmental changes (Thattai *et al.*, 2004) or to increase sensitivity in signal transduction processes (Hanggi, 2002). To model such stochastic systems, two main methods are used. The first is using stochastic differential equations (SDEs; derived from ODEs by adding noise terms to the equations), the solutions for which can be numerically obtained either by computing many trajectories (Monte Carlo methods) or approximating their probability distribution and then calculating statistical measures (such as mean and variance). Notably, with this method noise is imposed on the system and represented by mathematical terms chosen a priori, instead of arising from the underlying physical interactions. The second is a very successful and exact method introduced nearly 30 years ago (Gillespie, 1976; Gillespie, 1977), and recently enhanced to cope with different reaction timescales (Haseltine *et al.*, 2002; Rao *et al.*, 2003; Rathinam *et al.*, 2003) or space (Stundzia, 1996; Ander, 2004). With this approach, molecules are modelled individually and reaction events are calculated by the probability of meeting

and reacting. The price to pay for having a more physically realistic model is the considerable increase in computational time and the need for specialized algorithms (Alfonsi *et al.*, 2005; Salis *et al.*, 2005).

Space in modelling

Until recently, the majority of simulations ignored the fact that biological processes take place in heterogeneous and highly structured environments. Even prokaryotes are now known to possess a cytoskeleton and control the movement and location of molecules, so regulating cellular processes in both space and time (Gitai, 2005). Indeed, spatial segregation underlies many cellular strategies; reactions are prevented by physically separating molecules and molecular gradients within or between cells are used in pattern formation (Gorlich et al., 2003). Crucial as it may be for fundamental processes such as self-organization (Nedelec et al., 2003; Sawai et al., 2005), morphogenesis (Collier et al., 1996), cell division (Dens et al., 2005) or calcium waves (Wu et al., 2005), spatial information is still largely absent from interaction databases. Recent technological advances are addressing this dearth of spatial data, and theoretical advances are improving computational methods, making it now possible to simulate spatio-temporal models of biological processes in coarse-grained or realistic geometries (Lemerle et al., 2005).

Results Part One

As discussed in the Introduction, mathematical modelling and simulation of biological processes represent a powerful means to gain understanding on the mechanisms underlying these processes, often suggesting which experiments to do that would help corroborating or rejecting a working hypothesis. Although modelling could seem simple to an outsider, who might interpret the wealth and user-friendly appearance of simulation tools as an insurance of success, there are many conceptual pitfalls for the modeller that result in unrealistic predictions. The first step towards the generation of a good, informative model consists in understanding the limitations and advantages of the different available mathematical formalisms. In the following paragraphs, I give some examples of how modelling and simulations can lead to false predictions when the limitations of a given approach to represent reality are not taken into account.

Mathematical-formalism-independent errors

The precise order in which a series of reactions occurs can be consequential, yet is frequently disregarded. To show the impact that the choice of order of events can have on the predictions obtained by the corresponding model, I considered the case in which the formation of active dimers of a certain species is known to trigger downstream events, and, as an additional assumption, such a dimer is only active when both monomers are activated (for example, by phosphorylation). One can formulate a general model considering all possible dimerization and monomer activation/deactivation reactions derived from these hypotheses. Not knowing the order of events, three extreme possibilities can be formulated: two of total dependence (only activated monomers can dimerize or dimerization must occur before activation can) and one of total independence between activation and dimerization reactions. As Figure 2.1.1 shows, the different models lead to different steady-state concentrations of active dimer. If high concentrations (*e.g.* more than 200 molecules) but not low concentrations of this species can start a signalling cascade, only the system modelled as in the scheme corresponding to "activate and dimerize" will show a response.

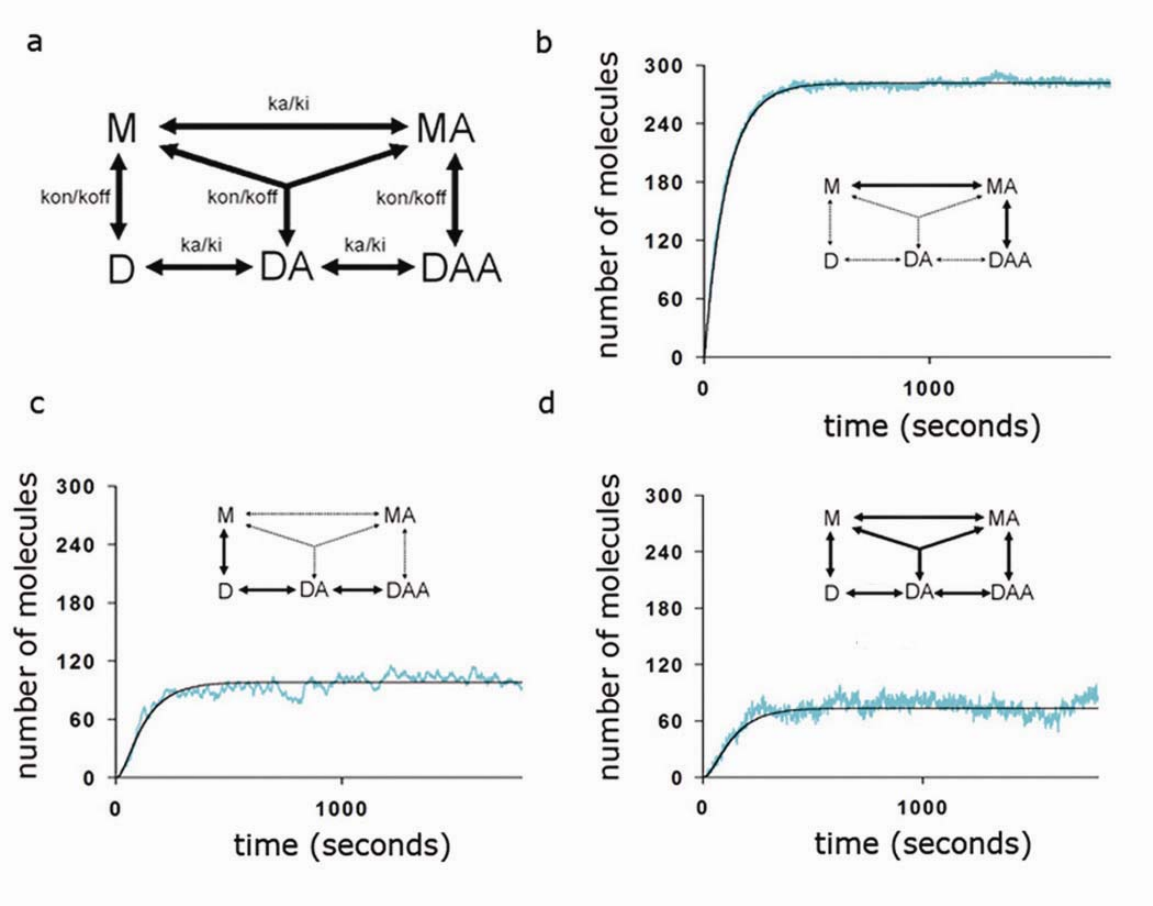

Figure 2.1.1 | **Example of mathematical-formalism-independent pitfalls in modelling.** If protein M is active as a post-translationally modified dimer DAA, the formation of DAA can be modelled differently, depending on assumptions made regarding the order of events and the nature of the active dimer. Here we assume that both monomers must be modified to form an active dimer. **a**, The scheme shows all reactions compatible with the experimental observations. M, monomer; MA, modified monomer; D, dimer; DA, dimer with one modified monomer; DAA, active dimer (both monomers modified). Each horizontal arrow corresponds to a reversible activation reaction and each vertical arrow corresponds to a reversible dimerization reaction. The two slanted arrows, together with the central vertical arrow, represent dimerization of a modified monomer with an unmodified one. **b**–**d**, Simulation runs for three different orders of events—respectively, 'activate then dimerize', 'dimerize then activate' and 'dimerize and activate together independently'—showing the deterministic (black) and stochastic (cyan) temporal evolution of DAA molecules. (see Materials and Methods for parameters used in the simulation and a mathematical derivation of the steady-state solution).

Mathematical-formalism-dependent errors

Choice of formalism

Problems can arise from the mathematical formalism used to simulate a system. To illustrate the impact of modelling choices, I simulated a simple gene network with negative feedback (protein B forms multimers and sequesters the activator protein AP responsible for its transcription) using three formalisms with different degrees of graininess (Figure 2.1.2): a simple boolean model, a quantitative deterministic model with ODEs, and a quantitative stochastic model (Ander, 2004). With the discrete-time boolean model, the built-in delay produces oscillations (Figure 2.1.2b). The other two models require additional events to be modelled explicitly (for example, degradation to balance production), and in contrast to what is observed with the coarser boolean model, oscillations do not occur unless multimerization is allowed (Figure 2.1.2c-f).

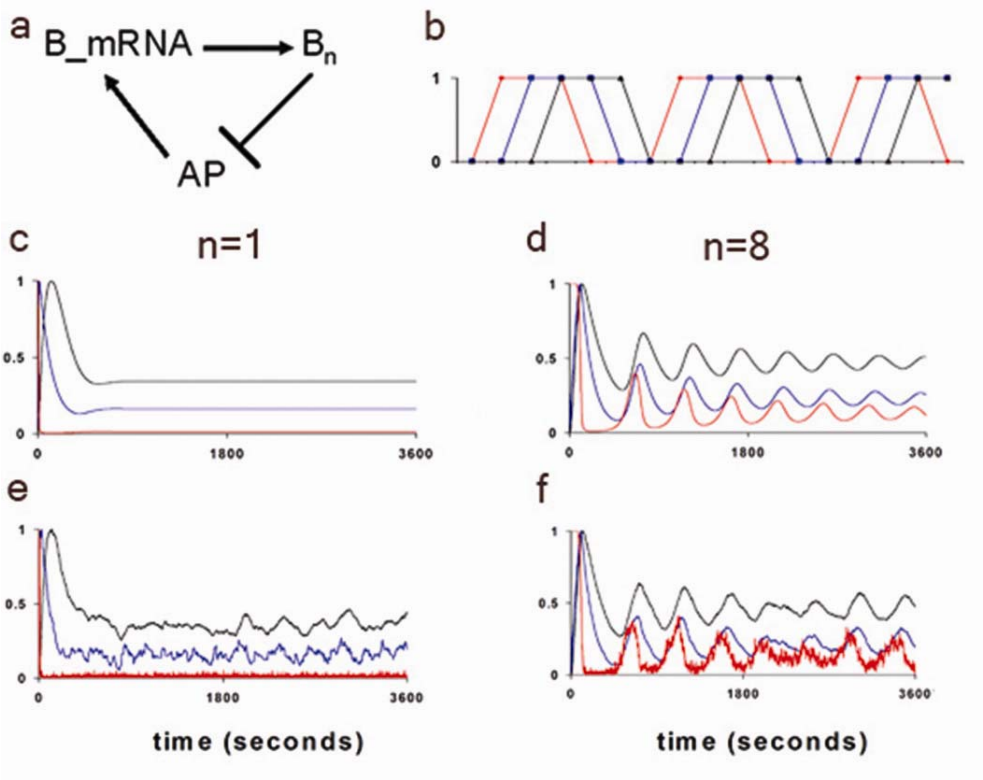

Figure 2.1.2 | Simulation of a simple network using different mathematical formalisms. **a**, Diagram of the negative feedback network used in the simulations. n, the number of B molecules in the active complex. **b**–**f**, Time courses of activator protein AP (red), *B* mRNA (blue) and B protein (black). The *y* axis represents the number of molecules, normalized for each species by the maximum value reached, except in **b**, in which it represents presence or absence of the molecules. Simulation of discrete time boolean model (**b**) with synchronous update. Deterministic (**c**, **d**) and stochastic (Ander, 2004) (**e**, **f**) simulations using specified parameters (see Materials and Methods), with B monomer (**c**, **e**) or octamer (**d**, **f**). Oscillations predicted by the boolean model are obtained in the deterministic/stochastic model only when B oligomerization is included.

Effect of localization of species on cellular processes

To illustrate the impact on predictions of accounting for constraints of cellular space, I modelled a simple network (Figure 2.1.3a), in which a phosphorylated transcription factor triggers the production, in one pole of the cell, of protein A that is involved in a positive feedback loop (resulting from mutual repression of species A and B). Starting from an initial state corresponding to a high concentration of B and no A, when the kinase and the phosphatase freely diffuse in the cell, the positive feedback acts

as a switch causing the disappearance of B and the accumulation of A (Figure 2.1.3d). When the kinase and the phosphatase are localized to opposite poles of the cell (Figure 2.1.3b), however, a gradient of the phosphorylated transcription factor is formed (Figure 2.1.3c), and the amount of A produced is insufficient to trigger the switch (Figure 2.1.3e).

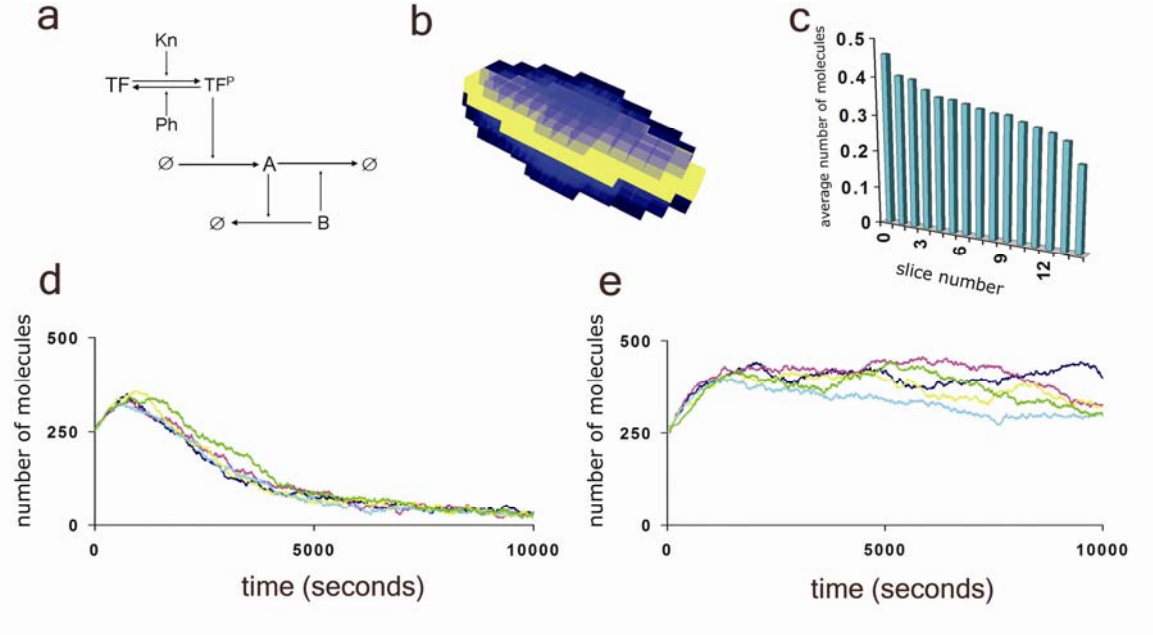

Figure 2.1.3 | Effect of localization of species on cellular processes. **a**, Diagram of a simple network in which a phosphorylated transcription factor TF^P triggers the synthesis of protein A that is involved in a positive feedback loop (resulting from mutual repression). Ø → indicates protein production, whereas → Ø indicates protein degradation. The behaviour will depend on the spatial constraints imposed on the kinase Kn and the phosphatase Ph. When they localize to opposite poles of the cell, switching behaviour does not take place. Production of protein A in both simulations (Ander, 2004) takes place in the pole of the cell where the phosphatase is localized. **b**, The model geometry (lattice unit is 1 μm). Yellow indicates the longitudinal cell slice along which the gradient is observed. **c**, Gradient of TF^P obtained with localization of species. **d**, **e**, Time course of protein B without (**d**) and with (**e**) localization of species (see Materials and Methods for parameters used in the simulation).

Continuous versus discrete concentrations

Because molecules are discrete species, continuous representations of molecular abundance are another source of artefacts. For example, contrary to what happens with discrete-value models, steady states take infinite time to be reached with continuous concentrations, a discrepancy that disappears by focusing instead on how fast the steady state is approached (that is, by introducing the concepts of half-life, rise-time and others; Figure 2.1.4a). Similarly, a probabilistic key is needed to interpret the non-integral values generated by the continuous-value deterministic models, as for discrete stochastic models. For low numbers, however, this interpretation is not error proof. If we consider a single, strictly autocatalytic species, B (Figure 2.1.4b), an ODE model would conclude (as would a related SDE model with a noise term that was only multiplicative) that there are two steady states: an unstable lower one (with zero molecules per cell) and a stable upper one. Simulation runs based on such models show that any non-zero initial state evolves asymptotically towards the upper steady state, whereas zero states are absorbing (that is, that once reached, they cannot be left). If important downstream events, such as cell differentiation or apoptosis, are triggered only by the absence of B molecules, a continuous model would lead us to wrongly conclude that these events never occur, whereas the more physically realistic, discrete stochastic model would reveal that, for each cell, it is only a matter of time before the triggering state is reached (Figure 2.1.4b).

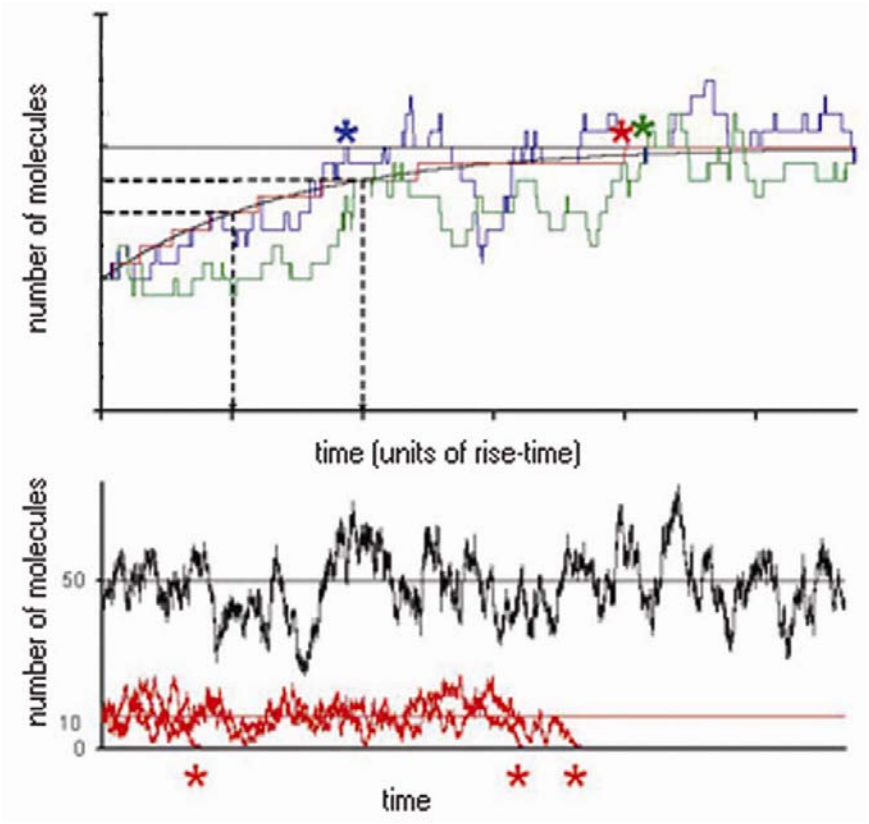

Figure 2.1.4 | Example of putative model-dependent pitfalls in modelling: continuous versus discrete concentrations. **a**, Simulation of a simple system in which a species is produced at a constant rate (16×10^{-3} molecules s^{-1}), and degraded with a first order decay rate of 1×10^{-3} s^{-1}, giving an asymptotic steady-state of 16 molecules per cell (plotted as a straight horizontal line). The initial state for all simulations is 8 molecules per cell. Two discrete stochastic runs are shown in blue and green. The corresponding ODE solution is shown in black, whereas the discrete approximation of it is shown in red (rounding each value of the continuous run to the closest integer). A star indicates, for each discrete run, when the steady-state value has been reached. Each broken line illustrates a geometric construction of the rise-time, as the time taken by the system to go, first from 8 to 4 molecules per cell away from steady state, then from 4 to 2. Each unit of rise-time is separated by tick-marks on the *x*-axis, which are identically spaced (as a property of exponential curves). The stochastic simulation shows that it is possible to reach steady-state values earlier or later than in the deterministic analysis. **b**, Superimposed stochastic (wavy lines) and deterministic (continuous straight lines) simulation runs of a system composed of a single autocatalytic species, with parameter values (see Materials and Methods) such that the upper steady-state solution is either high (black curves) or low (red curves) (respectively, 50 and 10 molecules per cell volume of 1 μm^3). A star indicates when a stochastic run has reached the zero absorbing state. In the lower case (red curves), the deterministic solution clearly differs from the average stochastic run, because all runs reach zero and stay there.

Results Part Two

Building the p53/Mdm2 synthetic oscillator in budding yeast (*Saccharomyces cerevisiae*)

Fundamental pre-requisites for the successful construction of the p53/Mdm2 synthetic oscillator in yeast are that:

a) p53 is stable when expressed alone and degraded only in the presence of Mdm2

b) Mdm2 triggers its own degradation and has a short half life

c) p53 can induce Mdm2 expression.

p53 has already been shown to bind in yeast to p53-responsive elements and start transcription of downstream genes (Oliner *et al.*, 1993), so we only need to ascertain that p53 is not being substantially degraded by some yeast enzyme in an Mdm2-independent fashion and that Mdm2 performs its E3 ubiquitin ligase activity in cooperation with the endogenous components of the ubiquitin pathway, finally leading to p53 proteasomal degradation.

Based on the results published by Lahav *et al.* (Lahav et al., 2004), we decided upon using the fusion proteins p53-ECFP and Mdm2-EYFP, since this allows monitoring single cells – with techniques such as time-lapse fluorescence microscopy or FACS.

p53-ECFP is stable when expressed alone in yeast

In order to determine whether p53-ECFP is degraded in yeast cells, I performed a pulse-chase-like experiment, in which p53-ECFP expression is triggered with the addition of galactose in the culture medium and either it is stopped adding glucose in the same medium or all protein synthesis is halted by adding cycloheximide. In the first case, we are blocking gene expression, while in the second we are blocking translation of any mRNA into protein. If p53 or Mdm2 mRNA is very stable, in fact, adding glucose to the medium could still result in accumulation of the protein over time. On the other hand, cycloheximide prevents translation of any mRNA in the cell (Emmerich *et al.*, 1975) (which makes it toxic in the long run), so it is not suited to study the degradation of p53 in the presence of Mdm2, since it would prevent formation of Mdm2 as well. In this case, in fact, Mdm2 must be kept at constant levels, while p53 must be given a pulse.

I therefore used cycloheximide only to check the stability of p53-ECFP and Mdm2-EYFP when they are expressed separately, but used glucose when p53-ECFP and Mdm2-EYFP are co-expressed, being respectively under the inducible GAL or constitutive TEF promoter.

The pool of molecules produced during the induction stage is then monitored over time, collecting samples at fixed intervals. If the protein is not degraded and repression is effective, we expect its levels to remain constant when equal volumes of sample are loaded on the gel. Figure 2.2.1 shows that p53-ECFP is stable under these conditions. I repeated the same experiment several times, monitoring the fusion protein levels for up to six hours and no degradation was observed (data not shown)[1].

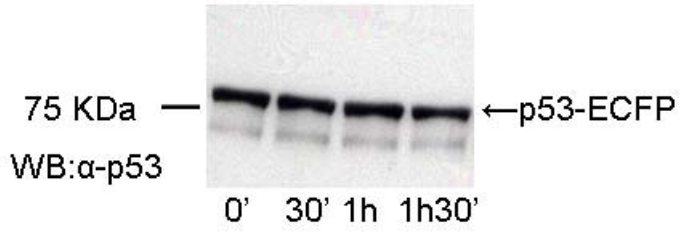

Figure 2.2.1 | p53-ECFP is stable in budding yeast. Human p53 wild type gene was fused to ECFP and cloned into a yeast plasmid under the inducible GAL promoter. Cells harbouring the p53-ECFP fusion protein were grown at 30°C and when they reached logarithmic growth phase, protein expression was induced by adding 2% final concentration (f.c.) of galactose to the medium. Induction lasted one hour; subsequently cycloheximide was added to 100 μg/ml f.c. Samples were collected every half an hour starting from the moment in which protein synthesis is stopped (time 0'), for a total period of one and a half hours. No significant degradation of the p53-ECFP fusion protein was observed in this experiment as well as in several other experiments where the protein levels were monitored for longer time.

p53-ECFP does not interfere with yeast gene expression under normal growth conditions

In order to proceed with the construction of the synthetic oscillator, we wanted to determine whether the p53-ECFP transcriptional activity would interfere with the normal

[1] For all results presented in the thesis, I performed at least two independent experiments under the same conditions. Each figure shows only one representative experiment.

gene expression in yeast cells. Bioinformatics predictions conducted for us by BioBase suggested that the yeast genome possesses many putative p53-responsive promoters. To eliminate the possibility that p53 could interfere with the normal expression profile of yeast cells and to get more confident that our synthetic circuit would not cross-talk with endogenous signalling pathways, the EMBL Gene Core Facility performed microarray analysis on total RNA extracted from exponentially growing yeast cells (ESM356-1), comparing the gene expression profiles of yeast cells containing an empty plasmid and cells containing the plasmid carrying the p53-ECFP fusion gene. Since there was no significant change in the expression profiles between control and p53-ECFP containing cells, we can rule out a significant effect of p53 on yeast transcription, which is a prerequisite for our circuit (Figure 2.2.2).

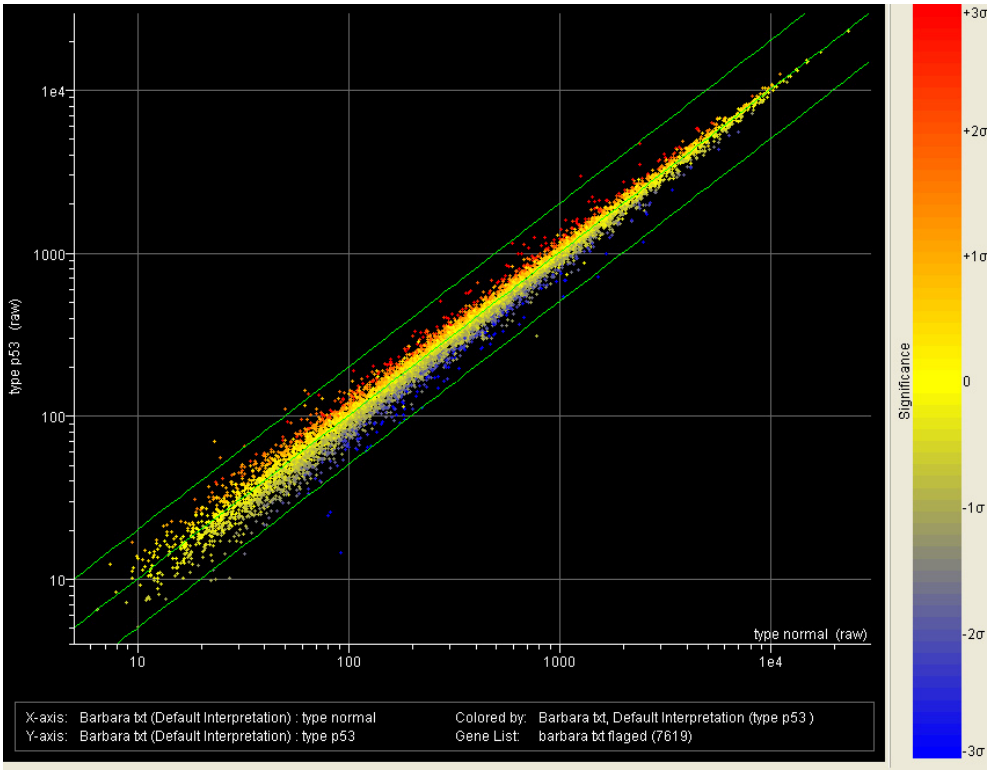

Figure 2.2.2 | Correlation between expression profiles of control (X axis) and p53-ECFP harbouring cells (Y axis). Cells carrying an empty plasmid and cells carrying the plasmid containing the p53-ECFP fusion protein were grown at 30°C and induced with GAL once they reached the exponential growth phase. Induction was carried on for two and a half hours, then cells were lysed and total RNA extracted and prepared for chip hybridization (see Materials and Methods). Comparing the expression profiles of control

and p53-ECFP containing cells, only few genes lied outside the significance threshold and they had no apparent relation to p53. Globally, the p53-ECFP transcription factor does not interfere with the normal gene expression in budding yeast.

p53-ECFP is diffused throughout the yeast cell nucleus and can be found at the septin ring

In order to determine the localization of the p53-ECFP fusion protein in budding yeast, I used fluorescence microscopy to image living cells. Figure 2.2.3 shows that the p53-ECFP fusion protein mainly concentrates in what seems to be the cell nucleus, but can also be detected in the cytoplasm, sometimes along a line. Since most Höechst 33352 fluorescence displays in the ECFP channel, staining the cell nucleus with this dye in the presence of a CFP-tagged protein yields ambiguous results if the protein of interest does localize in the nucleus. Nevertheless we could speculate that the p53-ECFP fusion protein resides in the nucleus by looking, for instance, at budding cells where the nucleus is easily detected at the interface between mother and daughter cells (see red arrow in Figure 2.2.3).

In human cells, p53 is found in the cytoplasm and in the nucleus (in a cell cycle dependent fashion) (Liang *et al.*, 2001), so the distribution of p53-ECFP in yeast cells seems to recapitulate what happens in human cells.

Interestingly, the protein is also found at the septin ring (Figure 2.2.4) and this localization is likely not an artefact, considering that for instance Mdm2 is never found there (see below) and that usually exogenous proteins expressed in yeast are either cytoplasmic or nuclear (Prof. Ed Hurt, personal communication).

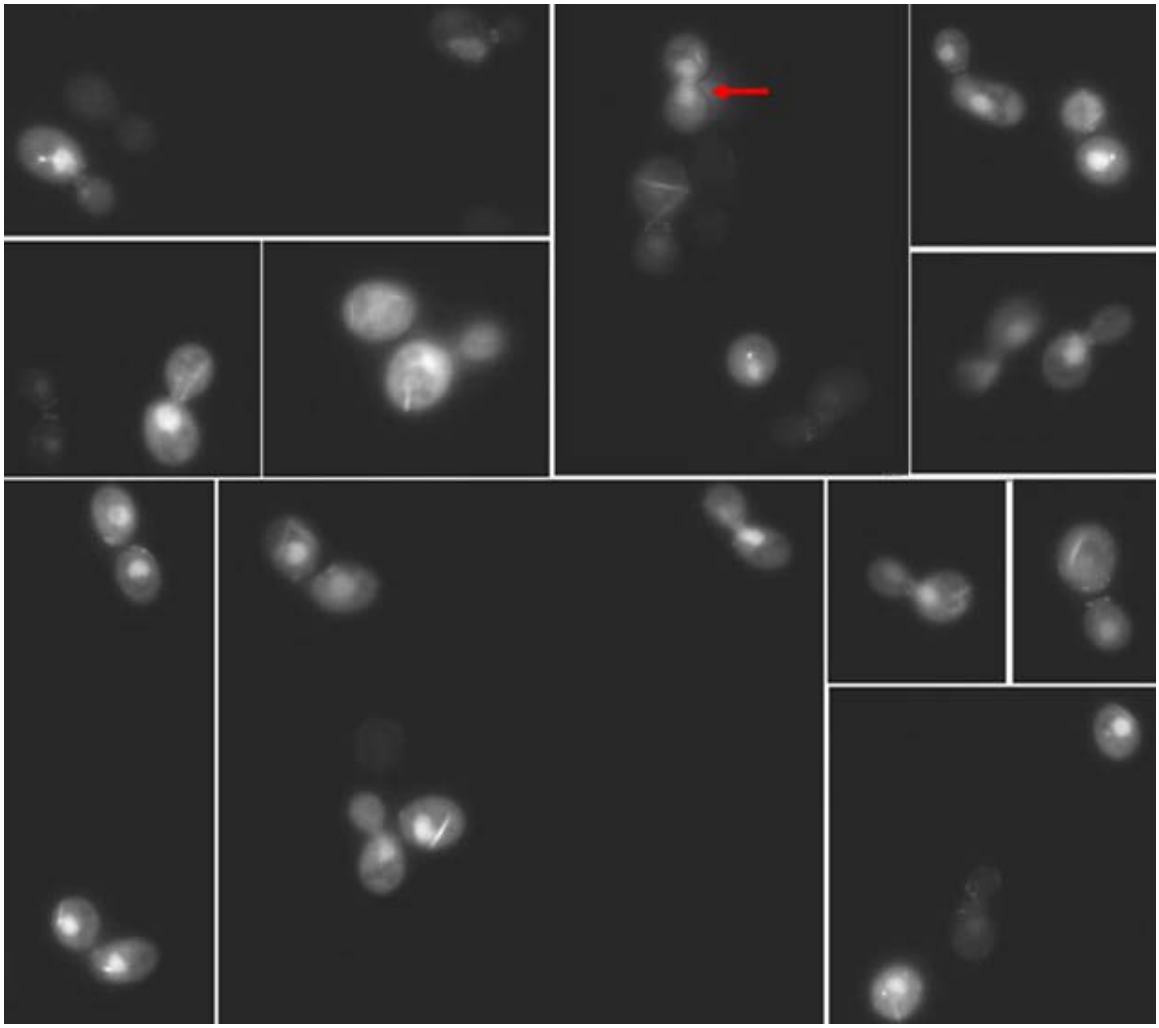

Figure 2.2.3 | Localization of p53-ECFP in yeast cells. Cells were grown at 30°C and gene expression was triggered by the addition of 2% f.c. galactose in the exponentially growing culture. After 1 hour of induction, the cells were imaged using excitation and emission filters for CFP (see Materials and Methods). p53-ECFP can be detected in both the cytoplasm and the nucleus of yeast cells, with higher nuclear concentration levels as compared to the cytoplasmic ones.

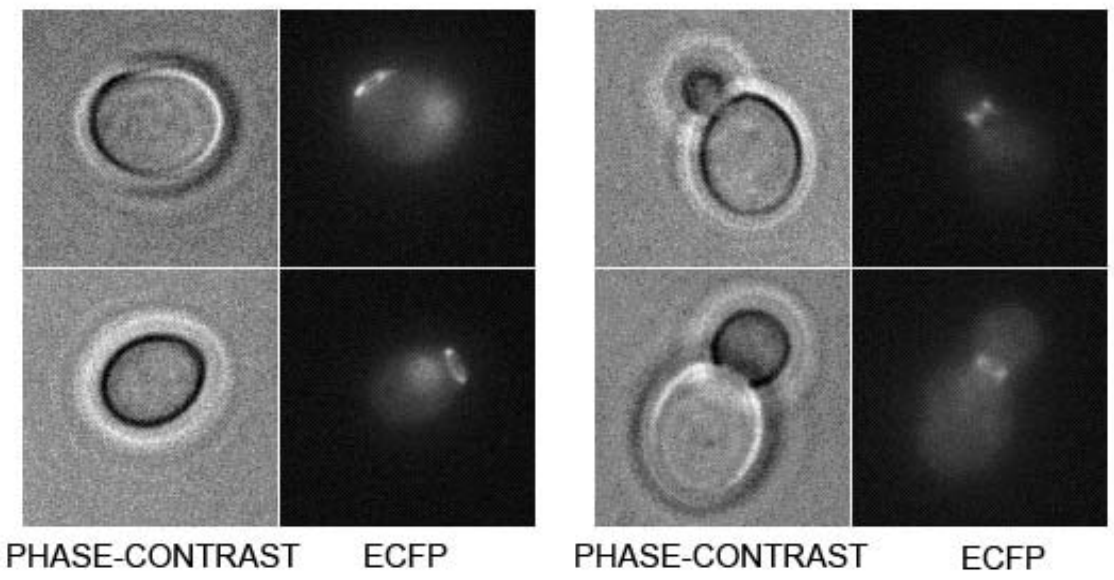

Figure 2.2.4 | p53-ECFP localizes to the septin ring. Cells were grown at 30°C and gene expression was triggered by the addition of 2% f.c. galactose in the exponentially growing culture. After 1 hour of induction, the cells were imaged using excitation and emission filters for CFP (see Materials and Methods). p53-ECFP localizes to the septin ring of yeast cells, suggesting an interaction of p53 with endogenous proteins localized there (see Discussion).

Once ascertained that the yeast copes well with the presence of the exogenous p53-ECFP fusion protein, that p53-ECFP exhibits a normal distribution in the cell and it does not get degraded when expressed alone, I went on testing whether Mdm2 was able to ubiquitylate itself, getting degraded by the proteosome.

Mdm2-EYFP is degraded in yeast

To look at Mdm2-EYFP fusion protein stability in yeast cells I used the same type of experiment performed with p53-ECFP. While in human cells the half life of Mdm2 is very short, ranging from 5 to 20 minutes, in yeast Mdm2 has a half life of about one hour (Figure 2.2.5). Considering that the average half life of a yeast protein is about 40 minutes (Belle et al., 2006), we can conclude that Mdm2 is not as rapidly degraded in yeast as in human cells.

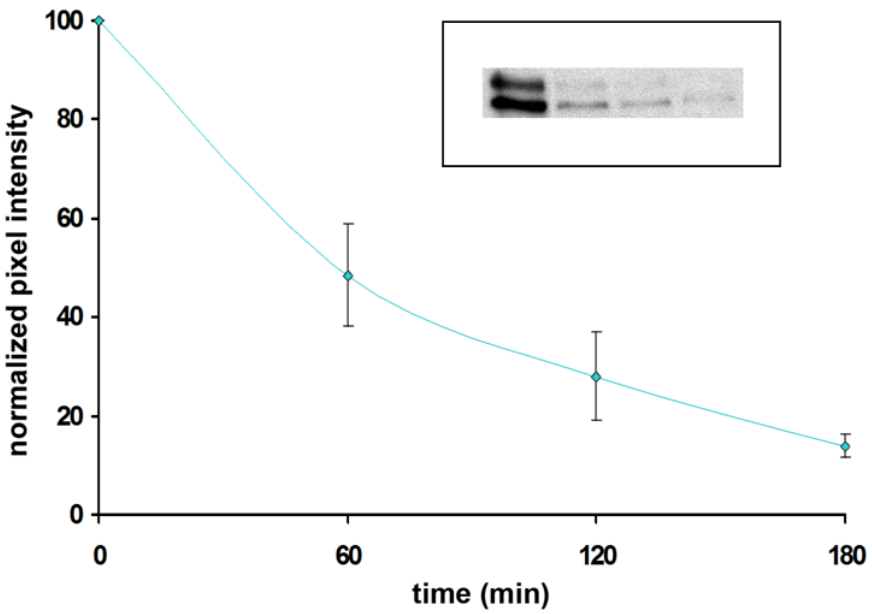

Figure 2.2.5 | Mdm2-EYFP is degraded in yeast. Cells were grown at 30°C and induced with 2% f.c. galactose once they reached exponential growth phase. To stop protein synthesis cycloheximide was added to 100 µg/ml f.c. Protein level was calculated using Adobe Photoshop as explained in Materials and Methods. Three independent experiments were used to calculate the average protein level for each time point. Inset: representative western blot to show the degradation of Mdm2-EYFP. Time course is as in the graph. Mdm2-EYFP reaches 50% of its initial level about one hour after protein synthesis is inhibited.

Mechanisms underlying Mdm2-EYFP degradation

From the previous experiment it is possible to conclude that Mdm2-EYFP fusion protein has a half-life of about one hour, but it is not possible to attribute this degradation solely to the autoubiquitylation activity of Mdm2. In fact, there could be four explanations:

a) degradation is due only to Mdm2 autoubiquitylation

b) degradation is only due to the action of some endogenous enzyme(s)

c) degradation is due to both autoubiquitylation and ubiquitylation by some yeast enzyme(s)

d) degradation is not ubiquitin dependent (it is vacuolar).

In order to shed some light on the mechanisms underlying Mdm2 degradation, I generated a mutant Mdm2, Mdm2H452A, which was shown not to ubiquitylate itself nor p53 in human cells, due to a mutation in its RING domain (Honda *et al.*, 2000). If Mdm2H452A-EYFP is stable, we can conclude that Mdm2 degradation is due only to autoubiquitylation. Unfortunately, since the mutant protein appears to be degraded to the same extent – or more (Figure 2.2.6 and 2.2.7) – than wild type Mdm2 (Figure 2.2.6), we can only eliminate possibility a, but we cannot distinguish between cases b, c and d. This result, however, mirrors what happens in human cells, where Mdm2 lacking its RING domain, or harbouring a point mutation in the active site, is still capable of being degraded, suggesting the presence of other mechanisms for keeping Mdm2 half life short (Brooks *et al.*, 2004).

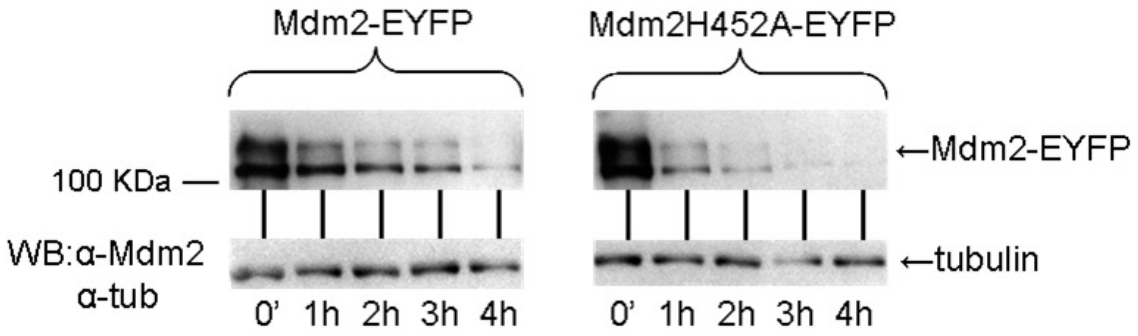

Figure 2.2.6 | Mdm2 carrying a mutation in its RING domain is degraded in yeast. Cells were grown at 30°C and induced with 2% f.c. galactose once they reached exponential growth phase. To stop protein synthesis cycloheximide was added to 100 µg/ml f.c. Samples were collected every hour starting from the moment in which protein synthesis is inhibited. Mdm2H452A-EYFP fusion protein, carrying a point mutation in the RING domain which inhibits the E3 ubiquitin ligase function, is degraded in yeast like the wild type protein, indicating that autoubiquitylation is not – if at all – the cause of Mdm2 degradation.

Mdm2-EYFP degradation is proteasome-dependent

To see whether Mdm2-EYFP degradation is mediated by ubiquitin, I used a yeast strain (pre1-1 pre2-2) for which proteasomal degradation is impaired (Heinemeyer et al., 1993). When the protein is expressed in this mutant strain, we expect to see a slowing-down in its degradation, provided it is proteasome-dependent. This is what we observe for both wild type and mutant Mdm2 (Figure 2.2.7).

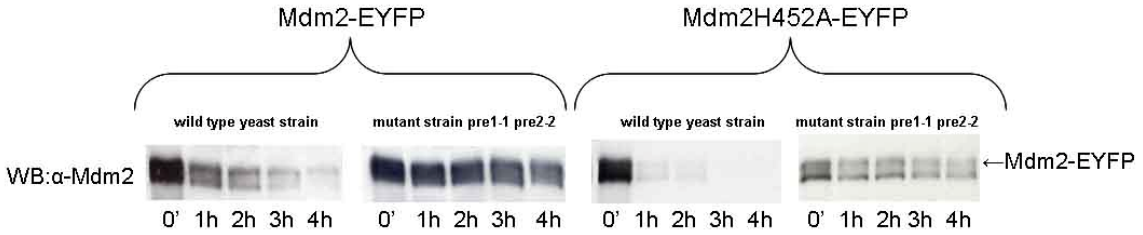

Figure 2.2.7 | Mdm2-EYFP degradation is proteasome-dependent. Plasmids containing Mdm2-EYFP and Mdm2H452A-EYFP genes under the GAL promoter were transformed (separately) in a wild type yeast strain and a mutant strain (pre1-1 pre2-2) impaired in proteasomal degradation. Induction was done with 0.5% f.c. galactose for 1 hour. Expression from the GAL promoter was blocked adding 3% f.c. glucose to the same medium. Time 0' corresponds to the moment in which protein synthesis is blocked. Samples are collected every hour, for a total of four hours. Degradation of both wild type and mutant Mdm2 proteins is slowed-down in the mutant strain, indicating that their degradation is proteasome-dependent.

From these experiments we can conclude that Mdm2-EYFP degradation is proteosomal and to a large extent independent of any autoubiquitylation activity.

Mdm2-EYFP localizes to the yeast nucleus and to one or several nuclear speckles

Mdm2-EYFP localization was determined by fluorescence microscopy (Figure 2.2.8) and indirect immunofluorescence (Figure 2.2.9). Both techniques reveal a nuclear localization, although only with fluorescence microscopy it is possible to detect one or more nuclear speckles in which Mdm2-EYFP accumulates.

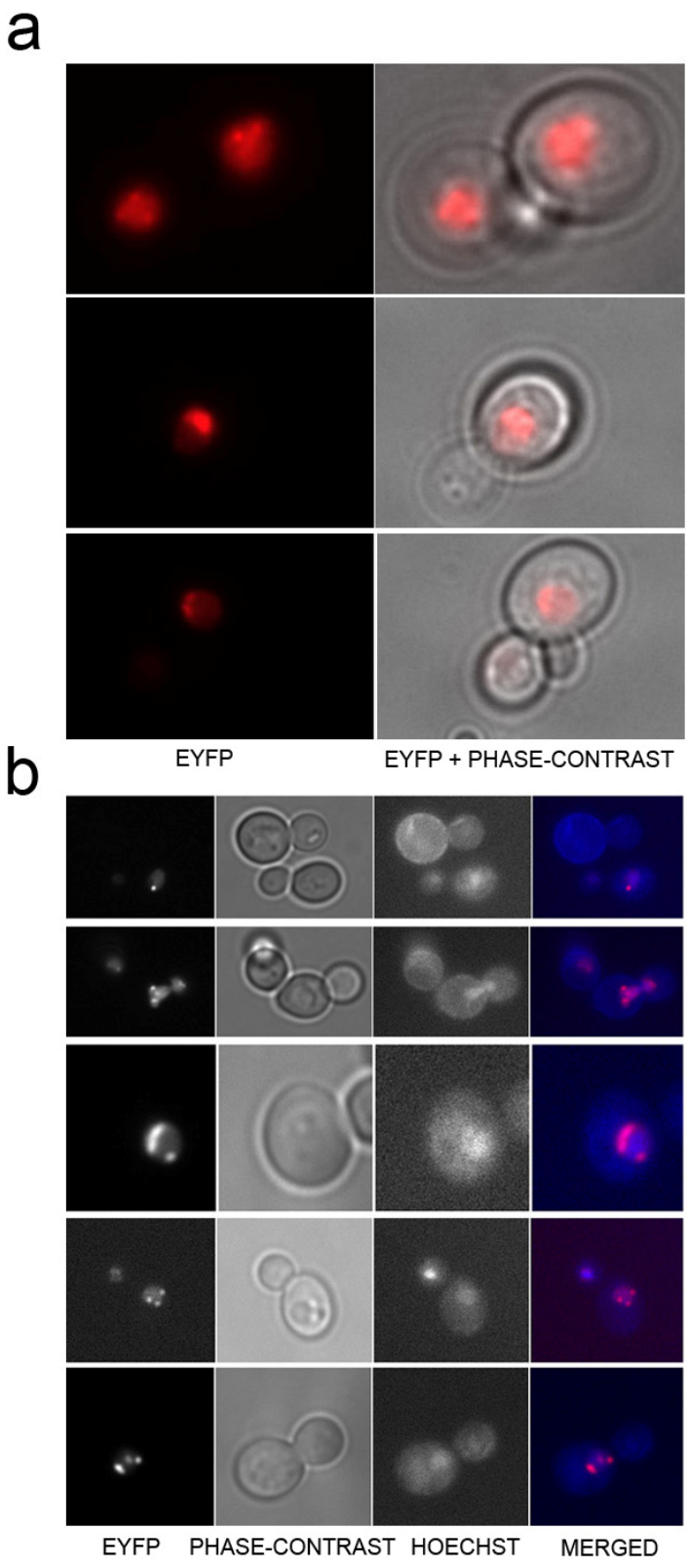
a
EYFP
EYFP + PHASE-CONTRAST
b
EYFP
PHASE-CONTRAST
HOECHST
MERGED

Figure 2.2.8 | Mdm2-EYFP fusion protein localizes to the yeast nucleus and to one or several nuclear speckles. In the merged image, the Höechst signal is shown in blue and the Mdm2 is shown in red. **a**, Cells were grown at 30°C and gene expression was triggered by the addition of 2% f.c. galactose in the exponentially growing culture. After 1 hour of induction, the cells were imaged using excitation and emission filters for YFP (see Materials and Methods). Mdm2-EYFP shows no localization in the cytoplasm as compared to p53-ECFP. **b**, Höechst 33352 was added to the medium to stain the DNA. These cells also contain the p53-ECFP plasmid, but were imaged before p53 gene expression was triggered with galactose.

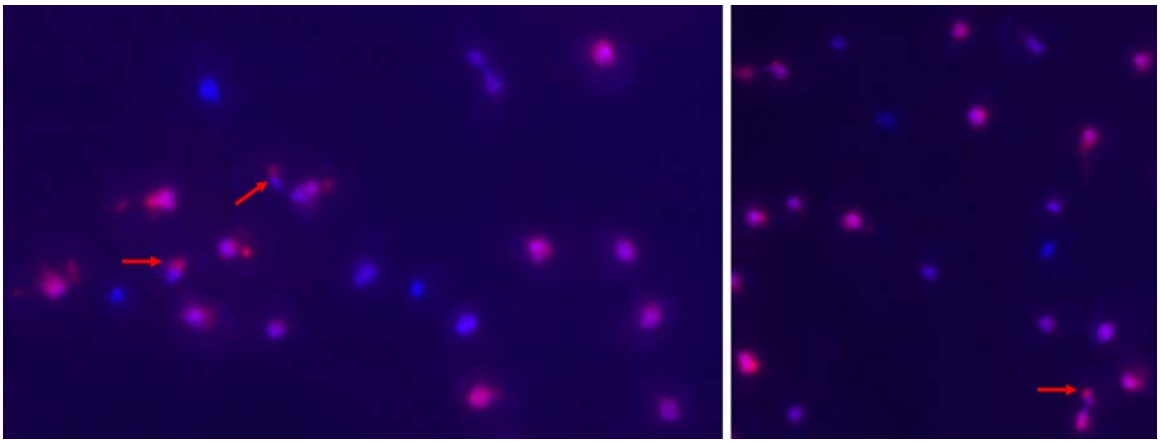

Figure 2.2.9 | Indirect immunofluorescence of yeast cells expressing Mdm2-EYFP fusion protein. Cells were grown at 30°C and gene expression was triggered by the addition of 2% f.c. galactose in the exponentially growing culture. Immunofluorescence was performed as described in Materials and Methods. DNA was stained with Höechst 33352 (shown in blue). Mdm2-EYFP was stained using the monoclonal SMP14 antibody (shown in red). Mdm2-EYFP localizes to the nucleus of yeast cells, sometimes accumulating in a round area at the tip of the Höechst signal (see red arrows and Figure 2.2.8b).

Comparing figures 2.2.8 and 2.2.9, it is evident that while with fluorescence microscopy the discrete dots in which Mdm2-EYFP localizes are visible, with indirect immunofluorescence Mdm2-EYFP appears mostly evenly distributed in the cell nucleus or at maximum concentrated in a single spot at the extremity of the DNA signal. One explanation for this difference is that the antibody used to detect the protein in the immunofluorescence cannot access the structures in which the protein is found, or that it cannot access the epitope it recognizes when the protein is localized in these structures. The antibody, then, binds only to the nuclear fraction of the protein pool, resulting mainly in a homogenous nuclear staining. In fact, only perfect fixation would immobilize the antigens, while retaining authentic cellular and subcellular architecture and permitting unhindered access of antibodies to all cells and subcellular compartments. Cross-linking reagents (such as formaldehyde) in general preserve well cell structure, but may reduce the antigenicity of some cell components.

Mdm2-EYFP localization is very dynamic

In order to follow the localization of the protein through time, I also performed time-lapse microscopy. Mdm2-EYFP non-homogeneous nuclear distribution, characterized by several dots often at the nuclear periphery, is very dynamic, with dots appearing and disappearing, fusing and sometimes separating again into single dots (Figure 2.2.10).

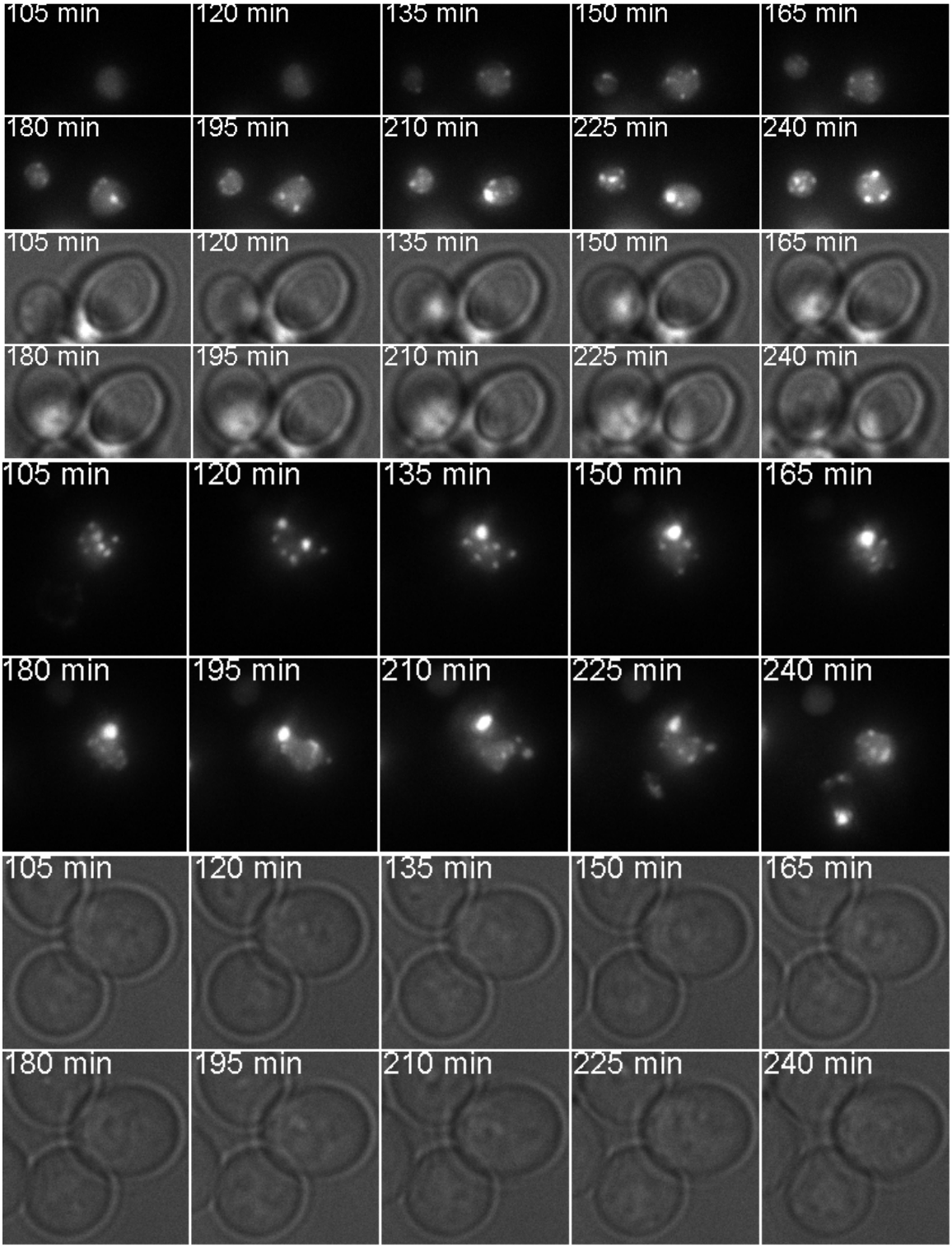

Figure 2.2.10 | Mdm2-EYFP localization is very dynamic. Cells harbouring the Mdm2-EYFP plasmid were grown at 30°C until they reached exponential growth phase. Cells were then adhered to the bottom of a Petri dish for live imaging (see Materials and

Methods). Galactose was added directly into the Petri dish and time-lapse started at this point. Movies are shown from the moment in which the fluorescent signal starts rising. In most cells, Mdm2-EYFP first appears distributed into discrete loci, which tend to fuse into a single very bright dot. Sometimes several dots appear in other regions of the nucleus as compared to the bright bigger dot.

In human cells, Mdm2 is mainly nuclear, (although it can shuttle between the nucleus and the cytoplasm), so the presence of Mdm2-EYFP in the yeast nucleus is not surprising. The dotty localization of the protein is instead very intriguing and does not have an immediate correspondent in human cells (see Discussion).

The first two requirements for the successful construction of the synthetic oscillator are satisfied – p53-ECFP being stable in the absence of Mdm2-EYFP and Mdm2-EYFP being degraded when on its own. Also, the fusion proteins do not show abnormal distributions inside the yeast cells, which would have prevented the use of this model organism to host our synthetic circuit. Next, I needed to determine whether the Mdm2-EYFP fusion protein is able to ubiquitylate p53-ECFP, targeting it for proteasomal degradation.

p53-ECFP is not degraded in the presence of Mdm2-EYFP

To analyse Mdm2-dependent p53 degradation, I transformed yeast cells with two plasmids, one harbouring the Mdm2-EYFP fusion gene under the constitutive TEF promoter, and another carrying the p53-ECFP fusion protein under the inducible GAL promoter. In this way, the cells have a constant level of the E3 ubiquitin ligase Mdm2 while p53 expression is given a pulse and then stopped. As previously mentioned, in this case gene expression from the GAL promoter is blocked by adding glucose to the medium. Notably, using the concentrations of galactose and glucose indicated in the literature (2% for both), the promoter was not completely shut off and protein degradation (in the case of Mdm2) was masked (data not shown). I found that inducing with 0.5% galactose and repressing with 3% glucose yielded the desired outcome.

Samples are collected as previously explained. To our great disappointment, the presence of Mdm2 does not affect p53 stability, leading us to conclude that Mdm2-EYFP is for some reason not able to ubiquitylate p53-ECFP under these conditions (Figure 2.2.11).

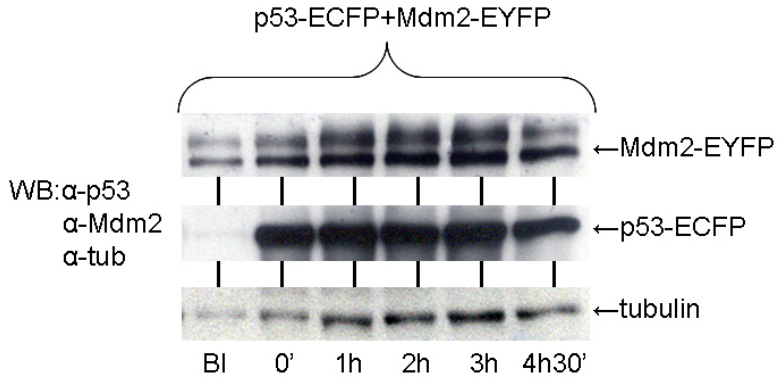

Figure 2.2.11 | p53-ECFP is stable in the presence of Mdm2-EYFP. Cells containing both p53-ECFP and Mdm2-EYFP – respectively under the GAL and TEF promoters – were grown at 30°C until exponential growth phase. Gene expression from the GAL promoter was triggered by adding 0.5% f.c. galactose to the medium and was inhibited by adding 3% f.c. glucose to the same medium. An equal volume of sample (1 ml) was collected at every time point and an equal volume of treated sample was loaded in each lane of the gel. BI stands for Before Induction. p53-ECFP is not degraded in the presence of Mdm2-EYFP.

p53-ECFP and Mdm2-EYFP interact and co-localize to a dot inside the yeast nucleus

Western blot analysis of cells expressing p53-ECFP and Mdm2-EYFP reveals that p53-ECFP is not degraded in the presence of Mdm2. This could be due to the fact that the proteins do not interact in the yeast cells. Fluorescence microscopy of living cells, expressing both p53-ECFP and Mdm2-EYFP, demonstrates that the proteins always co-localize to a dot, strongly suggesting that they do interact – directly or indirectly (Figure 2.2.12).

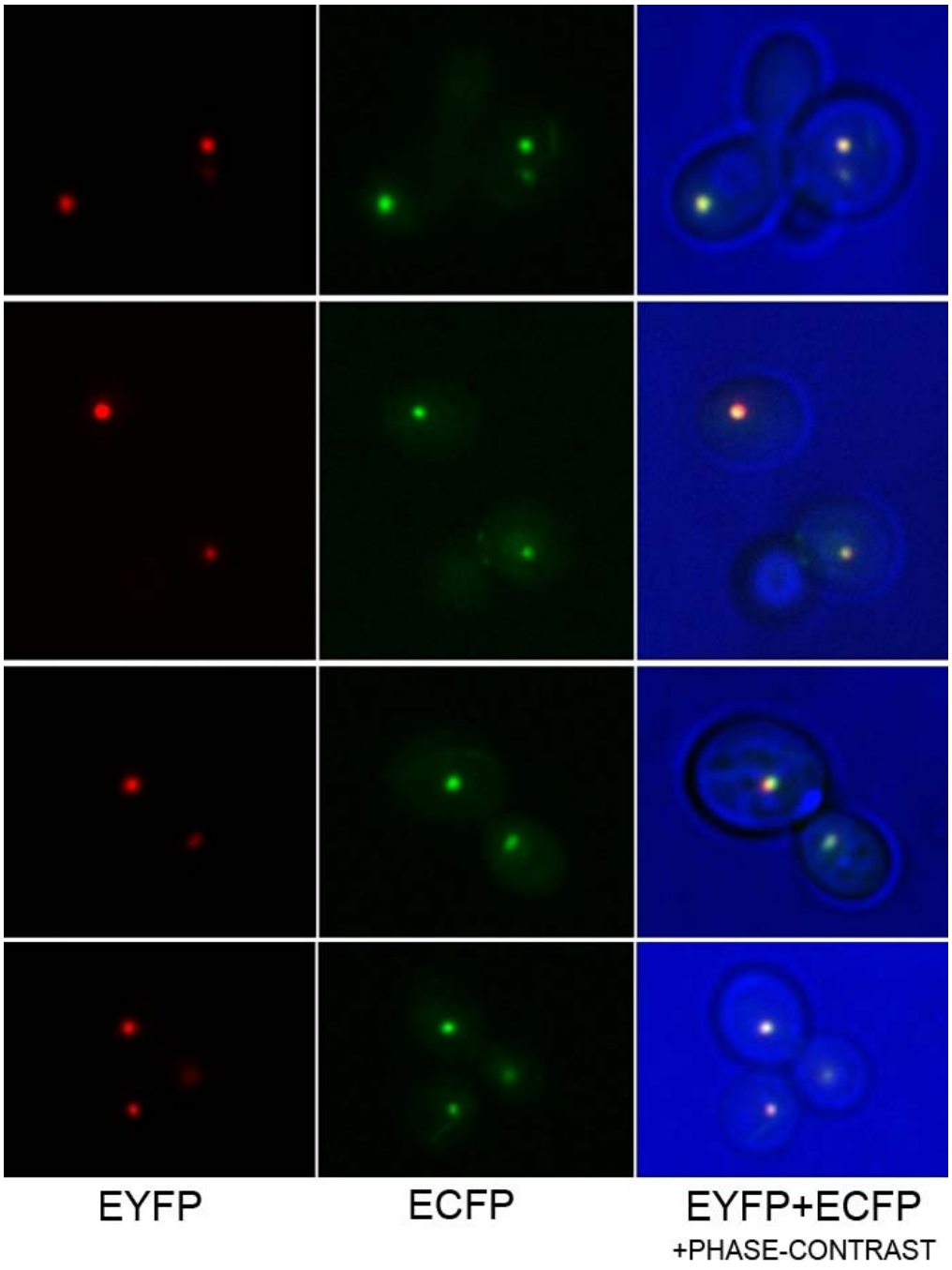

Figure 2.2.12 | p53-ECFP and Mmd2-EYFP co-localize to a dot in yeast cells. Cells were grown at 30°C and gene expression was triggered by the addition of 2% f.c. galactose in the exponentially growing culture. After 1 hour of induction, the cells were imaged using excitation and emission filters for CFP and YFP (see Materials and Methods). Mdm2-EYFP is shown in red and p53-ECFP in green. Co-localization results in yellow colour for the dot. Whenever the two proteins are expressed in the same cell, they co-localize.

To understand whether the dot formed by p53-ECFP and Mdm2-EYFP lied inside or outside the nucleus, I performed indirect immunofluorescence and used Höechst 33352 as a dye to stain the DNA, while detecting the fusion proteins with antibodies against p53 and Mdm2.

Although in some cells the dot overlaps with the Höechst signal, in most cells the dot appears to be in contact with the nucleus, but in a Höechst-minus region (Figure 2.2.13). Considering that a similar pattern is observed when using the Nop1 antibody to detect the nucleolus (with the Nop1 signal being in a Höechst-minus region despite the location of the nucleolus inside the nucleus, Figure 2.2.36), we should not interpret the absence of overlap as a clear indication that the dot is cytoplasmic.

Nonetheless, these results do not allow us to conclude that the dot resides inside the nucleus either. To clarify the localization of the dot in respect to the nucleus, we performed electron microscopy (see below) which showed unambiguously that the dot is indeed inside the nucleus.

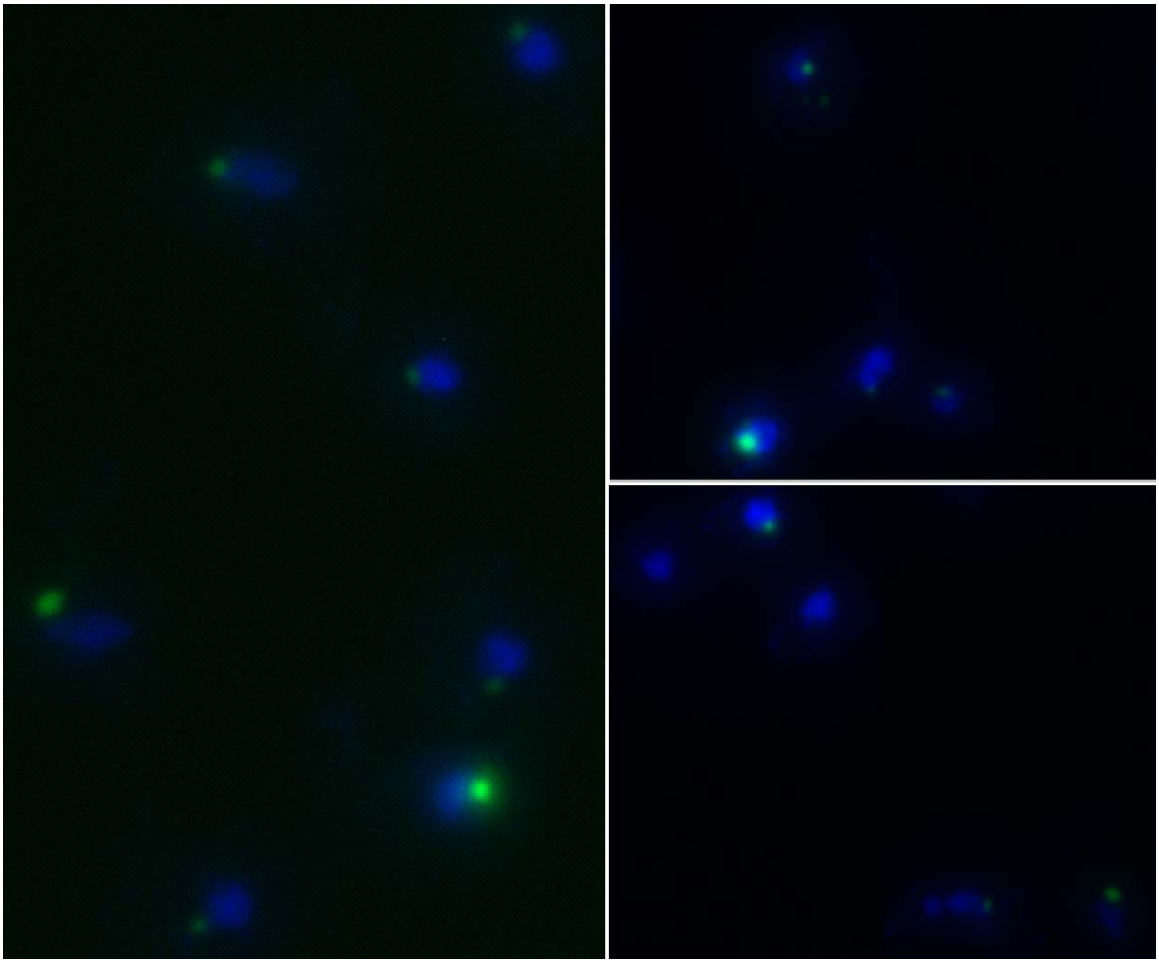

Figure 2.2.13 | p53-ECFP and Mdm2-EYFP co-localization in respect to the yeast nucleus. Indirect immunofluorescence was performed as described in Materials and Methods using the mouse monoclonal PAb 1801 anti-p53 antibody and the mouse monoclonal SMP14 anti-Mdm2 antibody. The DNA is shown in blue, while the p53-ECFP/Mdm2-EYFP complex in green. In most cells, the dot is detected at the edge of the nucleus, in a Höechst-minus region.

When a mutant p53 (p53W23S-ECFP) which does not bind Mdm2 due to a point mutation in the Mdm2 binding domain (Inoue et al., 2001) is co-expressed with Mdm2-EYFP in yeast cells, the dot is lost, suggesting that the binding of p53 to Mdm2 is required in order for the two proteins to co-localize (Figure 2.2.14). This result completely eliminates the possibility that p53-ECFP stability in the presence of Mdm2-EYFP is due to the inability of the proteins to interact with each other.

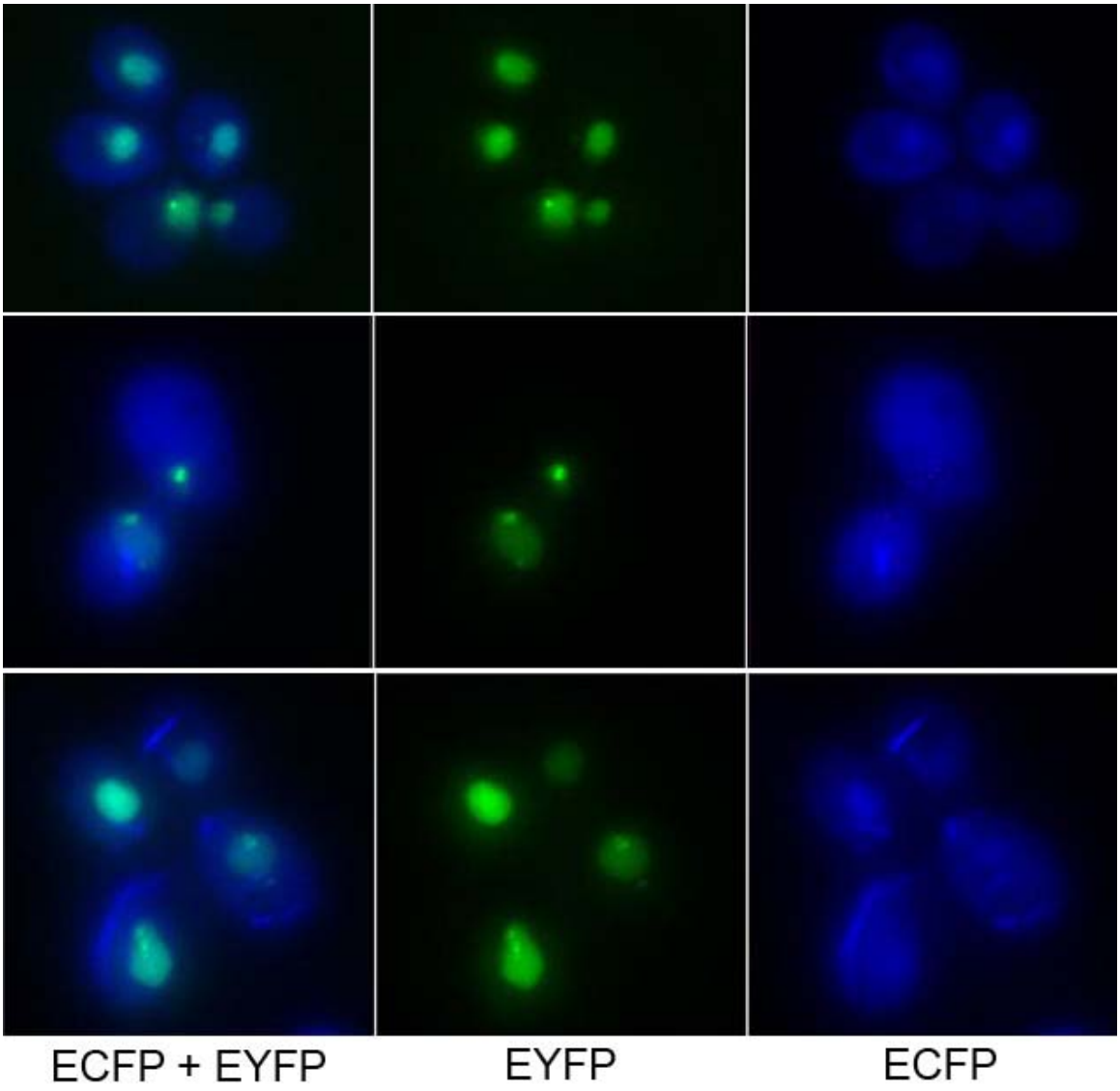

Figure 2.2.14 | Binding of p53 to Mdm2 is required for their co-localization. Cells were grown at 30°C and gene expression was triggered by the addition of 2% f.c. galactose in the exponentially growing culture. After 1 hour of induction, the cells were imaged using excitation and emission filters for CFP and YFP (see Materials and Methods). Cells express Mdm2-EYFP and a mutant p53 which does not bind to Mdm2 (p53W23S-ECFP). p53-ECFP is shown in blue, Mdm2-EYFP in green. In this case, the fluorescent signals in the CFP and YFP channels resemble those obtained with p53-ECFP alone and Mdm2-EYFP alone respectively.

At this point it seemed that we could not build the synthetic p53-Mdm2 oscillator relying only on these two proteins. We therefore revised our design several times, adding to the circuit different components that we thought could allow p53 degradation to happen.

On the road to degradation, first attempt: adding the human ubiquitin chain elongation factor p300 to the network

While this study was being done, a new type of enzyme in the ubiquitylation pathway was described: the E4, also called "chain elongation factor" due to its ability to ligate ubiquitin molecules to a nascent chain of ubiquitins on a substrate protein (see Introduction). Grossman *et al*. showed that the acetyltransferase p300 – previously known to acetylate and activate p53 after DNA damage – has also intrinsic E3 ligase activity and that together with Mdm2 it works as an E4 and targets p53 for proteasomal degradation catalysing p53 polyubiquitylation as opposed to monoubiquitylation catalysed by Mdm2 alone (Grossman et al., 2003). Using truncated versions of the protein, these authors could ascribe p300 catalytic activity to its N-terminus (a.a. 1-595). In light of these results, I interpreted the lack of p53 degradation to the fact that, without p300, Mdm2 can only monoubiquitylate p53, a signal which is not sufficient to target p53 to the proteasome. I therefore cloned human p300 N-terminus (p300(CH1)), hoping that this would represent the solution to problem. Unfortunately, p53-ECFP is stable also when Mdm2-EYFP and p300(CH1) are co-expressed in the cell (Figure 2.2.15)

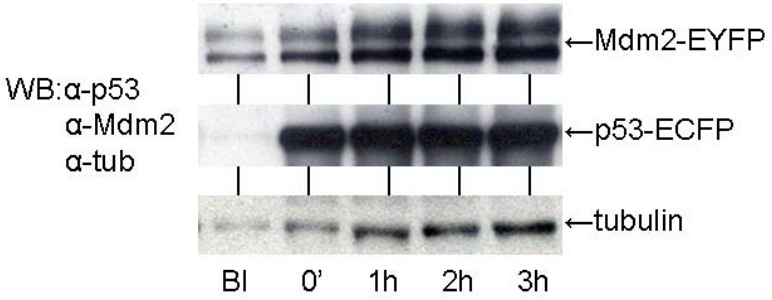

Figure 2.2.15 | p53-ECFP is stable in the presence of Mdm2-EYFP and p300(CH1). Cells containing three plasmids, one carrying p53-ECFP under the GAL promoter, one carrying Mdm2-EYFP under the TEF promoter and one carrying p300(CH1) under the TEF promoter were grown at 30°C until exponential growth phase. Gene expression from the GAL promoter was triggered by adding 0.5% f.c. galactose to the medium and was inhibited by adding 3% f.c. glucose to the same medium. An equal volume of sample (1 ml) was collected at every time point and an equal volume of treated sample was loaded in each lane of the gel. BI stands for Before Induction. p300(CH1) expression was not directly detected with an antibody, but the plasmid was sequenced to make sure that the gene sequence was correct and in the right frame. The same result was obtained using native p53 and Mdm2 and p300(CH1) fused to the FLAG tag (see Figure 2.2.18a), thus

we can conclude that Mdm2-EYFP and p300(CH1) do not suffice to trigger p53-ECFP degradation in yeast cells.

On the road to degradation, second attempt: Removing the fluorescent proteins from p53 and Mdm2

At this stage, we started wondering whether the presence of the fluorescent protein at the C-termini of p53 and Mdm2 could affect their proper folding, the accessibility of the residues to be modified (in the case of p53), or the enzymatic activity (in the case of Mdm2). Although we used exactly the same fusion proteins described in (Lahav *et al.*, 2004), we thought that the degradation of p53 that they observed in their cell line could be due to the activity of other E3 ubiquitin ligases present in those cells, thus leaving the possibility that Mdm2-EYFP might be impaired in its function. Also, the tight co-localization of the proteins to the dot might be due to aggregation (see below and Discussion) and since it is well known that GFP tends to aggregate (Tsien, 1998) (unless the modified monomeric GFP version is used) and considering that p53 forms a tetramer, we believed that ECFP and EYFP might prevent ubiquitylation to occur. Furthermore, protein over-expression might as well be the cause of aggregation; I therefore decided to clone the p53 and Mdm2 wild type genes this time under the weaker inducible GALS promoter and – when expression ought to be constant – the constitutive weaker ADH promoter.

Surprisingly, Mdm2 levels under the ADH promoter were not constant with time as it was supposed to be. Since Mdm2 levels need to be reliably constant if we want to increase our chances to degrade p53, I cloned the *mdm2* gene under the strong constitutive TEF promoter, the one used with the fusion protein Mdm2-EYFP. The choice of a strong promoter for the Mdm2 is also supported by the consideration that in the literature, for both *in vitro* and *in vivo* ubiquitylation assays, Mdm2 levels consistently appear to be at least twice those of p53 (see (Shimizu et al., 2002) for example).

Figure 2.2.16 shows that the native proteins behave like the fusion proteins when expressed alone and also when co-expressed, leading to the conclusion that the fusion

proteins are functional – as was shown by (Lahav *et al.*, 2004) – and that the failure of p53 degradation is not to be ascribed to the presence of the fluorescent proteins.

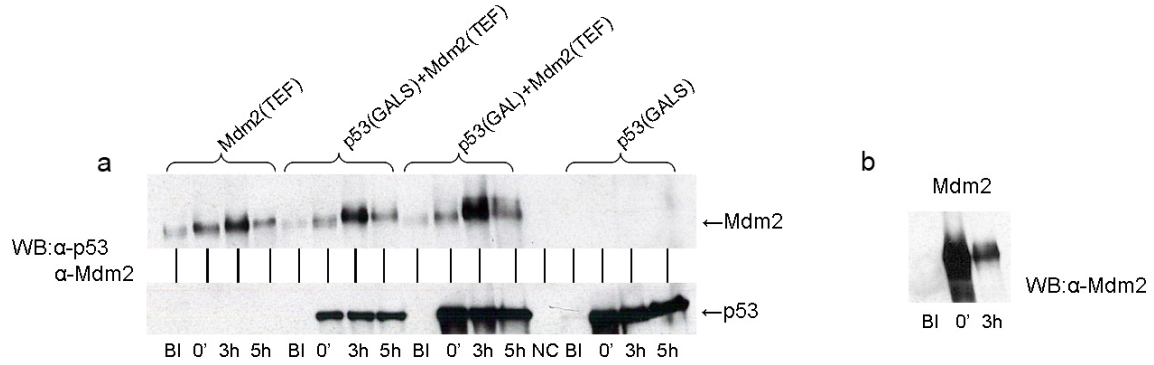

Figure 2.2.16 | Stability of the p53, Mdm2 native proteins in yeast. Cells were grown at 30°C until exponential growth phase. Gene expression from the GAL or the GALS promoter was triggered by adding 0.5% f.c. galactose to the medium and was inhibited by adding 3% f.c. glucose to the same medium. **a**, Samples were collected before adding the galactose (BI), when adding the glucose (0'), 3 hours (3h) and 5 hours (5h) after stopping induction. Mdm2 levels decrease at time point 5h independently of p53. p53 is stable regardless the presence of Mdm2. NC indicates the negative control. **b**, Mdm2 native protein is degraded fast, confirming what we observed with the fusion protein. BI refers to the sample collected before induction with galactose.

Since tagging a protein with the fluorescent protein GFP can sometimes alter its localization (Huh et al., 2003), I took advantage of having both native and fusion proteins to check whether their showed different localizations. Indirect immunofluorescence reveals no difference in the localization of native versus fusion proteins (data not shown).

On the road to degradation, third attempt: cloning the human E2, UbcH5B

Our belief that the human E3 ligase Mdm2 could function in budding yeast was based on the consideration that the human E2 (UbcH5B) – known to catalyze the passage of ubiquitin onto p53 in interaction with Mdm2 (Saville et al., 2004) – and its yeast homologue (Ubc4) share a very high homology (79% identities, 90% conservative changes). The stability of p53 in the presence of its negative regulator Mdm2 led us to

think that this homology might not suffice for the yeast E2-human E3 interaction to be efficient. Indeed, there exist several E2s in a cell, each interacting with only a subset of E3s, thus indicating a certain degree of selectivity already at the level of the E2s. In an attempt to correct for what we thought had been a naïve assumption responsible for p53 failed degradation, I cloned UbcH5B in a yeast expression plasmid and co-expressed it with only Mdm2 or with p53 and Mdm2 together. To our great surprise and disappointment, p53 was not degraded even under these conditions (Figure 2.2.17).

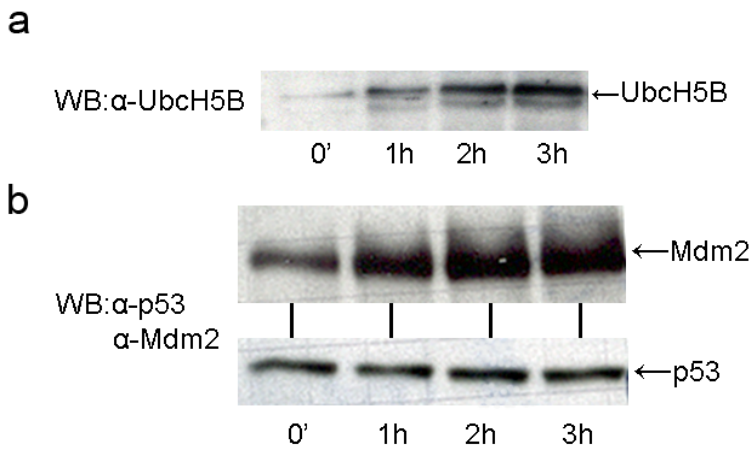

Figure 2.2.17 | p53 is stable in the presence of Mdm2 and UbcH5B. Cells were grown at 30°C until exponential growth phase. Gene expression from the GAL promoter was triggered by adding 0.5% f.c. galactose to the medium and was inhibited by adding 3% f.c. glucose to the same medium. **a,** Western blot analysis using an antibody against UbcH5B confirms expression of the protein. **b,** p53 is not degraded by Mdm2 in the presence of its human E2 partner.

On the road to degradation, fourth attempt: combining p300(CH1), UbcH5B and Mdm2

The fact that p53 is not being degraded when Mdm2 and UbcH5B are present in the yeast cells does not exclude the possibility that p300 is needed to polyubiquitylate p53 and order its degradation through the proteasome. Consequently, I built a plasmid

containing UbcH5B and p300(CH1) both under the TEF promoter and co-transformed it into cells together with a plasmid carrying the *p53* gene and a plasmid carrying the *mdm2* gene. As can be seen in Figure 2.2.18, p53 is still stable under these conditions.

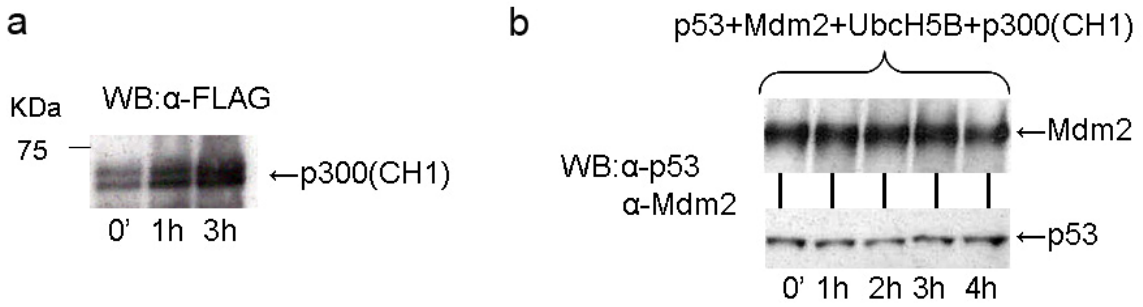

Figure 2.2.18 | p53 is stable in the presence of Mdm2, UbcH5B and p300(CH1). a, Western blot on cells containing p300(CH1)-FLAG to show that the protein is expressed. p300 is under the constitutive TEF promoter. **b**, In this experiment, cells were induced in the late exponential growth phase and last samples collected with the cells in stationary phase. Cell growth is thus limited and on the blot we do not see the accumulation of Mdm2 that we see in the other blots. I performed the same type of experiment later, this time under usual growth conditions and confirmed the result, eliminating the possibility that failed p53 degradation could be due to the cells being in stationary phase (data not shown).

On the road to degradation, fifth attempt: lowering the expression levels of p53; doubling the amount of Mdm2

Since little quantitative data are available for the p53 network, we don't know what the relative concentrations of p53 and Mdm2 allowing ubiquitylation to occur are. One could speculate that too much substrate inhibits the reaction and that we must have an excess of E3 ligase. Otherwise, we might assume that the substrate, E2 and E3 need to be at equimolar ratios or even that, being ubiquitylation an enzymatic reaction, little amounts of Mdm2 are sufficient to ubiquitylate p53. In principle, we should explore many different expression levels for p53 and Mdm2. In practise, this is very time-consuming, so we restricted ourselves to reducing p53 levels while keeping the same Mdm2 levels as we had before. In order to determine the minimal amount of galactose

that induces p53 to a level which is detectable on a western blot, I performed an induction curve of the p53 under the GALS promoter (Figure 2.2.19), and decided to use for further experiments galactose to a final concentration of 0.006%. It should be noted that the concentration of galactose had to be really low in order to have a non-saturated curve; in fact, when spanning concentrations ranging from 0.01% to 1%, p53 levels are already saturated (data not shown).

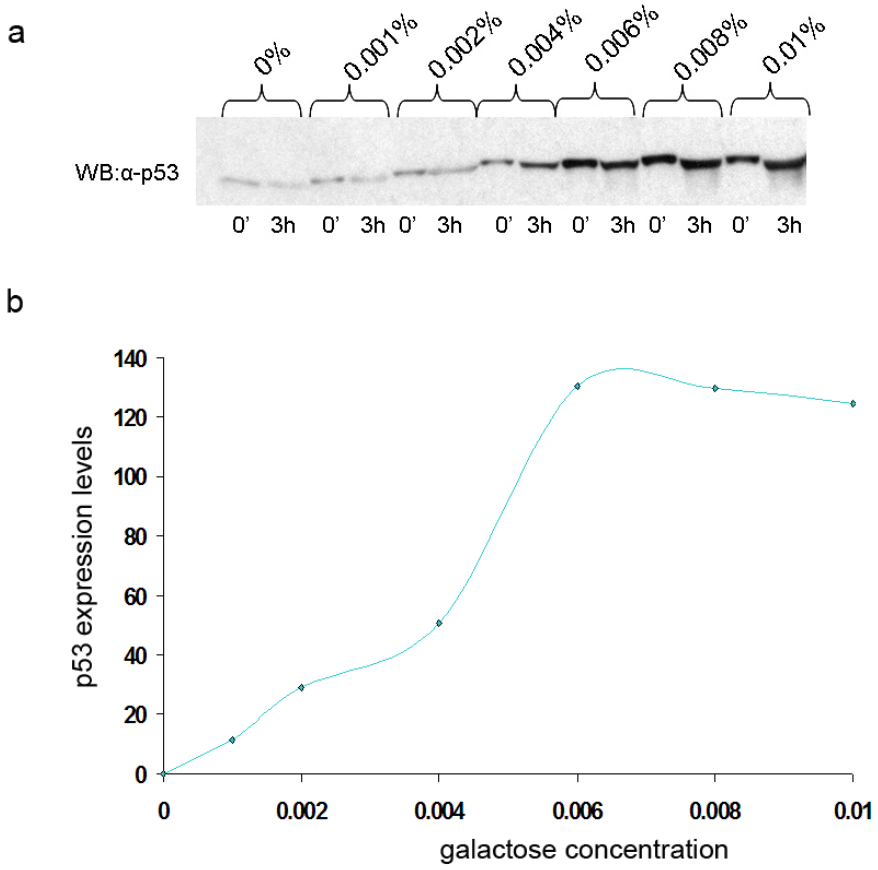

Figure 2.2.19 | p53 induction curve. Cells carrying p53 were grown up to exponential phase, then the culture was split in different subcultures, each of which was induced using an increasing amount of galactose. Samples were collected immediately and three hours after stopping induction with 3% f.c. glucose. **a,** western blot showing p53 levels as a function of galactose concentration; **b,** the western blot data were quantified using Adobe Photoshop (Materials and Methods) and the induction curve drawn in Excel. In the graph, the data point corresponding to no galactose (0%) is put to zero and this value is subtracted to all other data points.

Figure 2.2.20 shows that even when p53 expression levels are reduced, while keeping Mdm2 levels as before, degradation does not occur.

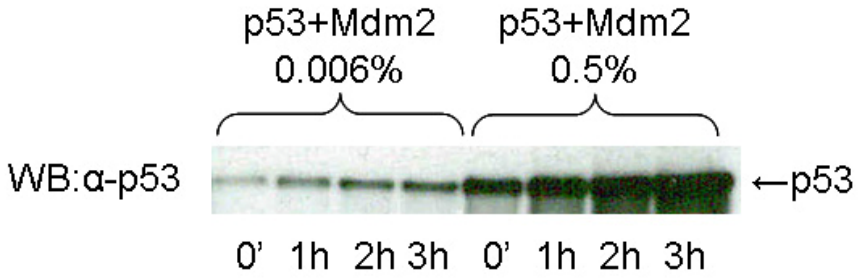

Figure 2.2.20 | Lowering expression levels of p53 does not bring degradation about. Cells were grown at 30°C until exponential growth phase. Gene expression from the GAL promoter was triggered by adding, respectively, 0.006% and 0.5% f.c. galactose to the medium and was inhibited by adding 3% f.c. glucose to the same medium. Samples were collected every hour, starting from the moment in which glucose was added to the medium, for a total amount of three hours. Lowering p53 expression level does not lead to its degradation.

On the road to degradation, sixth attempt: using a p53 mutant (p53F270A) that is hyper-ubiquitylated in human cells

Shimizu *et al*. have shown that mutating phenilalanine 270 to alanine renders the p53 hyper-susceptible to Mdm2-mediated ubiquitylation (Shimizu et al., 2002). I decided to generate the same mutant used in that study hoping that this would increase p53 ubiquitylated species, and consequently our chances to detect some degradation. To our surprise, I found that this mutant p53 is very unstable on its own and therefore we cannot conclude that degradation is due to the action of Mdm2 (Figure 2.2.21). Moreover, this mutant is not a good candidate for the construction of the synthetic oscillator, since we need a p53 protein that is stable on its own and degraded in an Mdm2-dependent fashion.

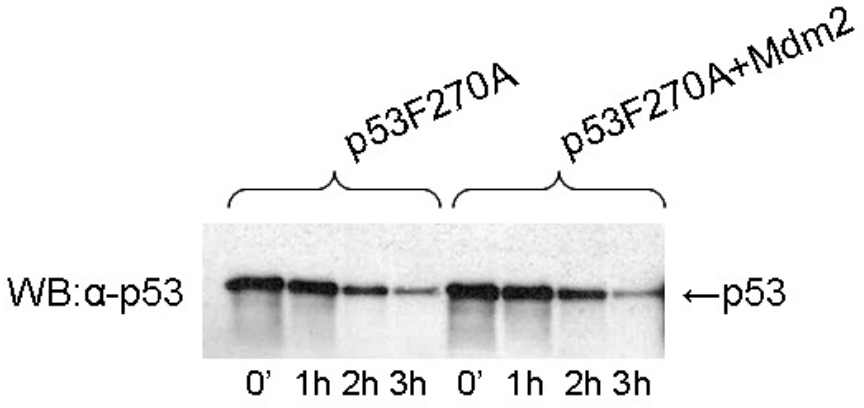

Figure 2.2.21 | p53F270A is degraded regardless the presence of Mdm2. Cells were grown at 30°C until they reached exponential growth phase. Gene expression from the GAL promoter was triggered by addition of 0.006% galactose to the medium and was inhibited by addition of 3% f.c. glucose to the same medium. Samples were collected in the moment in which glucose was added to the medium and every hour afterwards, for a total amount of 3 hours. p53F270A is unstable in the absence or presence of Mdm2.

Mdm2 is modified in yeast

Mdm2 is known to be subject, in human cells, to almost as many post-translational modifications as p53 itself. It is plausible, then, that Mdm2 is being modified in yeast in a way that affects its E3 ligase activity towards p53. One way to verify if this is happening is to compare Mdm2 status at different time points. To do this, we need Mdm2 to be under an inducible promoter, so that we can decide when the protein is made and follow it from that moment on.

As inducible promoter I decided to use a p53 responsive one – so that Mdm2 expression is p53-dependent – because, on the one hand I can double-check the ability of my p53 clone to activate transcription in yeast as previously described (Oliner et al., 1993) and, on the other hand, I can obtain information on the timings of Mdm2 expression in response to p53 induction, which can be useful for the construction of the synthetic oscillator (as well as for a mathematical model of the synthetic network). Remarkably, the P2 promoter that drives Mdm2 gene expression in human cells in response to p53 binding does not work in budding yeast (data not shown). Only when I used the same promoter described in Oliner *et al.*, which comprises several repeats of the p53 consensus

sequence, did I observe Mdm2 expression. From these results, we speculate that one or two repeats of the p53 consensus sequence do not suffice to start a p53 transcriptional response from such a promoter. Rather additional elements – such as enhancers and co-factors – are needed. Figure 2.2.22 shows p53-dependent Mdm2 induction in yeast cells. From this experiment, it is evident that Mdm2 is modified in yeast as specific higher molecular weight bands are observed.

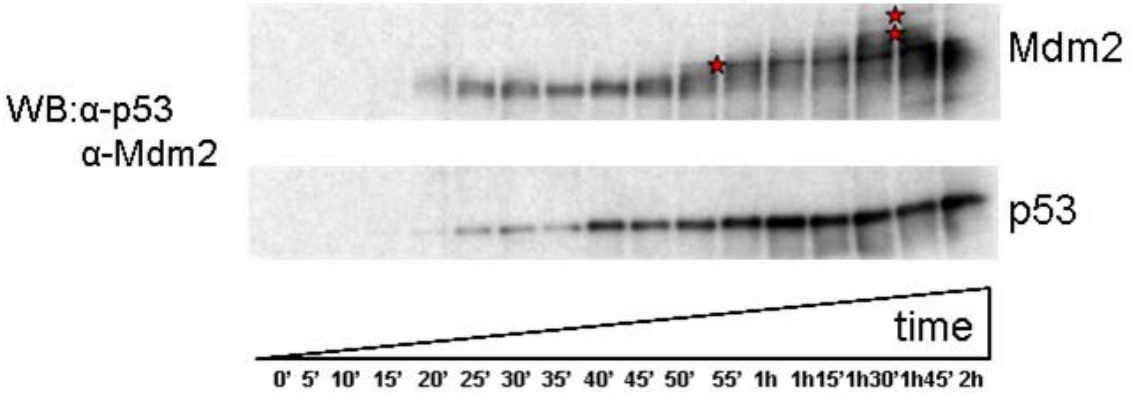

Figure 2.2.22 | p53-dependent Mdm2 induction in yeast. Cells carrying a plasmid with the p53 under the GAL promoter and a plasmid with Mdm2 under a p53-responsive promoter were grown up to exponential growth phase. Induction of p53 expression was done with 0.5% f.c. galactose. Glucose was not added to stop induction. The red stars indicate less mobile species which correspond to modified Mdm2.

Since we know that Mdm2 is being degraded through the ubiquitin-proteasome pathway, it is likely that the bands are ubiquitylated forms of the protein. I tried to purify the protein (6xHIS-tagged), but the amount of protein obtained was not sufficient to detect a signal when probing with an antibody against ubiquitylated proteins. Therefore, we cannot be sure of the nature of these modifications and we also cannot conclude that they are the cause of failed p53 degradation.

On the road to degradation, last attempt: changing E3 ligase

At this point, it was evident that, for some reason, the human E3 ligase Mdm2 cannot ubiquitylate p53 in yeast, at least not to an extent sufficient to trigger its degradation (see Discussion for an analysis of the reasons why Mdm2 might not lead to p53 degradation in budding yeast). Since, as mentioned in the Introduction, Mdm2 is not the only E3 ubiquitin ligase responsible for p53 ubiquitylation in human cells, I decided to test the behaviour of two other E3 ligases for p53, COP1 and Pirh2.

I first cloned the human COP1 into a yeast expression plasmid and analyzed p53 levels in its presence. Unfortunately, the COP1 antibody was extremely "noisy" and COP1 expression cannot be detected unambiguously. Therefore it is possible that p53 is not degraded because COP1 is not expressed (although the sequences of both the ORF and the promoter were verified before transforming the construct in yeast cells). Surely, p53 is not degraded when the E3 ligase Pirh2 (which I cloned introducing the 6xHIS tag and whose expression I could detect using an antibody against this tag) is used in place of Mmd2 (Figure 2.2.23).

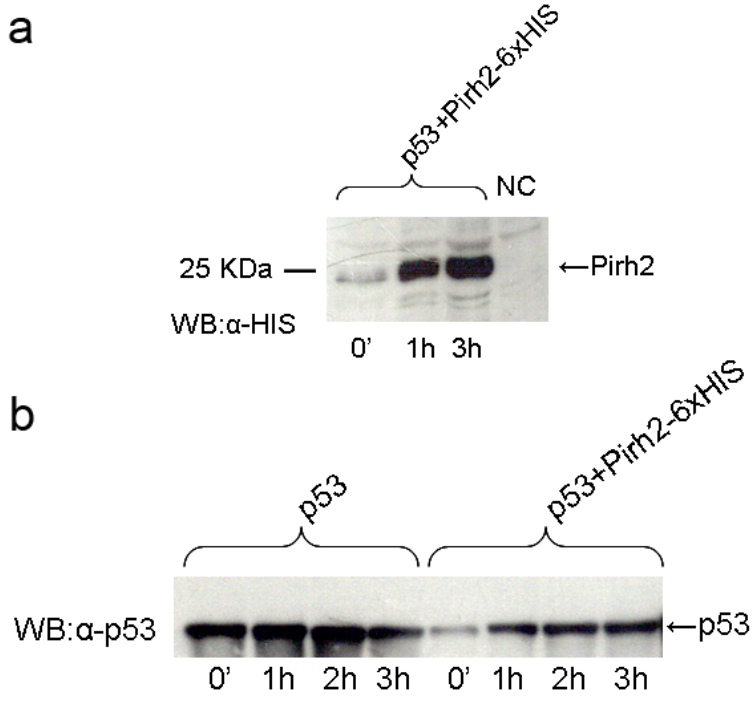

Figure 2.2.23 | p53 is not degraded in yeast by the human E3 ligase Pirh2. Cells carrying a plasmid with the p53 under the GAL promoter and a plasmid with the Pirh2

under the TEF promoter were grown up to exponential growth phase. Induction of p53 expression was done with 0.006% f.c. galactose. 3% f.c. glucose was not added to stop induction. **a**, Western blot showing that Pirh2 is expressed. Due to space limitation on the gel, only samples 0', 1h and 3h were run. **b**, Comparison between p53 levels in the absence (left) or presence (right) of the human E3 ubiquitin ligase Pirh2. p53 is stable in either case.

In conclusion, p53 is not being degraded in the presence of any of the ubiquitin E3 ligases tested in this study known to ubiquitylate p53 in human cells.

p53 is modified in the presence of Mdm2

Although p53 levels proved to be extremely stable under all the conditions I tested, I noticed that, when loading a sufficiently high amount of p53 on the gel, a less mobile p53 species appears on the western blot only in the presence of Mdm2 (Figure 2.2.24).

Since this band is about 8-10 KDa higher than wild type p53, we thought it might be a monoubiquitylated form of p53. In order to make sure that this band is not an artefact due to unspecific binding of the antibody, I used another antibody against a different epitope on p53 and obtained the same result (data not shown).

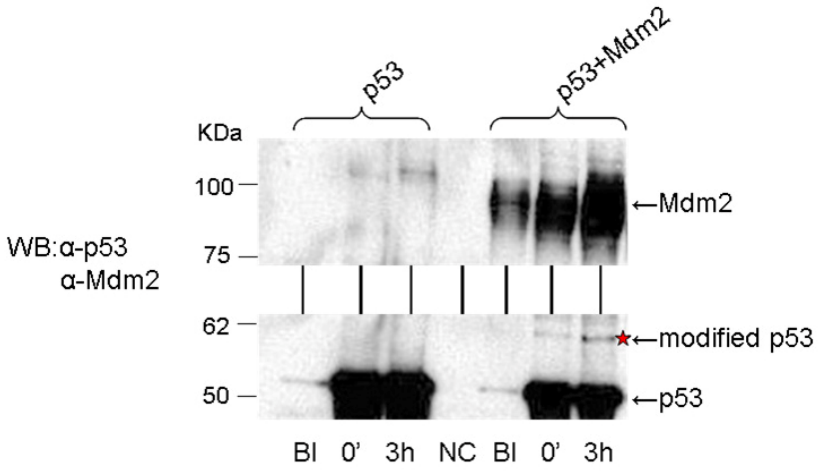

Figure 2.2.24 | p53 is modified in yeast in the presence of Mdm2. Yeast cells carrying only p53 or p53 together with Mdm2 were grown at 30°C to exponential phase. The first

sample (BI) was collected when 0.5% f.c. galactose was added to the medium to induce expression of p53. One hour later, induction was stopped through the addition of 3% f.c. glucose and a sample (0') was collected. Cells were grown for three hours before collecting the last sample (3h). The antibody against p53 recognizes an additional band (indicated by the red star) only in the samples obtained from cells expressing p53 and Mdm2.

p53 is similarly modified when Mdm2 is expressed together with p300(CH1), UbcH5B or p300(CH1) and UbcH5B contemporarily (Figure 2.2.25).

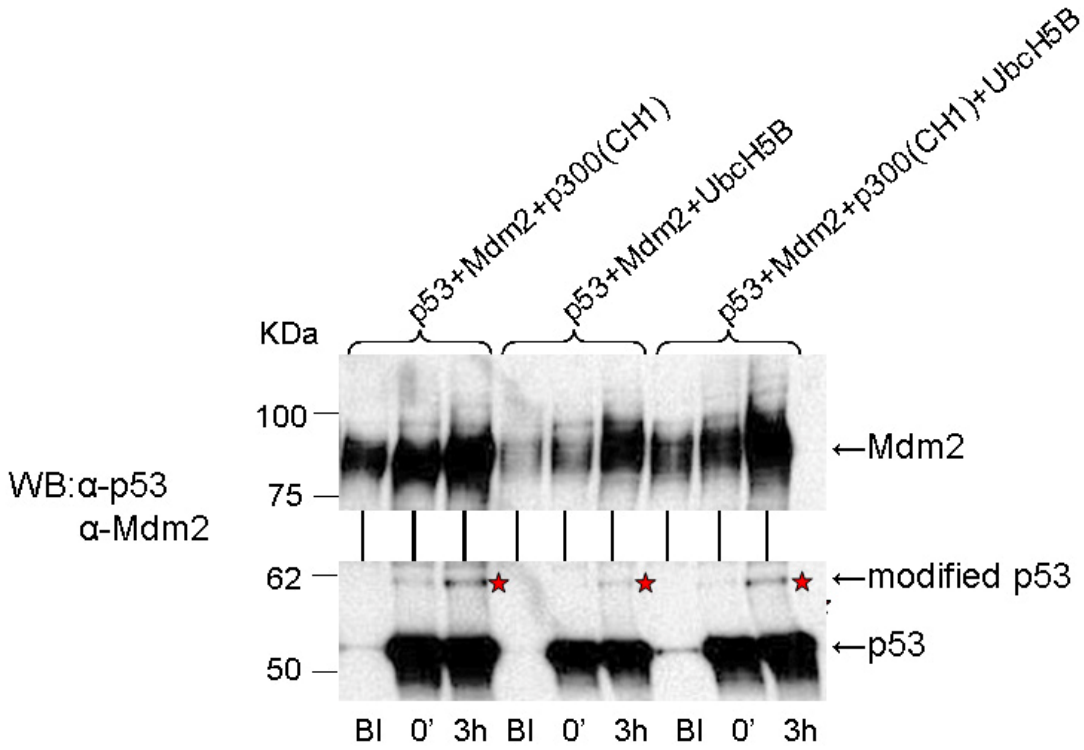

Figure 2.2.25 | p53 modification in the presence of p300(CH1) and UbcH5B. Yeast cells carrying the indicated constructs were grown at 30°C to exponential phase. The first sample (BI) was collected when 0.5% f.c. galactose was added to the medium to induce expression of p53. One hour later, induction was stopped through the addition of 3% f.c. glucose and a sample (0') was collected. Cells were grown for three hours before collecting the last sample (3h). p300(CH1) and UbcH5B (whose expression was previously verified, see Figures 2.2.17a and 2.2.18a) do not appreciably affect the action of Mdm2 on p53.

Is p53 monoubiquitylated?

There are several ways to understand what this modification is. The most elegant way is to use mass spectrometry, since this technique does not require any *a priori* knowledge on the nature of the modification and simply answers the question: "what is it?" Alternatively, one can use antibodies which can specifically recognize the modified version of the protein, such as antibodies against mono- and polyubiquitylated proteins. This method requires an *a priori* knowledge of the modification to select the right antibody. A third method is also an indirect one and it requires the generation of mutant proteins which are no longer modified. Again, we need to guess which is the modification and, if mutants have not been described before, one has to predict *in silico* which residues might affect the modification and then test the prediction experimentally.

While the first two methods require some sort of purification of the protein (*e.g.* a pull-down), the third one does not, since we simply need to see that the band disappears when using the mutant.

For the p53, a mutant protein in which the C-terminal lysines are mutated to arginines or alanines has been described to no longer be ubiquitylated by Mdm2 in human cells (Nakamura et al., 2000; Rodriguez et al., 2000). I therefore generated a p53 mutant (which I called p53δ) in which lysines 372, 373, 382 and 383 are mutated to arginines. If the higher molecular p53 band is a monoubiquitylated form of the protein, we expect it to disappear when using p53δ.

Strikingly, p53δ appears to be more modified than the wild type (Figure 2.2.26).

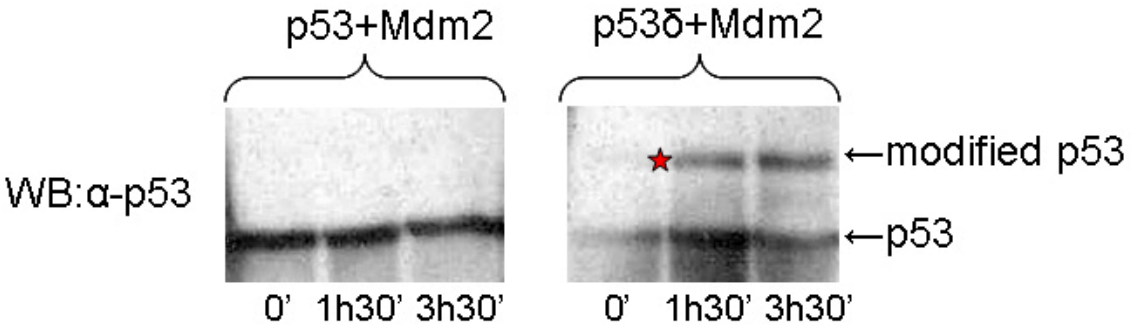

Figure 2.2.26 | p53δ is modified more than wild type p53. Cells were grown at 30°C up to exponential growth phase. Induction was done using 0.006% f.c. galactose. To stop

induction, 1% glucose was added after one hour to the same medium, and the first samples collected (0'). The second samples were collected one and a half hours later (1h30'), and three and a half hours later (3h30'). Notably, while the modified p53 – in the presence of Mdm2 – is not visible under these conditions (too little amount of p53 on the gel, too short exposure time), the band is very dark on p53δ + Mdm2 samples. p53δ alone does not have any additional band (data not shown).

Also, were the modification monoubiquitylation, the mutant Mdm2 carrying a mutation in its RING domain (Mdm2H452A) should not be able to modify p53. I find that, instead, the modification is present, and even somehow "stronger" than that obtained with wild type Mdm2 (Figure 2.2.27, compare the bands indicated by the red star in lanes 3 and 6).

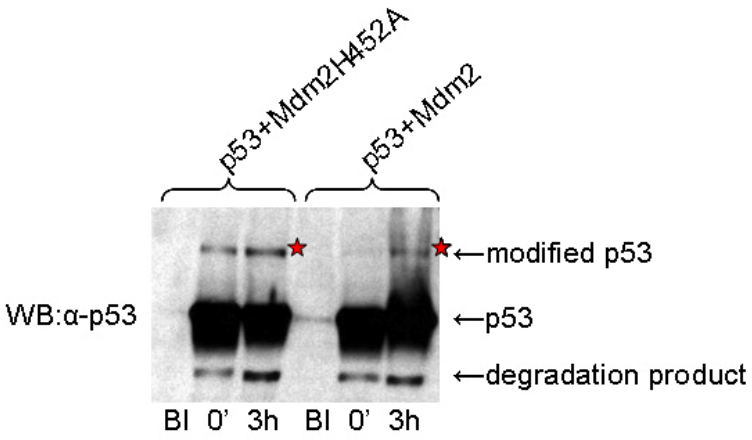

Figure 2.2.27 | Mdm2H452A retains its ability to modify p53 in yeast cells. Cells were grown at 30°C to exponential growth phase. The first sample (BI) was collected when 0.5% f.c. galactose was added to the medium to induce expression of p53. One hour later, induction was stopped through the addition of 3% f.c. glucose and a sample (0') was collected. The last sample was collected three hours later (3h). The fact that Mdm2H452A, which does not ubiquitylate p53 in human cells, is able to modify p53 in yeast argues against p53 modification being monoubiquitylation.

All the data collected were in contradiction with the hypothesis that the modification is ubiquitylation: a) Mdm2H452A, which should no longer function as a ubiquitin E3 ligase, works even better than the wild type Mdm2; b) p53F270A, which should be more

heavily modified appears to be less modified than the wild type; c) p53δ, which should not be ubiquitylated, is more strongly modified.

At this point, some pieces of evidence came that pointed towards the idea that the modification might be sumoylation, which is the only covalent protein modification that, like ubiquitin, leads to an increase in molecular weight of around 8 KDa.

Specifically, in the attempt to purify p53 to probe with an antibody specific for mono- and polyubiquitylated proteins, I realized that the band corresponding to modified p53 was being lost when lysing the cells under native conditions to perform an immunoprecipitation (IP) with low detergent concentration (*i.e.* a concentration that is used to immunoprecipitate soluble proteins, and not membrane proteins for instance) (Figure 2.2.28)

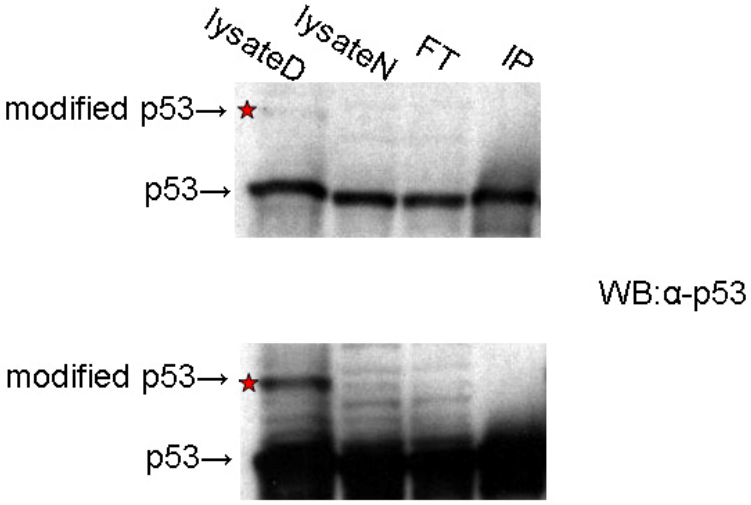

Figure 2.2.28 | Modified p53 is lost when performing immunoprecipitation. Yeast cells carrying p53 and Mdm2 were grown to exponential growth phase, induced with 0.5% f.c. galactose for two hours and then harvested. IP was performed using the DO-1 anti-p53 antibody as described in Materials and Methods. LysateD stands for "lysate obtained under denaturing conditions", while lysateN denotes "lysate obtained under native conditions". FT indicates the flow through, and IP the immunoprecipitation. Upper and lower panel represent the same film with different exposure times. The band corresponding to modified p53 is lost when lysing the cells under native conditions.

When, instead, I purified p53 (6xHIS-tagged) under denaturing conditions using a Ni^{+}-NTA column, the band could be detected, although it represents a very small fraction of the total protein (less than 5%, data not shown).

These results suggested that either this modified p53 is subject to de-modification in the cell lysate, or somehow the modified p53 protein is bound to something inside the cell, a membrane, a macromolecular complex or an organelle. From the microscopy studies, we knew that p53 co-localizes with Mdm2 in a very bright dot in the vicinity of the cell nucleus. Indeed, there seems to be a connection between the dot and the modification. Searching the literature for inspiration, I came across the work by Kim *et al.* in which they show that sumoylation of the human homeodomain-interacting protein kinase 2 (HIPK2) correlates with its localization to nuclear dots (Kim et al., 1999). Finally, p53 is itself sumoylated in human cells by Mdm2 and its sumoylation seems to correlate with its association with nuclear bodies (Gostissa *et al.*, 1999; Muller *et al.*, 2001). All these considerations led me to the conclusion that p53 might be sumoylated in yeast and that sumoylation correlates with the localization of p53 in the nuclear dot.

p53 is sumoylated in yeast by Mdm2

Using Ni^{+}-NTA columns, I purified p53 (6xHIS-tagged) from cells expressing only p53 or p53 together with Mdm2. I also included cells expressing either only p53δ or p53δ and Mdm2. This p53 mutant is more strongly modified than the wild type (Figure 2.2.26), so I thought it would increase the chance to retain the modified p53 after the purification. To exclude the possibility that the band is Mdm2-specific but not a modified p53, I used as a control cells expressing only Mdm2 (6xHIS-tagged). Figure 2.2.29 shows that p53 is sumoylated in yeast in the presence of Mdm2 and, as expected, this is more evident with p53δ.

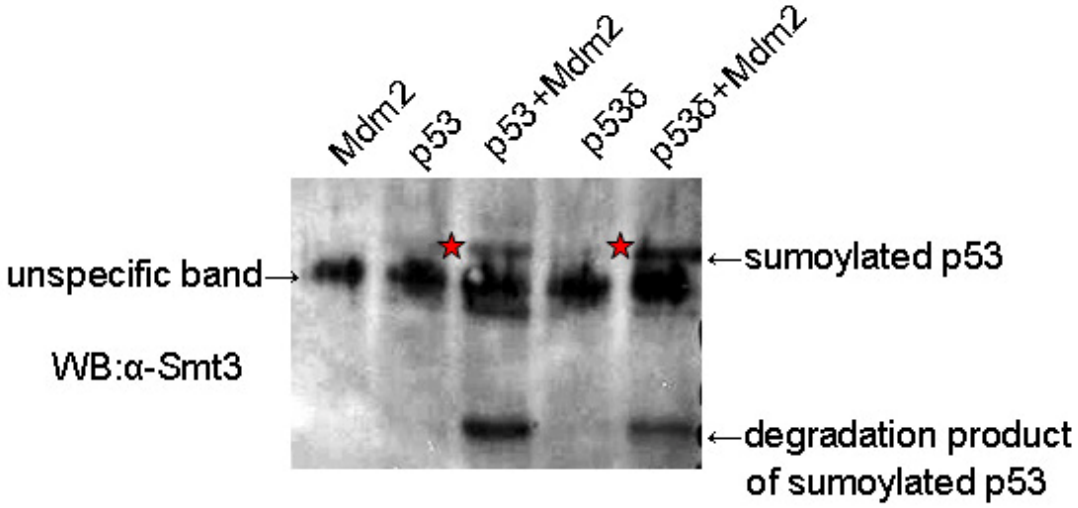

Figure 2.2.29 | p53 is sumoylated in yeast in the presence of Mdm2. Cells expressing only Mdm2-6xHIS (first lane starting from the left), only p53-6xHIS (second lane), p53-6xHIS and Mdm2 (third lane), only p53δ-6xHIS (fourth lane) and p53δ-6xHIS and Mdm2 (fifth lane), were grown at 30°C and induced with 0.5% f.c. galactose for two hours, then harvested. Purification on Ni^{+}-NTA columns was performed as described in Materials and Methods. Samples were run on a gel and sumoylated proteins were detected with western blot using the anti-Smt3 antibody. Only in the presence of Mdm2 it is possible to detect sumoylated p53 (indicated by red stars to the left of the corresponding band). As expected, p53δ is more strongly sumoylated than wild type p53 (compare bands indicated by red stars in lanes 3 and 5). Finally, a degradation product of p53 which is sumoylated is detected.

Direct binding of p53 to Mdm2 is necessary for sumoylation to occur. When p53W23S, which cannot bind Mdm2 due to a point mutation in the Mdm2 binding domain (Inoue *et al.*, 2001), is expressed with Mdm2 in place of wild type p53, sumoylation is strongly reduced (Figure 2.2.30).

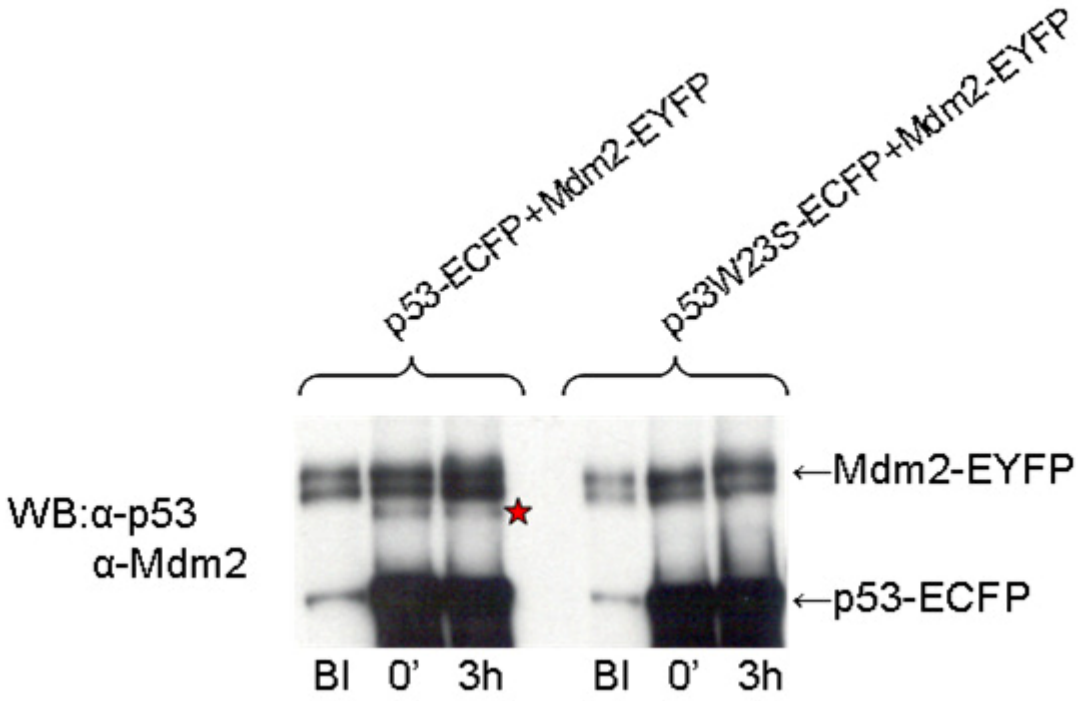

Figure 2.2.30 | Direct binding of p53 to Mdm2 is required for Mdm2-induced p53 sumoylation in yeast. Cells carrying the wild type p53–ECFP fusion protein together with the Mdm2-EYFP fusion protein or the mutant p53W23S-ECFP fusion protein and the Mdm2-EYFP fusion protein were induced with 0.5% f.c. galactose and induction was inhibited using 3% f.c. glucose. Although the band corresponding to sumoylated p53 (indicated by a red star) runs very close to the Mdm2-EYFP band, it is possible to see that the band is absent in the p53W23S-ECFP + Mdm2-EYFP samples.

SUMO conjugation to p53 in yeast cells requires lysine 386

In human cells, lysine 386 is known to be the major site for p53 sumoylation, since when this residue is mutated to arginine, p53 sumoylation is strongly impaired (Gostissa et al., 1999).

To prove that this holds true in yeast as well, I generated the same mutant (p53K386R) and compared its sumoylation levels to those of wild type p53 (Figure 2.2.31).

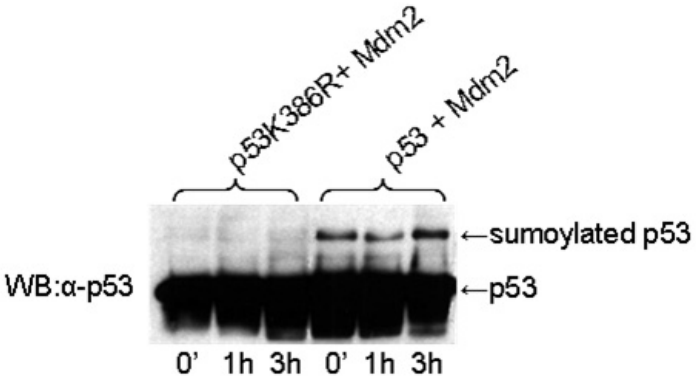

Figure 2.2.31 | Mutation of lysine 386 abolishes p53 sumoylation in yeast. Cells were grown at 30°C and induced with 0.5% f.c. galactose. To stop induction from the GALS promoter, 3% f.c. glucose was added to the same medium at time point 0'. When lysine 386 at the C-terminus of p53 is mutated to arginine, p53 sumoylation is abolished.

p14^{ARF} enhances Mdm2-dependent p53 sumoylation

Chen and Chen have shown that p14^{ARF} enhances Mdm2-mediated p53 sumoylation in human cells (Chen *et al.*, 2003). I decided to see whether this would happen in yeast cells as well. To this purpose, I cloned the human p14^{ARF} gene in a yeast expression plasmid and co-transformed cells with plasmids containing p53, Mdm2 and p14^{ARF}. As it can be seen from Figure 2.2.32, p53 sumoylation is strongly enhanced in the presence of p14^{ARF}.

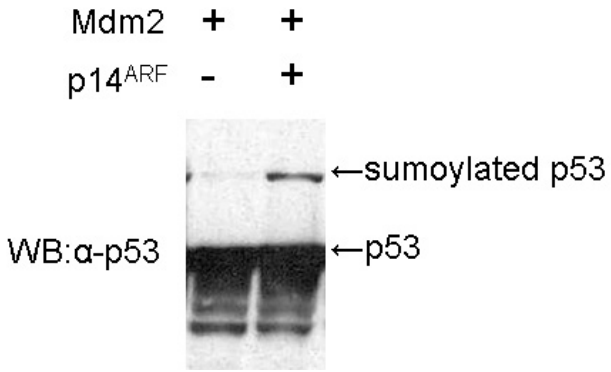

Figure 2.2.32 | p14^{ARF} strongly enhances Mdm2-mediated p53 sumoylation in yeast cells. Cells were grown at 30°C and induced with 0.5% f.c. galactose. p53 is under the inducible GAL promoter, while Mdm2 and p14^{ARF} are under the constitutive TEF

promoter. As in figure 2.2.26, while sumoylated p53 – in the presence of Mdm2 – is not visible under these conditions (too little amount of p53 on the gel, too short exposure time), sumoylated p53 can be detected in the presence of $p14^{ARF}$.

Sumoylation is responsible for p53 co-localization with Mdm2 to the nuclear dot

Sumoylation is known to affect the cellular localization of substrate proteins, often correlating with their affiliation with nuclear bodies (Kim et al., 1999; Muller et al., 2001). Since we find that p53 and Mdm2 co-localize to a specific cellular location in yeast and that p53 is sumoylated by Mdm2, I thought there might be a correlation between the modification and localization of p53 in yeast cells. This hypothesis is found to be true, since the co-localization of p53 and Mdm2 to the nuclear dot is lost when substituting wild type p53 with p53K386R which can no longer be sumoylated (Figure 2.2.33).

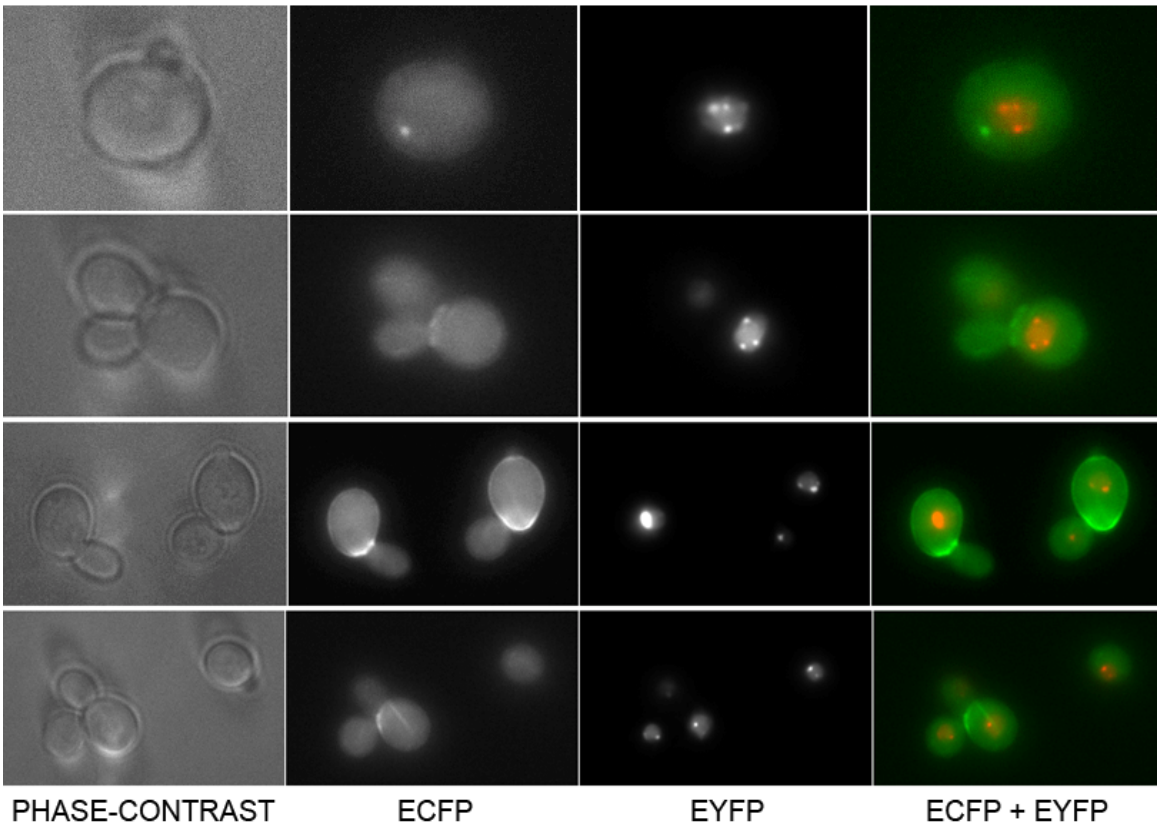

Figure 2.2.33 | p53K386R-ECFP does not co-localize with Mdm2-EYFP. Cells were grown at 30°C and gene expression was triggered by the addition of 2% f.c. galactose in

the exponentially growing culture. After 1 hour of induction, the cells were imaged using excitation and emission filters for CFP and YFP (see Materials and Methods). When p53 sumoylation is abolished (mutating the major site for sumoylation from lysine to arginine), p53-ECFP does not co-localize with Mdm2 and shows a diffuse fluorescence, sometimes being localized to the tip of the cell.

Aggresome or organelle?

From the data collected up to this point it is unclear whether the dot in which p53 and Mdm2 so tightly co-localize is an aggresome, *i.e.* a place in which the two proteins are confined because they are misfolded and not functional, or rather an organelle. Although I did not reach a clear-cut answer to this question, there are several evidences that discard the aggresome hypothesis in favour of the organelle one.

Considering that lower temperatures facilitate protein folding, I grew yeast cells at 20°C, 25°C and 30°C respectively and used fluorescence microscopy to see whether the dot would disappear at lower temperatures. Figure 2.2.34 shows that the dot is formed independently of the temperature at which the yeast cells are grown. Moreover, the dot is found also when p53 is expressed at very low levels (data not shown), which again argues against the aggresome hypothesis.

20°C

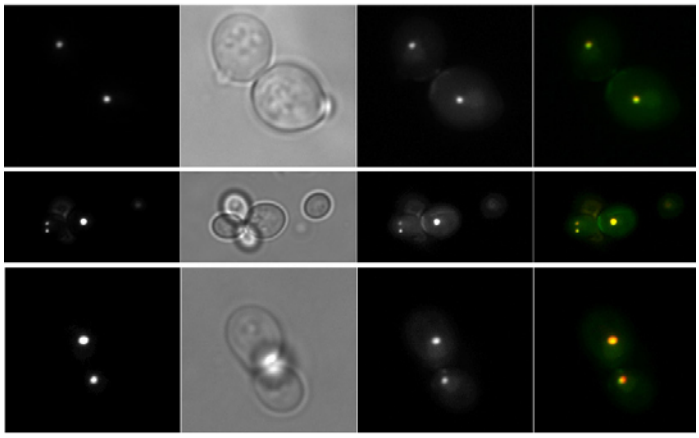

EYFP PHASE-CONTRAST ECFP EYFP + ECFP

25°C

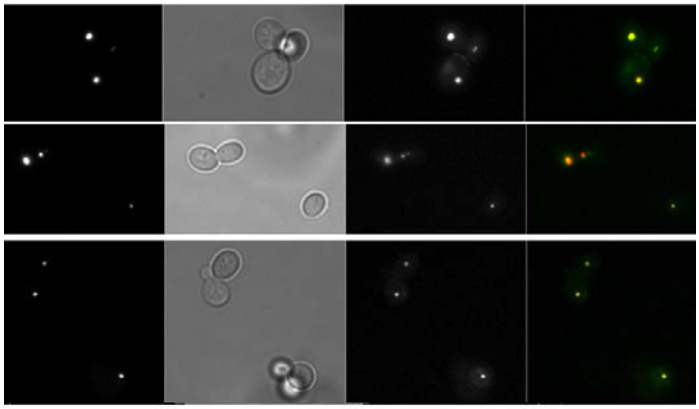

EYFP PHASE-CONTRAST ECFP EYFP + ECFP

30°C

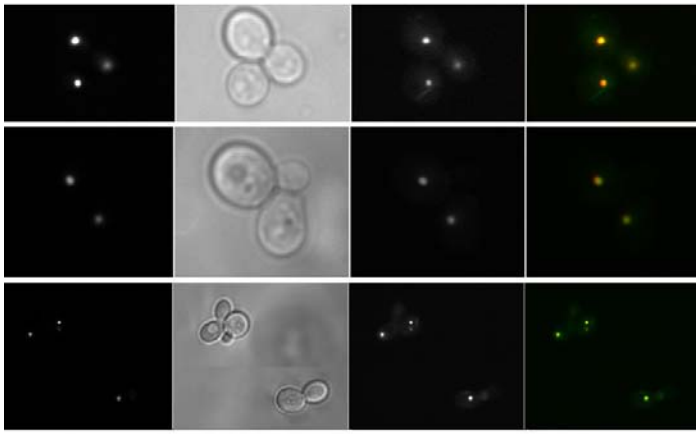

EYFP PHASE-CONTRAST ECFP EYFP + ECFP

Figure 2.2.34 | p53 and Mdm2 co-localize to the nuclear dot in yeast cells grown at different temperatures. Cells were grown at 20°C, 25°C and 30°C respectively. When cells reached exponential growth phase, p53 induction was trigger by adding 0.5% f.c. galactose to the medium (Mdm2 is constantly expressed). The first panel shows the signal obtained in the YFP channel, the second panel shows the phase-contrast image, the third panel shows the signal obtained in the CFP channel. The last panel shows the merged images for the CFP and YFP signals, where the CFP is pseudo-coloured in green and the YFP in red. Co-localization appears as a yellow signal. The dot is insensitive to the temperature at which the yeast cells are grown, arguing against the aggresome hypothesis.

To gain a better understanding on the nature of this dot, Charlotta Funaya in the EMBL Electron Microscopy Core Facility performed electron microscopy on yeast cells expressing p53 and Mdm2. I previously mentioned that it was difficult for us to understand whether the dot resided inside or outside the nucleus looking at indirect immunofluorescence pictures. Electron microscopy analysis ensures us that the dot is inside the nucleus (Figure 2.2.35).

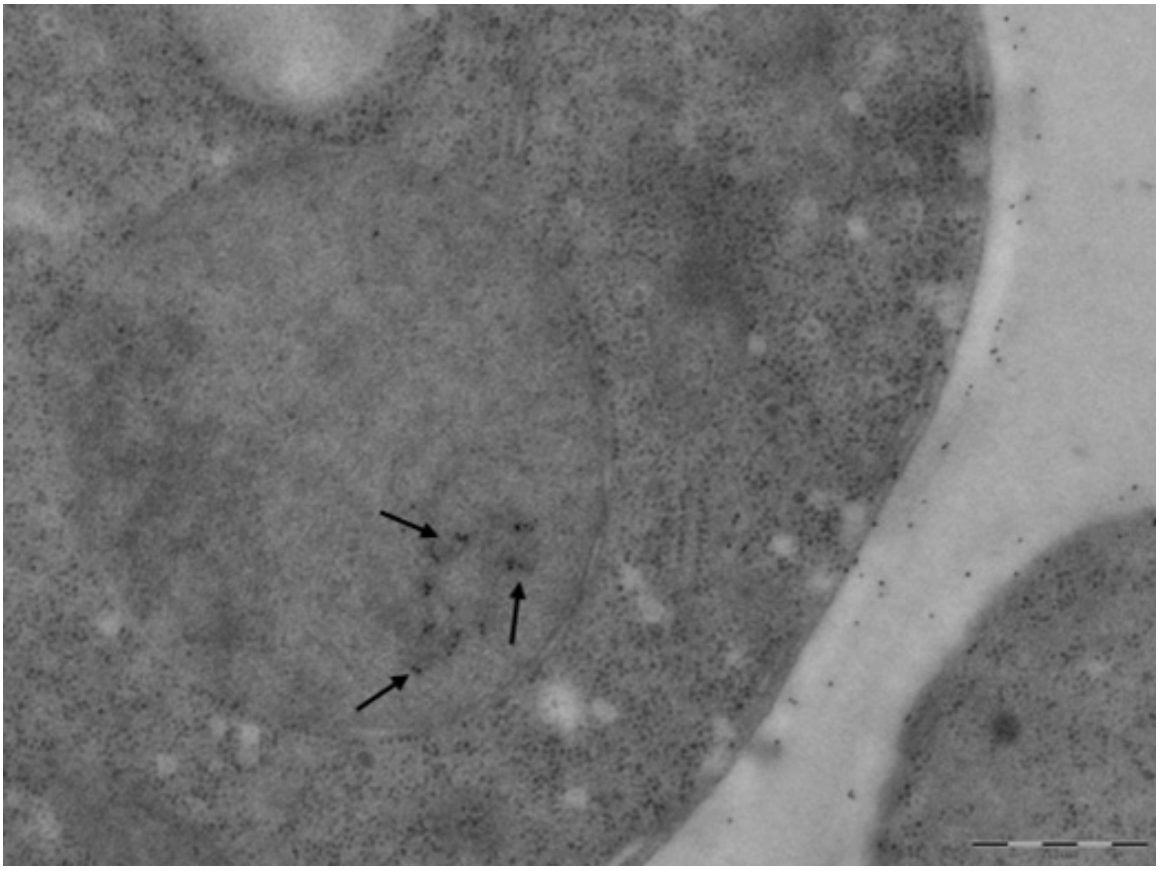

Figure 2.2.35 | Electron microscopy on a yeast cell expressing p53 and Mdm2. Cells were grown at 30°C and induced with 0.5% f.c. galactose when they reached exponential growth phase. Cells were then treated for electron microscopy as explained in Materials and Methods. The area where the gold particles are found is indicated by black arrows. The p53-Mdm2 complex is inside the yeast nucleus.

The position of the p53-Mdm2 nuclear dot is not random and is related to the yeast nucleolus

The electron microscopy pictures of cells expressing p53 and Mdm2 reveal that the nuclear dot formed by the two proteins is always adjacent to the yeast nucleolus (that can be recognized even without using a marker, due to its characteristic shape and its density compared to the rest of the nucleus). This is confirmed by indirect immunofluorescence, where using an antibody against the nucleolar protein Nop1 we find exactly the same pattern as in the electron microscopy pictures (Figure 2.2.36-37).

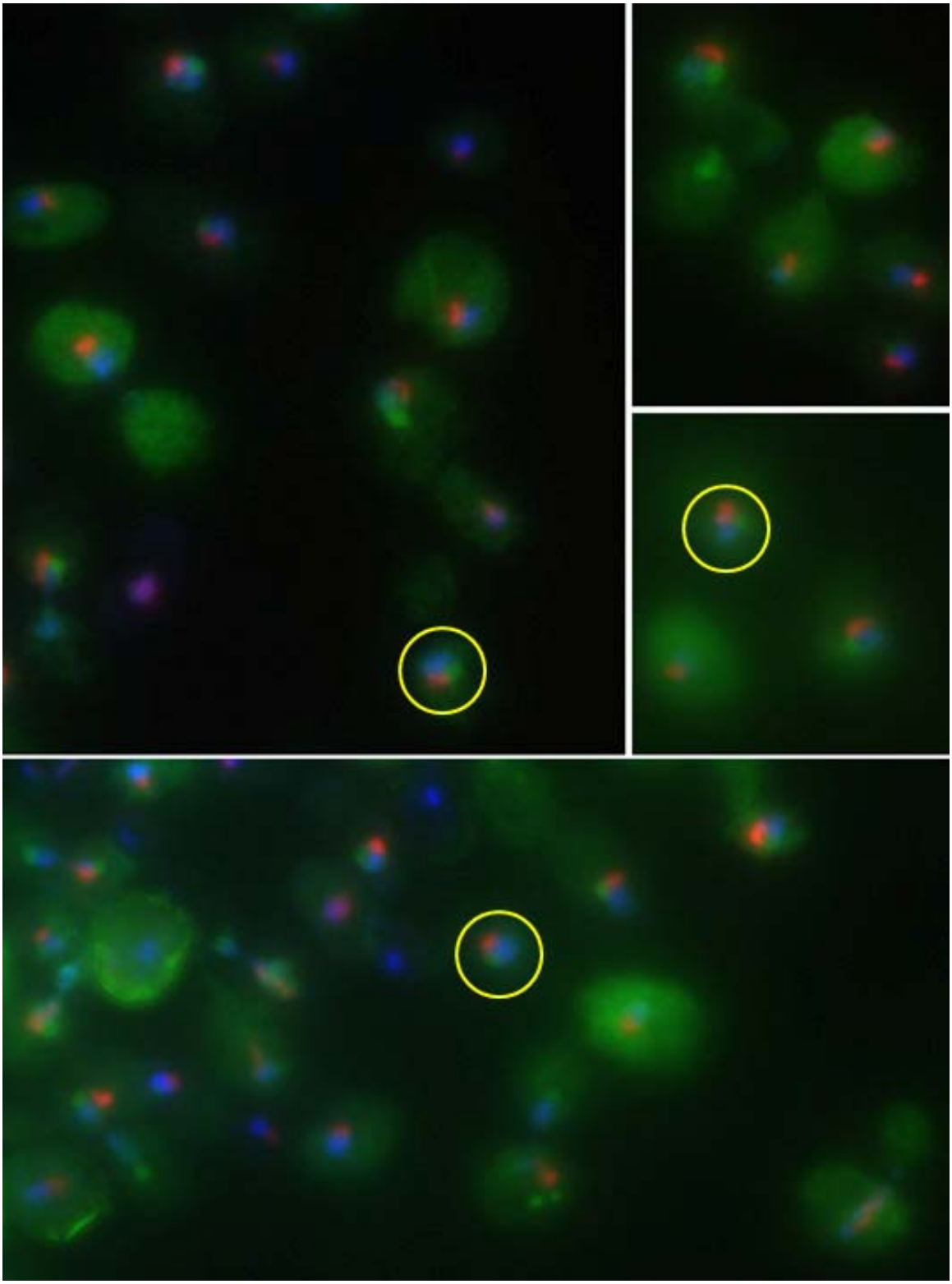

Figure 2.2.36 | Position of the p53-Mdm2 dot in respect to the yeast nucleolus. Cells were grown at 30°C and gene expression was triggered by the addition of 2% f.c. galactose in the exponentially growing culture. Immunofluorescence was performed as described in Materials and Methods. The DNA (stained with Höechst 33352) is shown in

blue, the nucleolus (stained with anti-Nop1 antibody) in red and the p53-Mdm2 complex (stained with anti-p53 and anti-Mdm2 antibodies) in green. The yellow circles surrounding the cells were inserted to highlight the typical disposition of the dot in respect to the DNA and the nucleolus.

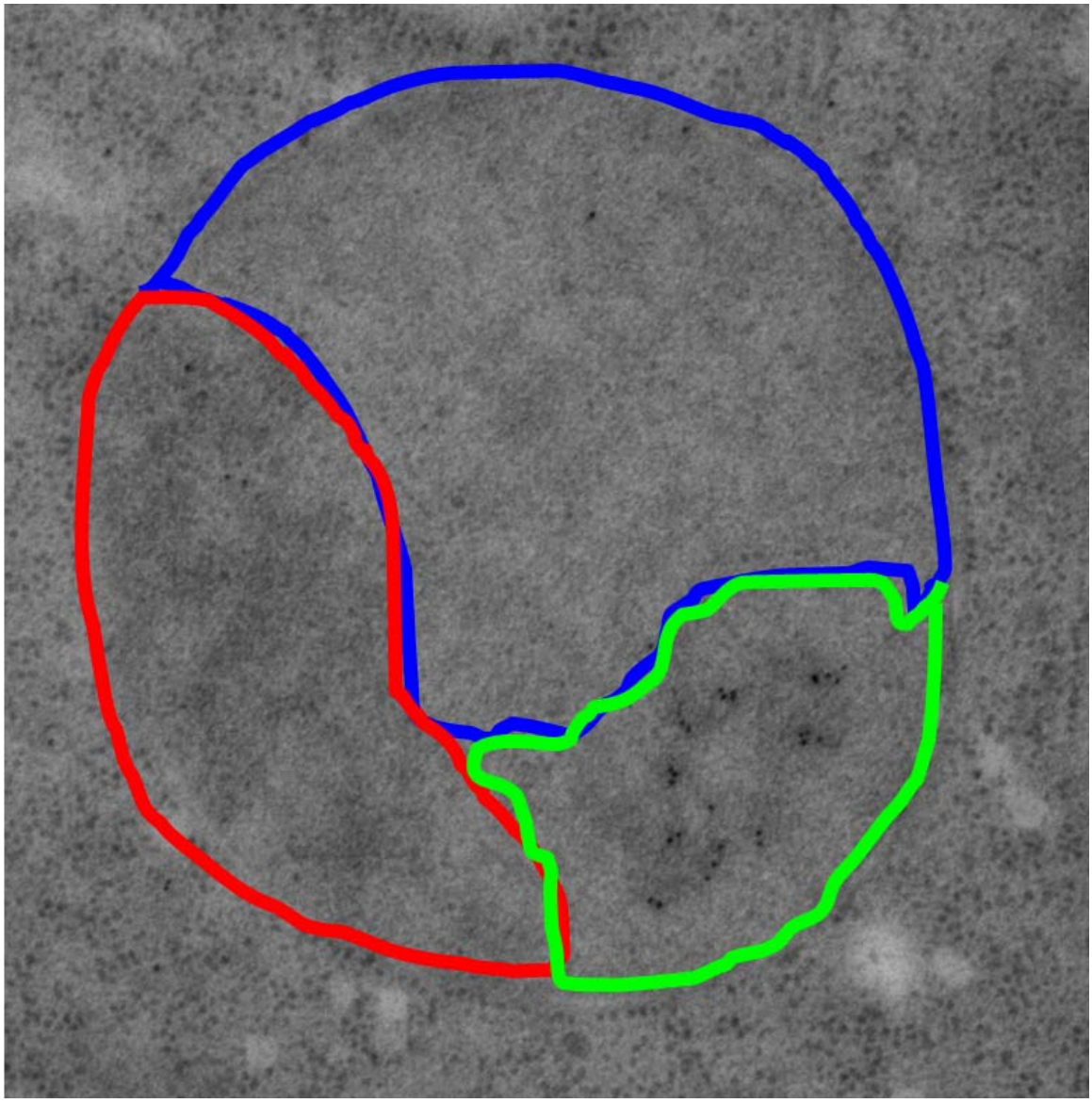

Figure 2.2.37 | The p53-Mdm2 dot is adjacent to the yeast nucleus. The same cell as in Figure 2.2.36 is shown here, but three different areas in the yeast nucleus are highlighted in colours: a light dense area corresponding to chromatin (blue), a denser area with no gold particles corresponding to the nucleolus (red) and a denser area with gold particles corresponding to the p53-Mdm2 dot (green). The p53-Mdm2 dot is found always in the proximity of the nucleus, confirming what we observe with immunofluorescence.

Considering that the vast majority of aggresomes described – until now – in human cells and in yeast are located in the cytoplasm (Corboy *et al.*, 2005; Haslbeck *et al.*, 2005), we consider this piece of information as another clue pointing towards the organelle hypothesis. Moreover, the distribution of the electron density over which the gold is found does not resemble that of aggregates and also the positioning of the gold particles is not that typical of aggregates (Prof. Ed Hurt, personal communication).

Surprisingly, the donut shape of the p53-Mdm2 dot is reminiscent of the nuclear bodies in which the human promyelocytic leukemia protein (PML) accumulates (Figure 2.2.38). This is an intriguing finding, considering the strong correlation between p53, sumoylation and PML bodies in human cells (see Introduction) and our results on the inability of p53K386R to localize to the nuclear dot with Mdm2 (see Discussion).

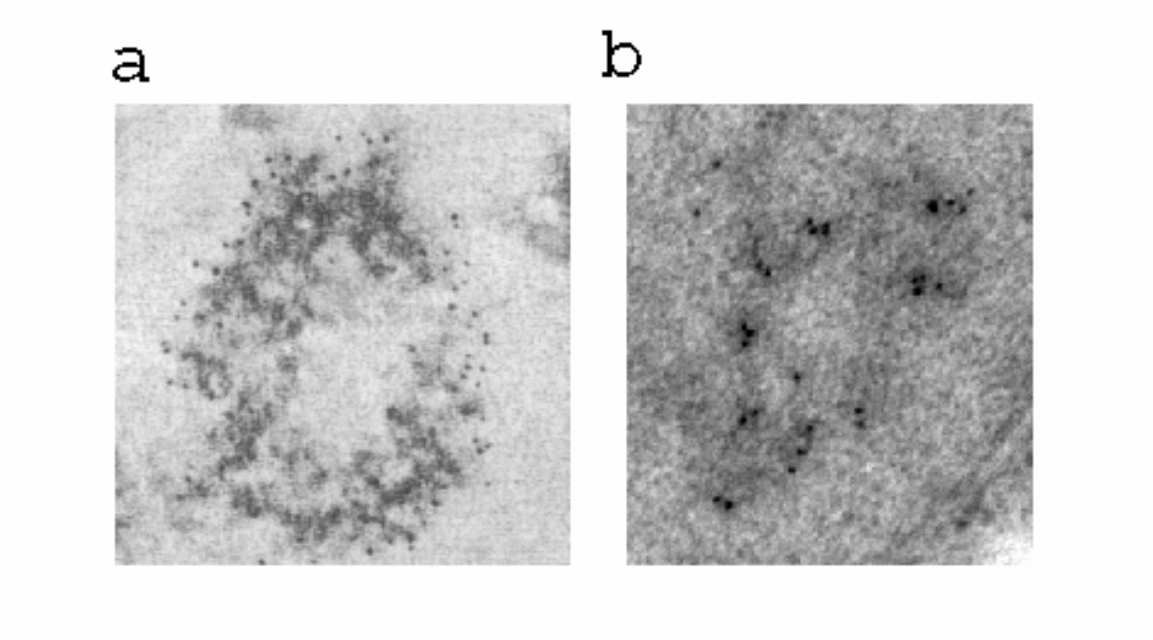

Figure 2.2.38 | The nuclear dot formed by p53 and Mdm2 is reminiscent of human PML bodies. a, Electron microscopy image of a PML body in Hela Cells (taken from (Weis et al., 1994)). **b,** Close-up on the p53-Mdm2 dot from the electron microscopy picture shown in Figure 2.2.35.

Dynamics of p53-Mdm2 nuclear dot formation

The nuclear dot formed by p53 and Mdm2 is not static but rather dynamic as can be seen by the time-lapse microscopy sequence in Figure 2.2.39. Actually, while in the electron microscopy we only see a single big structure recognized by the anti-p53 and anti-Mdm2 antibodies, with fluorescence microscopy it becomes evident that there are several dots. A common observed pattern is the fusion of these smaller dots to form a bigger one (which is likely the structure identified by electron microscopy), although from the time-lapse movies it is possible to detect cells in which several smaller dots co-exist with the bigger one (lower cell in Figure 2.2.39, for instance at the time-frames 40min, 70min, 80min). We can therefore conclude that the p53-Mdm2 dot is very dynamic, with dots fusing and sometimes splitting again into several dots. This also argues against an aggregation type of complex, and suggests that whatever the nuclear region involved in the dot formation is, it is rather dynamic.

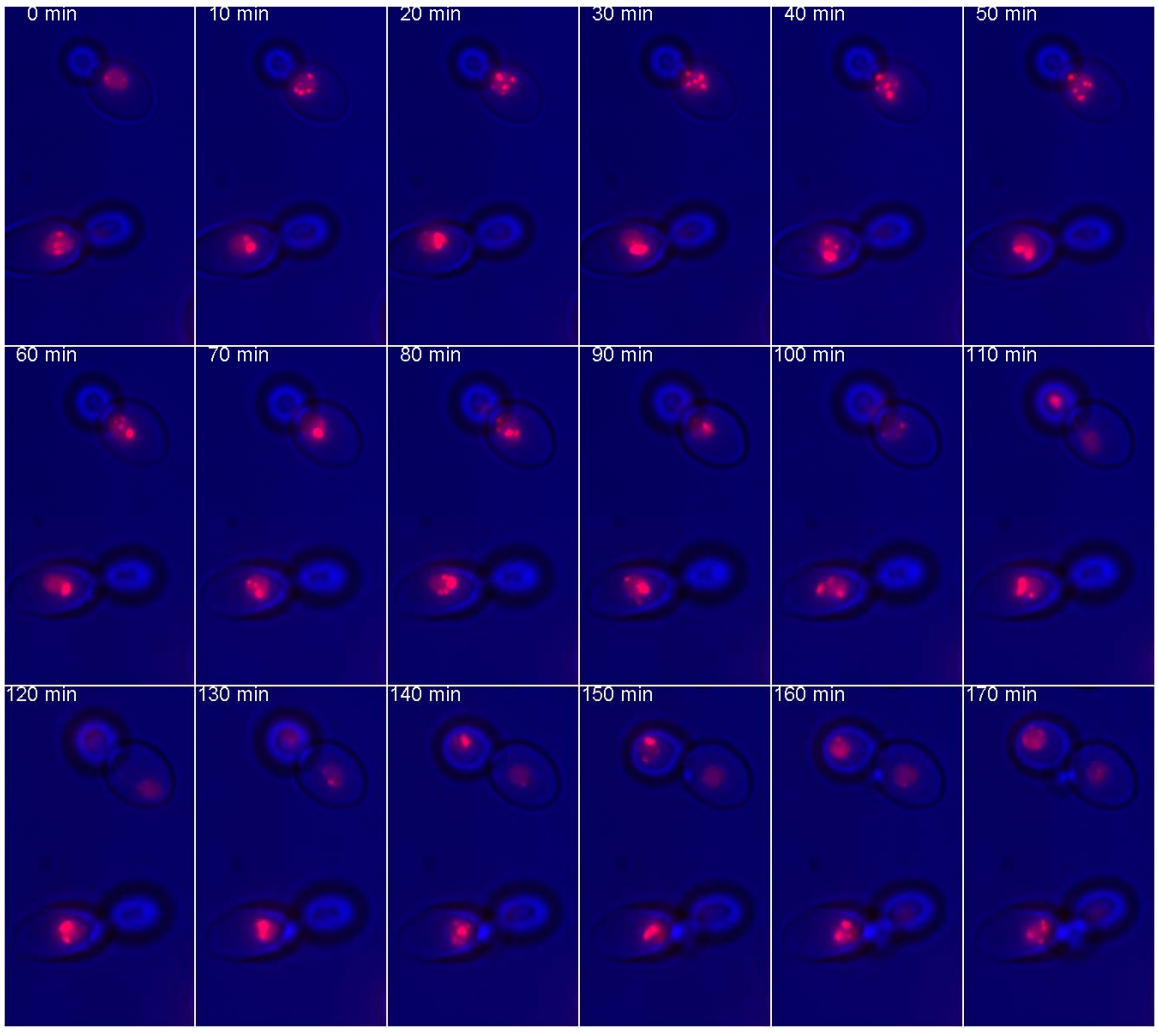

Figure 2.2.39 | Time-lapse microscopy on yeast cells expressing p53 and Mdm2. Cells harbouring the p53-ECFP and the Mdm2-EYFP plasmids were grown at 30°C until they reached exponential growth phase. Cells were then adhered to the bottom of a Petri dish for live imaging (see Materials and Methods). Galactose was added directly into the Petri dish and time-lapse started shortly after. Only Mdm2 position was tracked over time using the YFP filter to avoid bleaching the signals using also the CFP one. p53 appearance in each cell is verified taking stacks before and after the time-lapse (data not shown). Mdm2 is shown in red, and the phase-contrast image of the cells in blue. In the cells in which p53 is made, the many small dots always get together to form a bigger one, which sometimes splits again into smaller ones.

Mdm2 and the yeast nucleolus

An intriguing result concerns the shape of the yeast nucleolus in the presence of Mdm2. When looking at the localization of Mdm2 alone or in the presence of p53 with

electron microscopy we observe a striking difference: the dense area corresponding to the nucleolus seems to be scattered through the nucleus when compared to cells expressing both Mdm2 and p53 (compare Figures 2.2.40 and 2.2.35 and see Table 2.2.1 for statistics). This could indicate that Mdm2 on its own produces a reorganization of the yeast nucleolus. Notably, for the statistics we analyzed only a small number of cells (thirty precisely) and since the thin sections that were cut through the yeast nucleus for electron microscopy analysis could either completely miss the nucleolus or cut it in a way that the typical shape is not visible, we should enlarge the data set in order to confirm these observation.

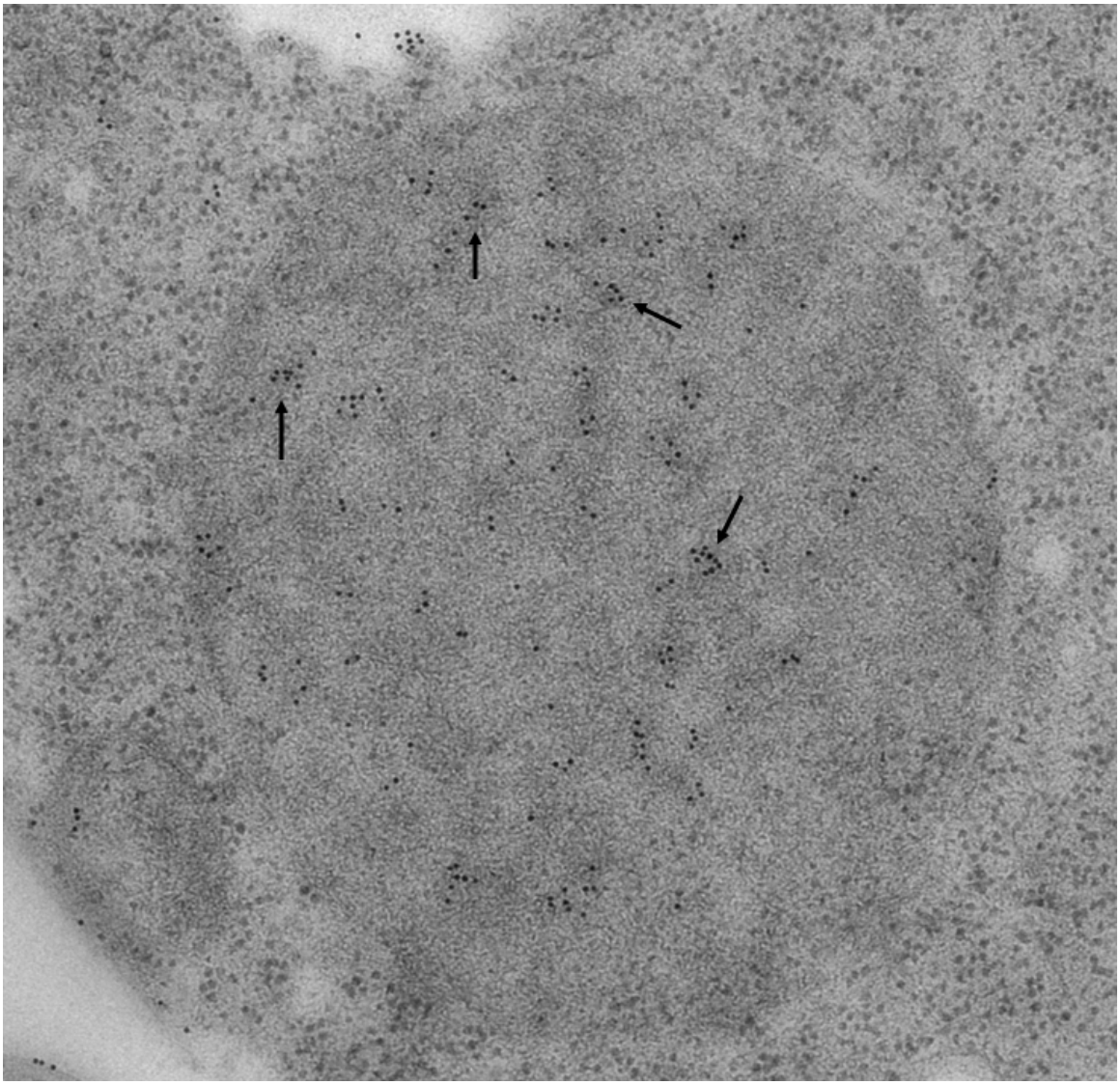

Figure 2.2.40 | Electron microscopy on a yeast cell expressing only Mdm2. Cells were grown at 30°C and induced with 0.5% f.c. galactose when they reached exponential growth phase. Cells were then treated for electron microscopy as explained in Materials and Methods. In twenty-nine out of thirty cells analyzed, the yeast nucleolus is not visible. Denser areas are scattered throughout the cell and the gold particles (indicating Mdm2) are mostly found on top of these dense areas (see black arrows).

	p53	Mdm2	p53+Mdm2
% cells with a visible nucleolus	70%	3%	83%

Table 2.2.1 | Statistics on yeast cells analyzed by electron microscopy. A set of thirty cells was analyzed and percentages of cells with a visible nucleolus calculated.

Discussion

Discussion

The aim of this study was to test the sufficiency of the p53-Mdm2 negative feedback for generating oscillations in the context of budding yeast *Saccharomyces cerevisiae*, while taking advantage of this minimalist approach to understand better the biological relevance of such dynamic interactions. This type of circuit differs from previously described synthetic oscillators in that the negative action of Mdm2 on p53 does not occur at the level of transcription, but at the protein-protein interaction and post-translational modification levels, with ubiquitylation playing a key role for the oscillations. The underlying assumption on which we relied for the successful construction of the synthetic p53 network in yeast was that, since targeted degradation by ubiquitylation is conserved in eukaryotes, Mdm2-dependent p53 degradation should occur in yeast cells, conformingly to what happens in human cells. To our great surprise, under all the conditions tested in the course of this study, we failed to detect p53 degradation; even when UbcH5B – which is the human E2 that interacts with Mdm2 to ubiquitylate p53 – or p300 – the human E4 that was shown to transform monoubiquitylated into polyubiquitylated p53 – are expressed together with Mdm2, p53 is not degraded.

Remarkably, p53 is instead sumoylated by Mdm2 in yeast and we find that the residue which is the major target for this modification in human cells (lysine 386) is also responsible for p53 sumoylation in yeast. Furthemore we observe a strong enhancement of Mdm2-mediated p53 sumoylation in the presence of the human nucleolar protein $p14^{ARF}$, scenario which mirrors what happens in human cells as well. Finally, we find a correlation between p53 sumoylation and the formation of nuclear bodies in yeast cells, which look like the nuclear bodies formed by the promyelocytic leukemia protein (PML) in human cells, where p53 and Mdm2 are also localized under certain circumstances.

Why is p53 not degraded in *S. cerevisiae*?

There are several explanations which could account for the failure of Mdm2-mediated p53 degradation in budding yeast.

Mdm2 and p53 are not interacting in yeast

In order for Mdm2 to ubiquitylate p53, the two proteins need to be in the same compartment (Xirodimas *et al.*, 2001). If in yeast p53 and Mdm2 are localized to different cellular addresses, ubiquitylation and subsequent p53 degradation cannot occur. Our data on p53 and Mdm2 localization (when each is expressed alone or when they are expressed together), using both the fusion p53-ECFP and Mdm2-EYFP proteins and the native ones, exclude this possibility (see Figures 2.2.3, 2.2.8 and 2.2.12 in Results Part Two). As a matter of fact, p53 and Mdm2 always co-localize to a dot inside the yeast nucleus (see Figure 2.2.37 in Results Part Two), and this co-localization is lost when using a mutant p53 protein for which binding to Mdm2 is disrupted (see Figure 2.2.14 in Results Part Two). Hence, we can discard the possibility that Mdm2 cannot ubiquitylate p53 because the two proteins are far from each other.

p53 and Mdm2 aggregate

Even though we are sure that p53 and Mdm2 interact in yeast, the proteins could be forming a non-functional aggregate. The first, instinctive reaction one has looking at the p53-Mdm2 dot, in fact, is that it is an aggregate caused by the over-expression of exogenous proteins in the host organism. Although we still don't have a clear answer to the question "aggresome or organelle?" (see Conclusions and future plans), there are several observations that favour the latter hypothesis.

First of all, the dot is inside the nucleus and, although recently nuclear aggresomes have been described (Fu *et al.*, 2005), aggregates have been generally identified as cytosolic deposits of misfolded proteins (Markossian *et al.*, 2004).

p53 being transcriptionally active in the presence of Mdm2 (see Figure 2.2.22 in Results Part Two) and Mdm2 being active as SUMO ligase for p53 (see Figures 2.2.29 and 2.2.31 in Results Part Two) also argue against the idea that p53 and Mdm2 are aggregating, as well as the fact that the dot is visible also with cells grown at 20°C (see

Figure 2.2.34 in Results Part Two) or when p53 expression levels are lowered (data not shown). In an attempt to better understand the internal arrangement of the p53-Mdm2 dot, we performed immunogold labelling on thin sections of high pressure frozen, lowicryl embedded yeast cells expressing only Mdm2 or p53 together with Mdm2. The electron dense region on top of which the gold particles are found does not resemble a typical aggregate (as assessed by comparing our images to published electron microscopy images of aggregates); rather, we find a strong similitude between the dot formed by p53 and Mdm2 in yeast and the nuclear bodies formed by the promyelocytic leukemia protein (PML) in human cells, in which p53 and Mdm2 are also recruited under certain circumstances (see Figure 2.2.38 in Results Part Two) (Pearson *et al.*, 2000; Kurki *et al.*, 2003). Furthermore, aggresomes are known to recruit components of the ubiquitin-proteasome pathway (Fu *et al.*, 2005) and proteins therein are usually ubiquitylated (Johnston et al., 1998). We do not detect, instead, any ubiquitylation of p53, on the opposite we find that p53 is sumoylated and sumoylation is involved in the association of proteins with nuclear (functional) bodies.

Mdm2, p53 or both are post-translationally modified in a way that prevents ubiquitylation to occur

We know that p53 and Mdm2 are subject, in human cells, to a series of post-translational modifications (phosphorylation, acetylation, *etc.*) which modulate their interaction as well as their localization or interaction with other proteins (see Introduction). We cannot exclude that p53, Mdm2 or both are modified in yeast in a way that prevents Mdm2-mediated p53 ubiquitylation. For instance, it has been shown that p53 acetylation inhibits Mdm2-mediated ubiquitylation in human cells with mechanisms that go beyond simple competition for the lysine residues to be modified (Li et al., 2002). Recently, it has been reported that phosphorylation inhibits sumoylation of c-Fos (Bossis et al., 2005), showing that two modifications occurring on different residues and in different domains on a protein substrate can also interfere with each other . It is possible, therefore, that p53 is post-translationally modified in yeast (*e.g.* acetylated) and that this modification keeps p53 from being ubiquitylated by Mdm2 (although mass spectrometry analysis did not identify any such modification).

Also, Mdm2 can be modified in a way that is consequential to its E3 ligase activity. From the results obtained in this study, it is in fact clear that Mdm2 is modified; with higher molecular weight bands becoming more detectable at later time points with respect to Mdm2 expression (see Figure 2.2.22 in Results Part Two). Since Mdm2 is degraded in yeast, these higher molecular weight species could be ubiquitylated forms of the protein (although I failed to detect them when probing Mdm2 purification with an antibody specific for mono- and polyubiquitylated proteins – data not shown). Mdm2 degradation is known to be subject to regulation in various ways, since Mdm2 stabilization leads to enhanced p53 degradation (Sharp *et al.*, 1999; Zeng *et al.*, 2003; Feng *et al.*, 2004). It would be intriguing, therefore, to attribute Mdm2 incapability to ubiquitylate p53 to the fact that the enzyme is busy with its own ubiquitylation. To test this hypothesis, I generated a mutant Mdm2 in which lysine 446 was exchanged for arginine, following the data published by Buschmann *et al.* which indicated residue 446 as the major site for Mdm2 autoubiquitylation (Buschmann et al., 2000). Preliminary results with this mutant show that p53 is stable (data not shown), although it is difficult to interpret them since I realized that the paper in which the mutation was described has been retracted (Fuchs *et al.*, 2002), making it arguable whether lysine 446 is indeed the major site for Mdm2 autoubiquitylation.

Post-translational modifications on p53 or Mdm2 required for efficient Mdm2-mediated ubiquitylation do not take place in yeast

The opposite situation could also be the cause for the failure of p53 ubiquitylation in yeast. In the literature, in fact, we find few examples of post-translational modifications which are required for effective p53 degradation in human cells (Chernov et al., 2001; Zhou et al., 2001). Were this the case, we should conclude that yeast is not an adequate model organism to study p53 ubiquitylation, unless we identified the required modifications and were able to either mimic or force them to happen.

Something is missing

When I started this project, Mdm2 was thought to be sufficient to polyubiquitylate p53 in the presence of ubiquitin, E1 and E2, both *in vitro* and *in vivo*. During the course

of this study, however, there has been a shift in paradigm: Mdm2 is now believed to catalyze only p53 monoubiquitylation, which is not sufficient to target p53 to the proteasome, whereas p300 – an acetyltransferase known to acetylate p53 thus enhancing p53 transcriptional activity – is the enzyme responsible for the conversion of monoubiquitylated species into polyubiquitylated ones (Grossman et al., 2003). This and other findings, which highlight the need for additional proteins in order for efficient Mdm2-dependent p53 degradation to take place (Gu et al., 2002; Gronroos et al., 2004), raise the possibility that Mdm2 alone is not enough to trigger p53 degradation., Some essential component(s) seems to be missing, although known candidates like p300 do not change p53 stability when expressed in yeast (see Figures 2.2.15 and 2.2.18 in Results Part Two), Most studies on p53 degradation are carried on in human cell lines expressing endogenous proteins which might be essential for p53 degradation without being identified as such. For years Mdm2 has been considered as the only E3 ligase for p53, so when researchers were performing *in vivo* ubiquitylation assays on human cells, they were not considering the fact that those cells have additional ligases which might account for the observed p53 degradation. In this respect, the use of yeast instead of human cells should facilitate the search for the minimal network able to support p53 degradation, being much more likely in this synthetic context the absence of additional proteins acting in the background (we confide that this would have some biological meaning and not be an artefact caused by the difference between human and yeast cells).

Yeast and human ubiquitylation pathways are incompatible

Although the ubiquitylation pathway is considered to be conserved in eukaryotes, it is possible that a human E3 ligase – like Mdm2 – cannot interact with the yeast homologue (Ubc4) of its interacting human E2 (UbcH5B), or that a human E2 cannot interact with a yeast E1. To discard the possibility that the failure of p53 degradation were caused by incompatibility between Mdm2 and Ubc4, I expressed in yeast UbcH5B and saw no change in p53 stability (see Figure 2.2.17 in Results Part Two).

We cannot discard the hypothesis that the human E1 is needed as well, since the classical view that there is no selectivity at the level of the E1 is changing. It is in fact being suggested that different members of the E1 enzyme family may have specialized

functions (perhaps preferentially transferring ubiquitin or ubiquitin-like proteins to particular E2 enzymes or directly to certain substrate proteins) and may be assigned to distinct cellular compartments (Hochstrasser, 1996).

p53 is ubiquitylated to an extent which is insufficient to signal its degradation

The fact that I never detected p53 degradation does not exclude that p53 is being (mono)ubiquitylated by Mdm2, but that the amount of ubiquitylated molecules is below detection on a western blot. Actually, the detection of protein ubiquitylation requires a careful methodological approach, because ubiquitination is a dynamic process that involves both ubiquitinating and deubiquitinating enzymes – and deubiquitinating enzymes are known to be very active in cellular extracts (Rajapurohitam *et al.*, 2002). Consequently, only a small fraction of the cellular pool of a protein that is destined for proteasomal degradation is modified by ubiquitin at any given time. As an example of the difficulty in detecting ubiquitylated p53 species, in the paper published by Krummel e*t al.*, the authors mention that attempts to detect endogenous ubiquitylation on wild type p53 failed even when exogenous Mdm2 was expressed and proteasome inhibitors used. To be able to detect p53 ubiquitylation, the authors had to transfect cells with exogenous p53, Mdm2 and ubiquitin (Krummel et al., 2005).

In this study, I tried various expression levels for p53, ranging from over-expression (using 2% galactose) to lower levels (down to 0.006% galactose), so one could argue that at least when over-expressing p53 in the presence of Mdm2, I should be able to detect some ubiquitylation. Instead, not even when pulling p53 down with an antibody or when purifying a 6xHIS-tagged version of the protein on columns, did I detect a signal using an antibody again mono- and polyubiquitylated proteins (data not shown). Considering that Mdm2 sumoylates p53 and that, despite the fact that the sumoylated fraction constitute less than 5% of the total protein pool, it is possible to detect this modification on a western blot using crude yeast lysates, I am prone to conclude that ubiquitylation is not happening at all, for some of the other reasons discussed here.

Mdm2 is after all not responsible for p53 degradation in normal cells

Although Mdm2 was the only known ligase to be in charge of p53 degradation when this study started, many additional ligases have been recently described (see Introduction). It is interesting that, for each of these newly discovered ligases, the respective authors claim a central role in p53 degradation, which is not confirmed by the data found in the other papers; for instance, in the work published by Dornan e*t al.*, showing that COP1 is an E3 ligase specific for p53, the authors perform RNAi on U2OS cell lines to show the effect on p53 levels of knocking down COP1, Mdm2 and Pirh2, singularly or in combination (Dornan et al., 2004). Looking at their data, p53 levels strongly increase with RNAi against COP1 or Mdm2. In the recently published paper by Chen *et al.*, which identifies ARF-BP1 as the ligase responsible for p53 turnover in unstressed cells, the authors show similar RNAi experiments on U2OS cell lines, but this time the effect on p53 levels of RNAi against COP1 is much weaker (Chen *et al.*, 2005). In light of these considerations, I decided to test other E3 ligases for p53, namely Pirh2 and COP1, trying to find the one which was able to catalyze p53 ubiquitylation in my yeast system. Unfortunately, none was successful (I also tried to combine two of them, like Mdm2 and COP1, Mdm2 and Pirh2, but failed to observe any change – data not shown).

Sumoylation wins over ubiquitylation

Our discovery of Mdm2-dependent p53 sumoylation in yeast brought the hope that this might represent the reason for failed degradation. In the literature, in fact, it has been proposed that sumoylation inhibits degradation of IkappaBalpha (Desterro *et al.*, 1998), while the role of sumoylation in contrasting p53 ubiquitylation is subject to debate (Gostissa et al., 1999; Muller et al., 2000; Rodriguez et al., 1999). We found that the non-sumoylatable mutant of p53 (p53K386R) is as stable as wild type p53. This suggests that sumoylation is not impeding p53 ubiquitylation. Another possibility is that the affinity of Mdm2 for Ubc9 is much higher than that for Ubc4 – the yeast homologue of the human E2 (UbcH5) which pairs with Mdm2 to ubiquitylate p53 – resulting in p53 being preferentially sumoylated and not ubiquitylated (small amounts of the protein might be

ubiquitylated, but again this could be below detection). This hypothesis is supported by the observation that Ubc9 has a remarkable ability to interact with other proteins, likely consequence of the distinct electrostatic potential distribution that characterizes Ubc9 as compared to other E2s (Tong et al., 1997).

p53 is sumoylated and not ubiquitinated in yeast

p53 sumoylation by Mdm2 in budding yeast came as a surprise, expecting as we were that Mdm2 would function as a ubiquitin E3 ligase, since this is well established in the literature. Mdm2 promoting p53 sumoylation is instead a rather recent finding, and the consequences of sumoylation on p53 await further studies (Chen *et al.*, 2003). Not only did we find that p53 is sumoylated by Mdm2 (see Figure 2.2.29 in Results Part Two), we also found that the lysine which is the major site for sumoylation in human cells (lysine 386) is also responsible for p53 sumoylation in yeast (see Figure 2.2.31 in Results Part Two). Even more intriguing is the finding that yeast cells co-expressing Mdm2 and $p14^{ARF}$ show enhancement in p53 sumoylation (see Figure 2.2.32 in Results Part Two). This is in perfect agreement with results obtained using human cell lines, where Mdm2 and $p14^{ARF}$ co-ordinately sumoylate p53 targeting it to the nucleolus (Chen *et al.*, 2003)

Functional role of p53 sumoylation

The role of sumoylation in p53 transcriptional activity is at the moment unclear, since results obtained up to now claim either its enhancement (Gostissa *et al.*, 1999; Rodriguez *et al.*, 1999) or its inhibition (Schmidt *et al.*, 2002) or no effect at all (Kwek et al., 2001). On the other hand, sumoylation has been reported to activate other transcription factors such as the heat shock transcription factor 2 (HSF2) (Goodson et al., 2001). Although we have not done yet extensive studies on this topic, our preliminary data suggest that sumoylation does not inhibit drastically transcription activity of p53 (see Figure 2.2.22 in Results Part Two), but further studies are needed to elucidate this point.

Sumoylated p53 exhibits different localization than non-sumoylated one

Our results indicate that sumoylation is necessary for the co-localization of p53 with Mdm2 to the nuclear dot, since when Mdm2 is co-expressed with the non-sumoytable mutant of p53 (p53K386R) the dot is not detected (see Figure 2.2.33 in Results Part Two). Looking at the distribution of p53K386R-ECFP in the cell, we notice that it is diffuse throughout the entire cell, but does not show a stronger staining into the nucleus like wild type p53 (compare Figures 2.2.3 and 2.2.33 in Results Part Two). If this on the one hand suggests that the nuclear levels of p53K386R are lower than those of the wild type p53, on the other hand we do not see an exclusion of p53K386R from the nucleus, therefore we believe that the failed co-localization with Mdm2 to the dot is not due to a failed interaction with Mdm2. This idea is supported by preliminary data of a cytoplasmic p53 mutant (which carries a mutation on lysine 305 which is essential for p53 nuclear import (Liang *et al.*, 1998)) which is found to co-localize to the dot with Mdm2 (data not shown). This result suggests that even if p53K386R is mostly cytoplasmic, Mdm2 could still interact and co-localize with it to the nuclear dot seemingly to what happens with cytoplasmic p53.

We suggest that sumoylation is the tag that re-directs p53 to the nuclear dot, in the same way in which sumoylation of the homeodomain-interacting protein kinase 2 (HIPK2) correlates with its localization to nuclear dots (Kim et al., 1999) and sumoylation of the PML protein is required for its localization into PML bodies (Muller *et al.*, 1998).

According to the western blot data, the fraction of p53 which is sumoylated is less than 5% of the total protein amount (which is in accordance with what was reported for other sumoylated proteins (Johnson *et al.*, 1999)), yet light microscopy on living cells shows that p53 is all concentrated in the dot with Mdm2, which we believe is made of sumoylated p53. This contradiction could either reflect an artefact of the microscopy set-up, in that p53 molecules are also somewhere else in the cell but the fluorescence in the dot is so high that the remaining fluorescence is undetectable, or it could be explained by a model in which sumoylation is required to target p53 to the nuclear dot, but once the protein is there, it gets rapidly desumoylated, so that the fraction of sumoylated p53 at any given time is very low.

What is the p53-Mdm2 nuclear dot?

From our indirect immunofluorescence analysis we notice a non-random positioning of the p53-Mdm2 dot in respect to the nucleolus (see Figures 2.2.36 and 2.2.37 in Results Part Two), so we suspect some sort of relation between the two. In fact, even if in the majority of the cells there is no overlap between the nucleolus (detected using an antibody against Nop1) and the p53-Mdm2 signals, this could reflect a limited accessibility to the antibody of the dense nucleolar structure (similar antibody accessibility problem has been reported for other nucleolar proteins (Wansink et al., 1993) and for p53 itself (Rubbi *et al.*, 2000). Moreover, Nop1 resides in the dense fibrillar component (DFC) of the nucleolus and the p53-Mdm2 complex could be located in another area of the nucleolus not stained by an antibody against Nop1.

Indeed there is a strong relation between p53, Mdm2 and the nucleolus in human cells (see Introduction) and moreover Mdm2 carries a cryptic nucleolar localization signal (NoLS) (Lohrum *et al.*, 2000) and it is found in human nucleoli under different circumstances (Kurki et al., 2003; Bernardi et al., 2004). It would therefore not be surprising if there were a connection between the nucleolus and the p53-Mdm2 cellular location.

Another intriguing possibility is that p53 and Mdm2 are triggering in yeast the formation of PML body-like structures, given the resemblance of the p53-Mdm2 dot to a PML body in human cells (see Figure 2.2.38 in Results Part Two). Actually, PML bodies are suspected to play some role in RNA-processing events (Borden, 2002), and in human cells are often found close to other nuclear bodies like the Cajal bodies (Borden, 2002), which in turn are related to the nucleolus (Gall, 2000).

Who brings whom to the dot?

An important aspect to be clarified is whether Mdm2 is simply mediating p53 sumoylation and localizes to the dot because of this function, or if Mdm2 itself is dictating the cellular address to which p53 has to go. Fluorescence microscopy on yeast cells expressing p53 and Mdm2 shows that, when p53 expression is low, the two proteins co-exist in several small dots, which resemble Mdm2 foci (data not shown). Since I performed time-lapse microscopy following only Mdm2 (I used only YFP excitation

since using also the CFP one would lead to bleaching of the signal), it is unclear whether p53 is recruited to sites in which Mdm2 is already present or if the two proteins go together somewhere else. Although Mdm2 foci are also dynamic and move towards each other to fuse into a brighter bigger dot, their behaviour is different from that observed in the presence of p53, which always lead to the (rapid) formation of the bigger dot. Electron microscopy images seem to confirm that the distribution of Mdm2 when alone is different from that in the presence of p53, and that the two proteins accumulate in a single donut-shape structure rather than in many smaller areas, but this could also reflect a detection limit of the immunogold labelling.

Mdm2 localization in yeast

Mdm2 localization is *per se* fascinating. Light microscopy clearly shows that the protein is distributed in several nuclear – very dynamic – dots, often at the periphery of the nucleus (see Figures 2.2.8 and 2.2.10 in Results Part Two). Sometimes, Mdm2 appears as a half-moon that resembles the nucleolus (see Figure 2.2.8 in Results Part Two). Considering that, as mentioned above, Mdm2 carries a cryptic NoLS, it could be that the protein localizes to the nucleolus or to some extra-nucleolar region at least during some stages of the cell cycle. Moreover, when expressing Mdm2 together with $p14^{ARF}$, a human nucleolar protein, Mdm2 localization does not change, or rather, the nuclear speckles become more evident (data not shown). Although I did not detect directly $p14^{ARF}$ localization in yeast, there is in principle no reason for its NoLS not to be recognized in this organism, living the question whether Mdm2 is nucleolar very much open.

More promising is the finding that the yeast telomere-binding protein Rap1 has a cellular distribution strikingly similar to that of Mdm2 (Figure 3.3). The resemblance is so remarkable that we are prone to believe that Mdm2 also binds telomeres in yeast.

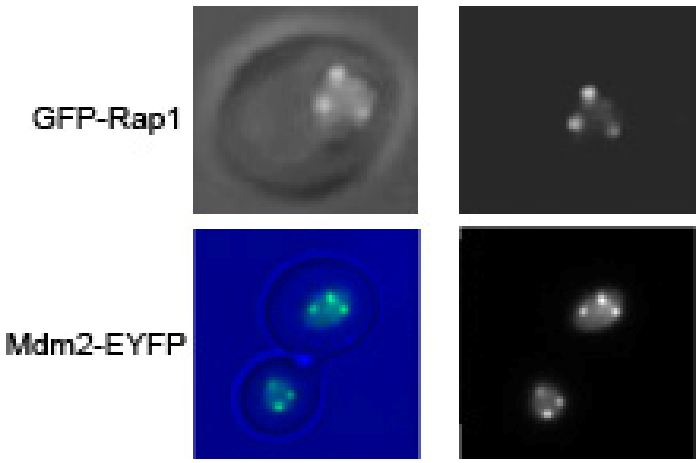

Figure 3.3 | Comparison between GFP-Rap1 and Mdm2-EYFP localization in budding yeast. GFP-Rap1 localization has been adapted from (Laroche et al., 2000). The left panel shows the merged image between phase-contrast and the fluorescent image. The right panel shows the GFP and YFP channel alone, respectively.

Mdm2 binding to telomeres has never been described in the literature, while the ability of Mdm2 to bind to DNA (Zhao et al., 2005) and RNA in general (Elenbaas et al., 1996), as well as p53-depedent Mdm2 association with chromatin (White et al., 2006), have been documented. Mdm2 putative nucleolar localization and association with yeast telomeres do not exclude each other, since in the literature we find examples of proteins which localize to the nucleolus and to telomeric foci (Gotta et al., 1997).

Re-shaping the nucleolus?

While looking at the electron microscopy pictures of a yeast cell expressing only Mdm2 and a cell expressing p53 and Mdm2, we noticed that only in the latter case it was possible to visually detect a darker (denser) region which we identified as the nucleolus (compare Figures 2.2.35 and 2.2.40 in Results Part Two). A statistical analysis on a small set of cells confirmed the observation that around 97% of the cells expressing only Mdm2 have a dispersed nucleolus, while circa 80% of the cells expressing p53 and Mdm2 have a visually detectable nucleolus. We could speculate that the presence of Mdm2 somehow inhibits the proper assembly of the yeast nucleolus or re-organizes it in a way that prevents us to detect the nucleolus in the electron microscopy pictures. Typical nucleolar shape is restored in the presence of p53.

These are, though, only speculations and more experiments are necessary to clarify this point. For instance, for the statistics we analyzed only a small number of cells and since the thin sections that were cut through the yeast nucleus for electron microscopy analysis could either completely miss the nucleolus or cut it in a way that the typical shape is not visible, we should enlarge the data set in order to confirm these observation.

Conclusions

Conclusions

The secrets of nature lie very well hidden from the grasp of our senses. We try through a continuous cycle of observations/experiments and theories/models to approach the truth as much as possible, though the depths of knowledge we can reach are unambiguously limited by the tools we use in our quest. This iterative process also dictates that we must accept parts of previous knowledge as true, even temporarily, and use them as working hypotheses to move forward. Sometimes such hypotheses lurk unquestioned for so long that we tend to confuse them with solid facts. Fortunately for science (and maybe unfortunately for the frustrated researcher) new tools and new approaches sometimes give results which shake the very foundations of these hypotheses. The p53-Mdm2 module could not have escaped such fate, since its extreme biological significance has been an irresistible temptation for a plethora of scientists, generating huge amounts of data at an amazing rate. However, one could argue that the countdown for bringing down such dogmas in this field started about one year ago when Krummel and colleagues published a paper which has important consequences on our understanding of p53 function (Krummel *et al.*, 2005). With their work on transgenic mice, these authors showed that the C-terminal lysines believed to be critical to p53 regulation are instead dispensable, since homozygous mutant mice where the seven C-terminal lysines were changed to arginines (Trp-53(7KR)) are surprisingly viable and phenotypically normal. Their explanation for the discrepancy between their results and previous ones is that usually studies on p53 are carried out either *in vitro* or over-expressing the protein, therefore in conditions of perturbed stoichiometries between p53 and its regulators. The work by Krummel and colleagues is not alone in its provocative appeal for revisiting the knowledge that has been accumulated over the years on p53 and its negative regulator Mdm2 (Brooks *et al.*, 2006).

In this study we tried an approach which combines advantages of the previous *in vivo* and *in vitro* studies; a synthetic p53-Mdm2 module was implanted in a eukaryotic organism to which it was completely foreign. Thus, the system was allowed to operate "in isolation" from other characterized or unknown components, like *in vitro*, while it enjoyed all other luxuries, provisions, but also limitations, of its more "natural" environment, the eukaryotic cell. The emergent properties of the synthetic network in

this context should be affected from the properties of each component much more than in the wild type system, since there are no other components or putative alternative pathways to buffer the effect. Taking this into consideration, it is not surprising that our first attempts were unfruitful, since they were based on previous "facts" about the properties of p53 and Mdm2 which are now in question.

Nonetheless this synthetic approach proved to be a powerful tool since studying the properties of the proteins in such isolation emphasized some of their underestimated previously described properties (like the sumoylation of p53 by Mdm2) and paves the way to clarify certain ambiguities like the effect of sumoylation on p53 degradation or localization.

Furthermore the synthetic system gives rise to a whole new set of issues which might or might not be specific for the yeast background. For instance, "is Mdm2 binding to telomeres?", "are p53 and Mdm2 able to trigger the formation of nuclear bodies (NBs) in yeast?", "what is the functional significance of such NBs?", "is p53 interacting with yeast septins?"

The localization of p53 to the yeast septin ring is an exciting discovery that deserves further investigation. Indeed, the fact that SUMO and sumoylated proteins are found at the bud neck and that p53 is itself a SUMO substrate, suggests that p53 may directly interact with SUMO or with SUMO substrates. Since the localization of sumoylated septins to the ring is cell cycle dependent (Johnson *et al.*, 1999), it would be interesting to see whether p53 localization to the septin ring follows a similar temporal pattern. It is also intriguing to investigate the relation between Mdm2 and the yeast nucleolus structure, to assess whether Mdm2 is effectively re-shaping it.

We therefore believe that the synthetic biology approach used in this study provides a different but complementary framework that not only helps in re-evaluating the relationship between p53 and its regulators, but also unlocks completely new areas of research.

Materials and Methods

Strains

Bacterial strains

All yeast plasmids used in this study can be propagated in *E. coli* to facilitate cloning. For manipulation of constructs until final version – to be transformed in yeast – I used any of the following *E. coli* strains:

XL1-Blue (*recA1 endA1 gyrA96 thi-1 hsdR17 supE44 relA1 lac [F' proAB lacI^{q} ZΔM15 Tn10(Tet^{r})], stratagene)*

BL21(DE3) (*E.coli B F^{-} dcm ompT hsdS(r$_{B}^{-}$ m$_{B}^{-}$) gal λ(DE3), stratagene)*

*TOP10 (F^{-} mcr*A Δ(*mrr-hsd*RMS-*mcr*BC) φ80*lac*ZΔM15 Δ*lac*X74 *deo*R *rec*A1 *ara*D139 Δ(*ara-leu*)7697 *gal*U *gal*K *rps*L (Str^{R}) *end*A1 *nup*G, *invitrogen*)

Yeast strains

For the analysis of Mdm2 proteasome-dependent degradation I used the following strains (kind gift of Dr. Dieter H. Wolf):

YWO 0607	*Mat***a** *ura3 leu2-3,112 his3-11,15 Cans Gal+*
YWO 0612	*Mat***a** *pre1-1 pre2-2 ura3 leu2-3,112 his3-11,15 Cans Gal+*

For all other experiments described in this thesis I used the strain ESM356-1 (*Mat***a** *ura3-53 leu2Δ1 his3Δ200 trp1Δ63*, kind gift of Dr. Michael Knop)

Plasmids

The plasmid pRS314-SN containing wild type *p53* gene was a kind gift of Prof. Bert Vogelstein. For all experiments with the fusion protein I used this plasmid, in which I substituted the original *p53* gene with the *p53-ECFP* fusion gene. For all experiments with native p53, I used the pRS314-SN plasmid as a template from which to amplify the p53 *gene*, which I cloned into the yeast vectors p413-GAL/GALS (kind gift of Dr. Michael Knop).

Mdm2 was amplified using pCDNA3.1-Mdm2 as a template (kind gift of Dr. Gaetano Gonzales). I then inserted the mdm2 gene into the yeast vectors p416-GALS/TEF.
All the p53 and Mdm2 mutants (performed as indicated in the respective references) were obtained with the PCR mutagenesis protocol (see below) and therefore remained in the same plasmids.
The plasmid pLPC containing $P14^{ARF}$ was a kind gift of Dr. Gaetano Gonzales. I restricted the gene out of this plasmid (BamHI-XhoI) and ligated it into the yeast vector p413-TEF.
Plasmids pEYFP-N1 and pECFP-N1 were a kind gift of Dr. Philippe Bastiaens. I used these vectors as templates from which I amplified the *ecfp* and *eyfp* genes respectively.
The plasmid pFLAG-CMV containing the *cop1* gene was a kind gift of Dr. Elisabetta Bianchi. I restricted the gene out of this plasmid and ligated it into p416-TEF.
For subcloning I used the plasmids pQE-30, PCM252 and PBluescriptII(+).

Growth media

The media used to grow *E. coli* (LB, SOC) were supplied by the European Molecular Biology Laboratory. *S. cerevisiae* cultures were grown in synthetic complete (SC) media, lacking one or more amino acids for maintenance of plasmids, with 2% raffinose in order to have a full response when adding galactose for gene expression induction. The materials and the recipe to prepare the SC medium are the following:

Materials

Yeast nitrogen base without amino acids but with ammonium sulfate (YNB)
Drop out powder

Protocol

For 1 L of medium, mix 6.7 g of YNB and 2 g of drop out powder in 700 ml of water. Stir for 20 min. Sterilize, add 100 ml of 20% raffinose (filter-sterile), top up to 1 L with water, filter again.

Yeast transformants were plated on SC plates with 2% glucose, which I prepared according to the following recipe:

Materials

YNB

Drop out powder

Agar

Protocol

For 1 L, mix 6.7 g of YNB with 2 g of drop put powder in 400 ml of water. Stir for 20 min. At the same time, add 20 g of Agar to 500 ml of water and stir for 20 min. Autoclave, then mix the two solutions, add 100 ml of 20% glucose, add water to reach 1 L final volume, mix well and pour plates.

Cultivation conditions

E. coli

E. coli strains were cultivated in LB medium at 37°C. Recombinant clones were selected in LB plates supplied with 100µg/ml Ampicilline.

S. cerevisiae

Wild type *S. cerevisiae* strains were grown in YEPD medium or plates at 30°C. Transformants were grown in SC + 2% raffinose medium or SC plates + 2% glucose. For pre-cultures, a medium size yeast colony was picked and transferred to 50 ml medium and grown at 30°C overnight. Cultures were grown on shakers at 230 rpm.

Freezing and storage of yeast strains

Yeast cells were scraped from a plate and were suspended into 1 ml of (sterile) 15% glycerol in water. The suspension was vortexed, immerged into liquid nitrogen and then stored at -80°C.

Galactose induction of protein expression

Strains carrying plasmids were cultivated at 30°C on a shaker at 230 rpm O.N. Cultures were diluted in the morning to an OD_{600} of 0.5. When the cells reached an OD_{600} of about 1.5, galactose was added to a final concentration of 0.006%, 0.5% or 2% depending on the downstream application. Cells were incubated typically for 1-2 hours before glucose to a final concentration of 3% was added to stop gene expression from the Gal promoter. Alternatively, cycloheximide was added to the medium to a final concentration of 100 µg/ml.

DNA and RNA isolation

Small scale plasmid DNA isolation from E. coli strains (minipreps)

5 ml of LB culture were grown O.N. at 37°C. Cells were harvested and minipreps were performed using the Qiagen MiniPrep Kit following the manufacturer's recommendations, with the following differences:

-the optional wash with PB was always done;

-the DNA was always eluted adding 40 µl of water to the column, waiting 5 minutes and finally centrifuging at top speed.

Isolation of RNA from S. cerevisiae

Total RNA extraction was performed according to the following protocol:

Materials

Citrate buffer

1.2 M sorbitol, 20 mM K_2HPO_4, 1 mM EDTA; pH 5.8

Denaturing solution

250g Guanidinthiocyanate, 293 ml DEPC-water, 24,6 ml 10% Sarkosyl, 17,6 ml 0,75 M sodium citrate, pH 7,0; heated at 65°C for dissolving

Protocol

O.N. cultures were harvested at 3-5K rpm for 5 min at 4°C and put on ice. Cells were resuspended in 10 ml citrate buffer, incubated with 1-5 mg/ml of Lytic enzyme (ISN) for 20-30 min at 37°C, and spun down at 5K rpm for 5 min at 4°C. Secondly, the cell were broken by suspending in 5 ml of denaturing solution and 5 ml of DEPC water, vortex for 1 min. Then 0.5 ml of 2M Na-acetate (pH 4,0), 5 ml phenol, and 1ml 44 $CHCl_3$/Isoamylalcohol (24:1) were added, this solution was vortex vigorously for 10 sec and placed on ice for 15 min. After centrifugation at 10K rpm for 20 min at 4°C the aqueous phase was pulled off to a fresh tube and precipitated with 5 ml of Isopropanol at –20 °C overnight. On the next day, the nucleic acids were centrifuged at 10K rpm for 20 min at 4°C. The pellet was washed with 80 % Ethanol, spun down at 10K rpm for 5 min, dried in a Speed-Vac as short as possible and dissolved in 300 µl of DEPC-water.

Isolation of DNA from Agarose gels

DNA was extracted from agarose gels cutting the band(s) at the appropriate size(s) and Qiagen Gel Extraction Kit was used to purify the DNA. Sometimes, to obtain purer DNA, ethanol precipitation was also used (see below).

Ethanol precipitation to purify DNA

The volume was adjusted to 100 µl in water. 1 µl glycogen (1µg) and 10 µl 3M NaAcO pH 5.5 were added and the solution vortex to mix well. 330 µl of pure EtOH were added, the solution vortex and then was frozen in liquid nitrogen. After spinning for 10 min at maximal speed (in a table-top centrifuge), the supernatant was carefully removed and washed once with 600 µl of 70% EtOH, which was completely removed. The pellet was finally resuspended in 10 µl of water.

DNA *in vitro* recombination methods

Restriction Enzyme Digestions of plasmids and PCR products

Purified plasmids or PCR products were digested with restriction enzymes to create appropriate cohesive ends for DNA ligation. Restriction enzymes were used in the appropriate salt buffers and under the conditions recommended by the manufacturers. The total reaction volume was always 50 µl and 2 µl of enzyme was used (total amount of glycerol in the reaction was always kept below 5% of final volume) when digestion was needed for further cloning or 0.5 µl when digestion was used to check for positive clones after ligation. Whenever possible, double digestions were performed (for this purpose, the NEB catalogue was consulted for compatibility of restriction enzymes), otherwise sequential digestions were performed according to the NEB recommendations. Incubations were generally carried out at 37˚C for 3 hours (for 1 hour when digestion was used to check positive clones after ligation). Digested species were purified either by agarose gel electrophoresis or by using the Qiagen PCR purification kit to remove small cleaved DNA fragments (see below). Plasmid dephosphorylation was avoided to increase efficiency of ligation when the restriction enzymes used produced non-compatible sticky ends (therefore likelihood of plasmid self-ligation is low).

Plasmid-insert ligations

During the course of this study, I tried many different protocols for ligations, eventually settling for O.N. ligation at 16°C (using a PCR machine). The final reaction volume was always 20 µl and contained 2 µl of ligase buffer (supplied with the enzyme), 1 µl of bacteriophage T4 DNA ligase (Roche), 2 µl of cut vector, 5 µl of cut insert and 10 µl of water. The following day, 10 µl of this reaction mixture were transformed using 20 µl of *E. coli* competent cells (to increase ligation efficiency, sometimes ethanol precipitation to purify the DNA was used prior to transformation, see above). The control ligation of the vector without the insert was always performed as an indication of restriction efficiency (the vector was not dephosphorylated whenever the used restriction enzymes produced incompatible sticky ends).

Enzymatic reaction clean-up

Products of restriction reactions were purified using the Qiaquick PCR purification kit, following the manufacturer's protocol for enzymatic reaction clean-up, when the restriction yielded undesirable fragments smaller than 80 bp. When the undesired products were higher than 80 bp the desired products were separated by preparative agarose gels and purified with the Qiagen gel-extraction kit.

Polymerase chain reaction (PCR) (Kleppe et al., 1971; Saiki et al., 1985)

The Polymerase Chain Reation (PCR) was used for amplifying DNA fragments, creating fusion genes, screening bacterial colonies for constructs and for mutagenesis. In all applications the final volume of the reaction mixture was 50 µl, containing 3 µl of 10 mM solution of each primer and 1µl of 10 mM dNTP mix. PCR screening was carried out using 0.2 units of *Taq* polymerase, whereas for the remaining applications 1-2 units of *Pwo* polymerase were used.

DNA amplification

The desired DNA fragments were amplified using 10-50 ng of template, for plasmid-borne templates, or by lysing a single bacterial colony, by boiling at 98°C for 5 min in water, for genomic templates. When the primers in use introduce a restriction site, extra bases are added to the 5' end of the primer to facilitate restriction. The exact number of these bases is specified for each restriction enzyme by its manufacturer (NEB). The procedure followed was:

- Heating at 97°C for 2 min (the polymerase is added at the end of these 2 min when hot-start is needed) ;
- Denaturation at 97°C for 30 sec;
- Annealing at 2°C below the lowest melting temperature of the primers, as calculated by the manufacturer (Sigma);
- Elongation at 72°C for X min where X is the size of the desired fragment in kb. For fragments smaller than 1 kb the time used was 1 min.
- Final elongation at 72°C for 8 min.

- Cooling at 4°C

The number of denaturation-annealing-elongation cycles was between 20 and 30 (the number of cycles was kept low to avoid introducing mutations and increased only when the PCR yield was insufficient for cloning purposes).

Fusion gene construction

Constructs which are the fusion of two DNA fragments were built as follows:

Each fragment was amplified for 10 cycles (if it was plasmid-borne) or for 30 cycles (if it came from genomic DNA). The primers used were such that the 3' reverse primer of the first fragment contained a complementary sequence to the 5' forward primer of the second fragment, marking the fusion of the two fragments (Figure 5.1). The overlap was such that the melting temperature was quite high (above 63°C).

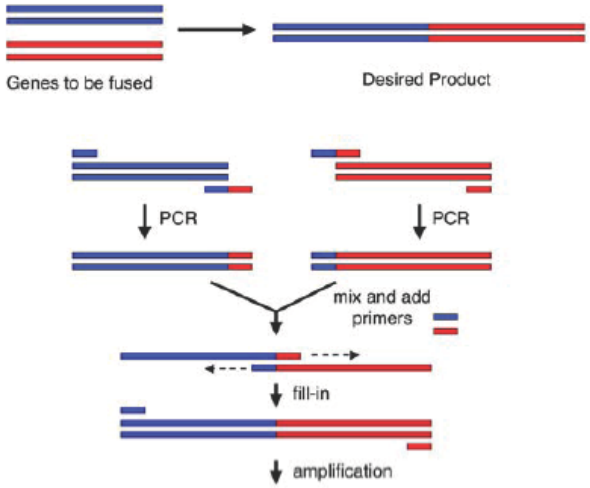

Figure 5.1 | Fusion of two genes by PCR. The two genes are amplified by using a 3' primer for the first gene and a 5' primer for the second one that contain the sequence at the fusion point and are complementary to each other. When the products of the two PCR reactions are mixed, under PCR conditions, the top strand of the first reaction will hybridize to the bottom strand of the second and the gaps will be filled-in by the polymerase leading to the full-length desired product. Including the external 5' and 3' primers (single colour rectangles) results in amplification of the latter product. Adapted from (Michalodimitrakis, 2005)

Aliquots from both reaction mixtures were directly mixed in a new tube, with fresh dNTPs, polymerase and the 5' forward primer of the first fragment and the 3' reverse primer of the second. The aliquots were such that the ratio of the aliquots' volume was roughly within the range of the ratio of the sizes of the two fragments.

In all applications PCR products were cleaned using the Qiaquick PCR purification kit (Qiagen), except when there were by-products. In those cases the desired product was purified by gel-extraction, after agarose gel electrophoresis, using the Gel-Extraction kit (Qiagen).

Mutagenesis

To create all point mutations used in this study I used the Quickchange site-directed mutagenesis (Stratagene). The reactions were always carried as indicated by the manufacturer.

DNA sequencing of PCR products

Once positive clones for ligation were obtained, constructs were sequenced by the EMBL Genomics Core Facility to make sure that the sequence of the insert was correct.

Agarose gel electrophoresis

Agarose gels were made with 0.8% - 2% (w/v) agarose in 25-50 ml TBE buffer. The percentage of agarose used depended on the size of the DNA fragments, although for preparative gels, 0.7% agarose was preferred in order to minimize the amount of agarose in the sample during the gel-extraction procedure. 2.5 µl of ethidium bromide solution (10 mg/ml) were added per 50 ml agarose gel. DNA samples were loaded with 6 µl non-denaturing DNA loading buffer. Gels were run at a constant current of 60 mA, in TBE buffer, for between 40 minutes and 1.5 hours. DNA was visualised by ethidium bromide fluorescence under ultraviolet (UV) illumination at 260 nm.

Transformation methods

Transformation of E. coli

Tubes were pre-chilled on ice for 20 min. The appropriate number of aliquots of competent cells was thawed on ice for 15 min. When the cells were thawed, few microliters of plasmid(s) were added to the cells and the tubes were left on ice for 30 min. Heat-shock was performed for 45 sec in a pre-warmed bath at 42°C. Tubes were put back on ice for 2 min. 1 ml of warm SOC medium was added to each tube and the culture grown for maximum 1h at 37°C. Finally, cells were plated on appropriate selection plates. When transforming a ligation product, cells were spun down (at maximal speed) so to remove 800 µl circa of supernatant. The remaining 200 µl were plated.

Transformation of S. cerevisiae

If aliquots of competent cells were not available, I first made fresh aliquots using the following protocol:

Heat-shock competent S. cerevisiae cells

Materials

LiSorb

100 mM LiOAc, 10 mM TRIS pH 8, 1 mM EDTA pH 8, 1 M Sorbitol (MERCK). Filter-sterilize

Carried DNA (Salmon Sperm)

Protocol

5 ml of YPD were inoculated with a single colony and incubated at 30°C on a shaker for 12 to 16 hours. This pre-culture was then diluted to a final concentration of OD600 0.15 in a final volume of 100 ml. The cells were grown at 30°C until OD600 was 0.5-0.7. They were then harvested at RT for 3 min at 2200 rpm, washed once with 0.1-0.5 volume of sterile water and once with 0.1-0.2 volume of LiSorb (always at RT). Supernatant was completely removed (to get rid of the LiSorb) and the pellet resuspended in a total

volume of 360 µl of LiSorb and 40 µl of carrier DNA (previously denaturated for 10 min at 99°C and cooled on ice for 3 min). The cell suspension was aliquoted in 50-100 µl fractions and directly stored at -80°C (knop et al., 1999).

Transformation

Materials

LiPEG

100 mM LiOAc, 10 mM TRIS pH 8, 1 mM EDTA pH 8, 40% PEG 3350. Filter-sterilize

Protocol

Competent cells in 50 µl aliquots were thawed on ice and typically 2 µl of DNA were added mixing well (snipping the tube). After waiting 2-3 min with the cells on ice, a 6 fold volume of LiPEG was added and the cells were well mixed and let incubate at RT for 30 min. The heat shock was performed in a water bath at 42C for 15 min. The cells were then washed once with water (spinning for 3 min at 2000 rpm at RT), sedimented with centrifugation, resuspended in 200 µl of water and plated on plates with SC-media lacking the appropriate amino acid or base. Plates were incubated at 30°C for two days, and transformants streaked out as single colonies. After two days one single, well growing colony was streaked out as a patch, frozen and stored at -80°C.

Protein analyses

Poly-Acrylamide Gel Electrophoresis under denaturing conditions (SDS-PAGE)

Materials

Loading buffer 2x (8ml)

100 mM NaPi pH 6.8, 6M Urea, 5% SDS, 1 mM EDTA, Bromphenol Blue (a dash), 1.5 % (w/v) DTT was freshly added prior to use

Running Buffer 10x (1L)

Tris 30.2 g, glycine 188 g, SDS 10g, H_2O up to 1L

Protocol

Criterion pre-cast gels (Biorad) Tris-HCl (7.5% or 15%, dependently on the size of the proteins) were loaded with the samples, then run at constant 170 V for approximately 1h. Visualization of the proteins was done with Western Blotting.

Western Blotting

Materials

Transfer buffer 10x without EtOH (1L)

Trizma 30 g, glycine 144 g

Transfer buffer 1x +EtOH (1L)

Transfer buffer 10x 100 ml, EtOH 200 ml, H_2O up to 1L

PBS (obtained from the European Molecular Biology Laboratory)

PBST(1L)

PBS 1L, Tween 20 50 µl (0.05%)

Protocol

Western Blots were performed using the Criterion Blotter system from Biorad, according to the manufacturer's instructions. However, optimal transfer conditions were constant current at 380 mA for 30 min. After the transfer, the nitrocellulose membrane was washed with water and stained with Ponceau S Solution (Sigma), in order to visualise the total amount of protein in each lane. Background staining was removed by washing with de-ionised water. The membrane was then scanned with an Agfa Duoscan f40 scanner or a photocopy was made. The stain was subsequently removed by washing with PBS. The membrane was blocked at RT for 1h with 5% milk in PBST and then exposed to the primary antibody for 1h at RT and to the secondary antibody, which is for 45 min. Each step with an antibody was followed by four 10 min washes with PBST. After the final wash, GFP bands were visualised with the ECL Western blotting analysis kit from Amersham Biosciences and the exposed films were scanned.

Blots quantification

Using Adobe Photoshop, a rectangular area was define into each band to quantify and the corresponding mean intensity obtained through the function "Histogram". To this number the background – calculated in the same way – was subtracted.

Stripping blots

Materials

Stripping buffer

100 mM TRIS/HCl pH 6.8, 2% SDS, βME 0.007 v.v or 143x

Protocol

Antibodies were stripped from the membranes through incubation of the latter ones in stripping buffer, at 60°C for 30 min. The membranes were then washed 6 times with PBS 1x to get rid of the stripping buffer. At this point, normal western blot procedure was carried on, starting from the blocking step (see western blot procedure paragraph in this chapter)

Analysis of protein turnover in yeast cells

Material

HU buffer

100 mM NaPi pH 6.8, 6M Urea, 5% SDS, 1 mM EDTA, Bromphenol Blue (a dash), 1.5 % (w/v) DTT was freshly added prior to use

Protocol

Cells were grown and induced following the previously described procedures. Samples were collected at different time points (typically, one sample right before addition of galactose – referred to as BI – one sample when glucose is added to stop induction – referred to as time 0' since from this moment on the protein's levels are followed – and once every hour, for up to 3-6 hours). Sample collection was done adding 150 µl of 1.85

M NaOH + 7.5 % βME to 1 ml of culture and throwing the tube into liquid nitrogen. When all samples were collected, they were thawed on ice. To precipitate proteins, 150 µl of 55% TCA were added to each sample and tubes were kept on ice for 10 min. They were then spun down for 5 min at maximal speed in a cold centrifuge and the supernatant completely removed. Pellets were resuspended in HU buffer, heated at 65C for 10 min, spun down 5 min at RT. Equal amounts of samples were analysed by SDS-PAGE followed by Western Blotting. Remaining volumes of samples were stored at -20°C for at least one repetition of the western blotting analysis.

Purification of 6xHIS-tagged proteins

Materials

Binding Buffer

50 mM TRIS/HCl, 100 mM NaCl, 20 mM imidazole, 1 mM DTT, (8M urea if purifying under denaturing conditions), pH 8.0

Washing Buffer

50 mM TRIS/HCl, 100 mM NaCl, 50 mM imidazole, 1 mM DTT, (8M urea if purifying under denaturing conditions), pH 8.0

Elution Buffer

50 mM TRIS/HCl, 100 mM NaCl, 300 mM imidazole, 1 mM DTT, (8M urea if purifying under denaturing conditions), pH 8.0

Depending on whether the buffers contained or not 8M urea, the purification was done under denaturing or native conditions respectively.

Protocol

2 L yeast culture was grown and induced as previously described (see normal growth and galactose induction of proteins paragraphs in this chapter), except that induction was carried on for 3 hours in order to have more protein for the purification step. Cells were then centrifuged at 4000 rpm for 10 min, washed with PBS + 0.5 mM PMSF at RT and

transferred to a 50 ml Falcon tube. Lysis buffer was added to have a final volume of 25 ml to which an equal volume of glass beads was added. The suspension was poured into a planet mill beaker and cells were spun at 350 rpm 3 times, each time for 3 min. The cell lysate was then first centrifuged in a 50 ml Falcon tube at 4000 rpm for 10 min, then the supernatant was poured into an ultracentrifuge tube and ultracentrifuged for 1 h at 33.500 rpm. For the purification, the lysate was filtered through a 0.22 µm filter, then loaded on a Ni-NTA column, which was pre-equilibrated with 5 volumes (respect to the column volume) of Binding Buffer. The column was washed with 10 volumes of Washing Buffer and elution was done with Elution Buffer. Protein concentration was estimated by the Bradford method using BSA as a standard and a gel was run with the elution fractions to analyse the purification result.

Immunofluorescence

Materials

KPi buffer

1M KPi pH 6.5, 0.5 mM MgCl2

SP buffer

3M Sorbitol, 100 mM KPi pH 6.5, 0.5 mM MgCl2

SPβ buffer

SP with 14 µl βME for 10 ml of SP (added fresh)

Mounting medium

55% Glycerol in PBS with 0.5 µg/ml of DAPI or Hoechst

Protocol

Cells were grown O.N.. When OD_{600} reached 0.5-1, induction of proteins was triggered adding galactose to a final concentration of 2%. Induction was done for 1 or 2 hours. 40 ml of cells were fixed at RT for 90 minutes (with occasional inversions of the tubes) adding 5 ml of KPi buffer and 5 ml of 37% Formaldehyde (Sigma). Cells were subsequently washed 3 times in 1 ml of SP buffer (cells were transferred to 1.5 ml tubes

after the first wash). Centrifugations were carried out at 1500 RPM for 3-5 min. Cells were always resuspended by spinning the tube. Cells were then digested for 75 min at 30°C on a roller in 1 ml of SPβ buffer with 200 µg/ml of Zymolyase 100 T (added from stock: 10 mg/ml in SP, stored at -20C). To recognize properly digested cells, 5 µl of sample were observed under the microscope to see whether more than 80% of the cells no longer showed phase contrast. Cells were washed 3 times in SP buffer and finally resuspended in 0.5 ml SP buffer with 2 mM PMSF (from stock: 200 mM in DMSO). Slides were prepared coating each well with ca. 100 µl of Polylysine 0.1% for 5 min followed by 5 washes with water. 35-50 µl of cells were added to each well and let settle for 20 min in a humid chamber in the cold. Cells are then aspirated using a 0.2 ml tipp and a vacuum pump. 10-15 µl of PBS-1%TX100 are added to each well and let incubate for 1 min. This step was repeated once. Cells were washed 3-5 times with PBS-1%BSA. Cells were incubated in PBS-1%BSA for 40 min at RT, followed by incubation with the primary antibodies (diluted in PBS-1%BSA) for 2 hours in a humid chamber. Cells were then washed 5 times with PBS. Incubation with secondary antibodies (always diluted in PBS-1%BSA) was performed for 1 hour in a humid chamber. Cells were washed 5 times with PBS-1%SBA, 3 times with PBS (letting two of the three washing solutions for 5 min on the wells). PBS was carefully aspirated from the wells and 3.5 µl of mounting medium were added to wells, after letting them dry for 3 min. A coverslip was glued to the slide using nail polish and slides were stored at -20°C for successive analysis.

In vivo staining of the yeast nucleus

Materials

Höechst 33352 (5 ng/ml)

Protocol

Höechst 33352 was added directly into the cell culture and incubated for 5 min before imaging the cells.

Microscopic techniques

For live cells imaging, cells were adhered with Concavalin A on small glass bottom Petri dishes (MaTek). All live cell experiments were performed at RT. Live cell imaging was performed on an imaging system (DeltaVision Spectris; Applied Precision) equipped with CFP, YFP, Cy3 filters (Chroma Technology Corp.), a 10x NA 1.4 oil immersion objective (plan Apo, IX70; Olympus), softWorRx software (Applied Precision), and a CoolSNAP HQ camera. ImageJ software was used to mount the images and to produce merged colour images. No image manipulations other than brightness adjustment were used. For certain fluorescence images, always stacks encompassing at least the thickness of the cell nucleus were recorded (spacing 0.5 µm). Maximum projections of the fluorescence images were generated, coloured and sometimes superimposed with the phase-contrast image using ImageJ software.

Electron microscopy

Immunolabelling

Materials

Blocking buffer

1.5% BSA + 0.1% Fish skin gelatin in PBS

Antibodies

rabbit polyclonal Mdm2 (H-221), mouse anti-rabbit linker antibody

Protein A Gold 10nm

Protocol

Yeast cells were high pressure frozen, lowicryl embedded and sections prepared. Non-specific binding sites were blocked by incubating sections with blocking buffer for 15 min. Sections were then rinsed in blocking buffer 3x 10 min each. Incubation with primary antibody went on for 30 min, then non-reacted primary antibody was removed with 10 min washes with PBS. Sections were then incubated on mouse anti-rabbit

antibody for 20 min. Sections were washed with PBS for 10 min with PBS. Sections were then incubated with Protein A Gold 10nm for 20 min and then rinsed in blocking buffer and PBS for 1 h total. Sections were fixed in 1% glutaraldehyde in PBS for 5 min, rinsed with water and stained with UAc, PbCi. Grids were placed section down onto droplets of 1 part 1% (v}v) aqueous uranyl acetate and 9 parts 2% (v}v) aqueous olyvinyl alcohol (MW 10000, Sigma) solution for 10 min on parafilm and air dried after removal of excess solution. Sections were then viewed and photographed with a transmission electron microscope.

Antibodies

All the antibodies used in this study are listed here:

Primary Antibodies

Mono- and poly ubiquitylated proteins, multi ubiquitin chains, mouse mAb (clone FK2), BIOMOL international, LP

p53 (FL-393), agarose conjugated, rabbit polyclonal, Santa Cruz biotech

p53 (DO-1), mouse monoclonal, Santa Cruz biotech

p53 (Pab 1801), mouse monoclonal, Santa Cruz biotech

p53 (N-19), goat polyclonal, Santa Cruz biotech

Mdm2 (H-221), rabbit polyclonal, Santa Cruz biotech

Mdm2 (SMP14), mouse monoclonal, Santa Cruz biotech

PCAF (H-369), rabbit polyclonal, Santa Cruz biotech

COP1, rabbit polyclonal, BIOMOL

P14ARF (ab3642), rabbit polyclonal, abcam

UbcH5, rabbit polyclonal, BostonBiochem

Anti-HIS antibody, kind gift of Dr. Elena Conti

Anti-FLAG M2 antibody, mouse monoclonal, Sigma

NOP1, mouse monoclonal, kind gift of Dr. Michael Knop

Cdc14, rabbit polyclonal, kind gift of Dr. Michael Knop

tubulin, rabbit polyclonal, kind gift of Dr. Michael Knop

PGK, mouse monoclonal, kind gift of Dr. Michael Knop

Secondary antibodies

peroxidase-conjugated donkey anti-mouse, Jackson Immuno Reasearch Laboratories

CY3-conjugated donkey anti-mouse, kind gift of Dr. Michael Knop

Reaction network and parameters for the simulation of the models discussed in Results Part One

Figure 2.1.1

In all three cases considered, rates corresponding to reactions of the same type were given identical values, such that the same parameter set was used each time, specifying constants for all four reaction types (counting forward and reverse reactions).

Parameters:

Dimerization rate: k_{on}=1e09 $M^{-1}s^{-1}$

Dissociation rate: k_{off}=1 s^{-1}

Monomer modification rate: k_a=1e-02 s^{-1}

Monomer demodification rate: k_a=1e-02 s^{-1}

Initial conditions: 600 M molecules, 0 molecules all remaining species.

Figure 2.1.2

Reaction Network for model simulated deterministically (c) and stochastically (e) in which B represses its transcription by binding to its own transcription activator AP.

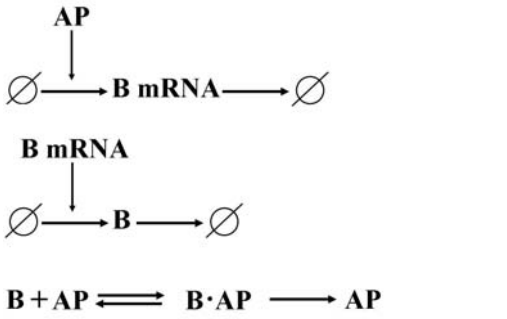

Parameters used for simulation:

k_1=0.1 s^{-1} (B_mRNA production)

k_2=0.5 s^{-1} (B production)

k_{on}=1e09 M^{-1} s^{-1} (complex formation)

k_{off}=0.01 s^{-1}

k_{deg}=log(2)/80 s^{-1}

Initial conditions: 100 AP molecules, 0 molecules for remaining species

Reaction Network for model simulated deterministically (d), stochastically (f) in the case in which B oligomerization is considered. B octamer is now the species that binds to the transcription factor AP, repressing B transcription.

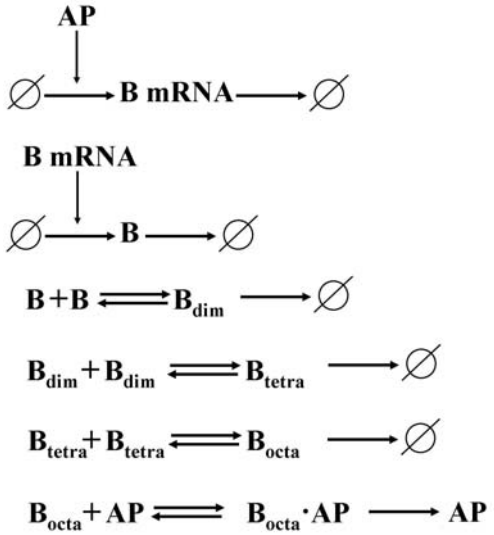

Parameters used for simulation:

k1=0.1 s^{-1} (B_mRNA production)

k2=0.5 s^{-1} (B production)

kdeg=log(2)/80 s^{-1}

kon=1e09 M^{-1} s^{-1} (complex formation between B_8 and AP)

koff=0.01 s^{-1}

kon_2=1e06 M^{-1} s^{-1} (dimer formation)

$koff_2$=0.01 s^{-1}

kon_4=1e06 M^{-1} s^{-1} (tetramer formation)

$koff_4$=0.01 s^{-1}

kon_8=1e09 M^{-1} s^{-1} (octamer formation)

$koff_8$=0.1 s^{-1}

Initial conditions: 100 AP molecules, 0 molecules for remaining species

Figure 2.1.3

Reactions considered for the simulation

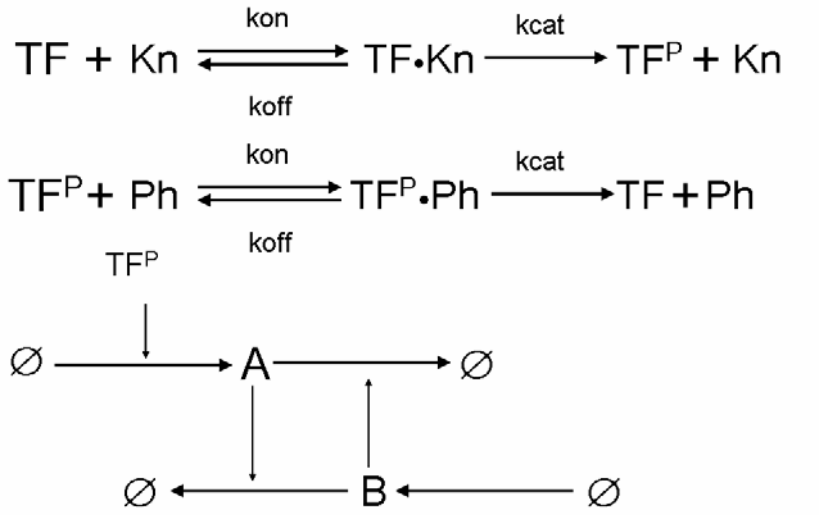

Parameters used for simulation:

D= 0.8 μm^2 s^{-1}

k_{on}=1e07 M^{-1} s^{-1}

k_{off}=1 s^{-1}

k_{cat}=1 s^{-1}

k_{pA}=1 s^{-1} (protein A production)

k_d=1e06 M^{-1} s^{-1} (proteins A and B degradation)

k_{pB}=7e-04 M^{-1} s^{-1} (protein B production)

Initial conditions: TF=200 molecules, TF^P=TF•Kn=TF^P•Ph=A=0 molecules, Kn=Ph=60 molecules, B=250 molecules

Figure 2.1.4

Scheme of the model: B can form a complex with its promoter prom, giving B_prom. B_prom catalyses the production of B. B degradation occurs by first order decay.

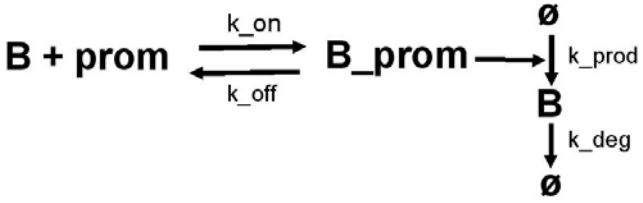

Parameter values used for the simulations of the HIGH and LOW cases:

Reactions constants (units)	**HIGH**	**LOW**
k_on (M^{-1} $s^{-1)}$	10^8	10^8
k_off (s^{-1})	8.3	1.66
k_prod (s^{-1})	1	0.2
k_deg (s^{-1})	10^{-2}	10^{-2}

References

Kobayashi, K.*, et al.* (2003). Essential Bacillus subtilis genes**,** *Proc Natl Acad Sci U S A*, 100, 4678-83

Smith, H. O.*, et al.* (2003). Generating a synthetic genome by whole genome assembly: phiX174 bacteriophage from synthetic oligonucleotides**,** *Proc Natl Acad Sci U S A*, 100, 15440-5

Noireaux, V. and Libchaber, A. (2004). A vesicle bioreactor as a step toward an artificial cell assembly**,** *Proc Natl Acad Sci U S A*, 101, 17669-74

Martin, V. J.*, et al.* (2003). Engineering a mevalonate pathway in Escherichia coli for production of terpenoids**,** *Nat Biotechnol*, 21, 796-802

Herrera, S. (2005). Synthetic biology offers alternative pathways to natural products**,** *Nat Biotechnol*, 23, 270-1

Gilbert, E. S.*, et al.* (2003). A constructed microbial consortium for biodegradation of the organophosphorus insecticide parathion**,** *Appl Microbiol Biotechnol*, 61, 77-81

Benner, S. A.*, et al.* (2003). Synthetic biology with artificially expanded genetic information systems. From personalized medicine to extraterrestrial life**,** *Nucleic Acids Res Suppl*, 125-6

Hutter, D.*, et al.* (2002). From phosphate to bis(methylene) sulfone: Non-ionic backbone linkers in DNA**,** *Helv. Chim. Acta*, 85, 27777-2806

Geyer, C. R.*, et al.* (2003). Nucleobase pairing in expanded Watson-Crick-like genetic information systems**,** *Structure*, 11, 1485-98

Yeger-Lotem, E.*, et al.* (2004). Network motifs in integrated cellular networks of transcription-regulation and protein-protein interaction**,** *Proc Natl Acad Sci U S A*, 101, 5934-9

Hartwell, L. H.*, et al.* (1999). From molecular to modular cell biology**,** *Nature*, 402, C47-52

Kashtan, N. and Alon, U. (2005). Spontaneous evolution of modularity and network motifs**,** *Proc Natl Acad Sci U S A*, 102, 13773-8

Becskei, A. and Serrano, L. (2000). Engineering stability in gene networks by autoregulation**,** *Nature*, 405, 590-3

Gardner, T. S.*, et al.* (2000). Construction of a genetic toggle switch in Escherichia coli**,** *Nature*, 403, 339-42

Becskei, A., *et al.* (2001). Positive feedback in eukaryotic gene networks: cell differentiation by graded to binary response conversion, *Embo J*, 20, 2528-35

Kobayashi, H., *et al.* (2004). Programmable cells: interfacing natural and engineered gene networks, *Proc Natl Acad Sci U S A*, 101, 8414-9

Kramer, B. P., *et al.* (2004). An engineered epigenetic transgene switch in mammalian cells, *Nat Biotechnol*, 22, 867-70

Pourquie, O. (2003). The segmentation clock: converting embryonic time into spatial pattern, *Science*, 301, 328-30

Blatten, C. (2004). Preliminary designs for synthetic chemotactic oscillators, *MIT Summer Synthetic Biology Competition*,

Guido, N. J., *et al.* (2006). A bottom-up approach to gene regulation, *Nature*, 439, 856-60

Hooshangi, S., *et al.* (2005). Ultrasensitivity and noise propagation in a synthetic transcriptional cascade, *Proc Natl Acad Sci U S A*, 102, 3581-6

Pedraza, J. M. and van Oudenaarden, A. (2005). Noise propagation in gene networks, *Science*, 307, 1965-9

Rosenfeld, N., *et al.* (2005). Gene regulation at the single-cell level, *Science*, 307, 1962-5

Dublanche, Y., *et al.* (2006). Noise in transcription negative feedback loops: simulation and experimental analysis, *Mol Syst Biol*, 2, 41

Hooshangi, S. and Weiss, R. (2006). The effect of negative feedback on noise propagation in transcriptional gene networks, *Chaos*, 16, 26108

Elowitz, M. B. and Leibler, S. (2000). A synthetic oscillatory network of transcriptional regulators, *Nature*, 403, 335-8

Atkinson, M. R., *et al.* (2003). Development of genetic circuitry exhibiting toggle switch or oscillatory behavior in Escherichia coli, *Cell*, 113, 597-607

Fung, E., *et al.* (2005). A synthetic gene-metabolic oscillator, *Nature*, 435, 118-22

Chen, M. T. and Weiss, R. (2005). Artificial cell-cell communication in yeast Saccharomyces cerevisiae using signaling elements from Arabidopsis thaliana, *Nat Biotechnol*, 23, 1551-5

Ball, P. (2004). Synthetic biology: starting from scratch, *Nature*, 431, 624-6

Pomerening, J. R.*, et al.* (2005). Systems-level dissection of the cell-cycle oscillator: bypassing positive feedback produces damped oscillations**,** *Cell*, 122, 565-78

Naef, F. (2005). Circadian clocks go in vitro: purely post-translational oscillators in cyanobacteria**,** *Mol Syst Biol*, 1, 2005 0019

Hoffmann, A.*, et al.* (2002). The IkappaB-NF-kappaB signaling module: temporal control and selective gene activation**,** *Science*, 298, 1241-5

Lewis, J. (2003). Autoinhibition with transcriptional delay: a simple mechanism for the zebrafish somitogenesis oscillator**,** *Curr Biol*, 13, 1398-408

Takigawa-Imamura, H. and Mochizuki, A. (2006). Predicting Regulation of the Phosphorylation Cycle of KaiC Clock Protein Using Mathematical Analysis**,** *J Biol Rhythms*, 21, 405-16

Tomita, J.*, et al.* (2005). No transcription-translation feedback in circadian rhythm of KaiC phosphorylation**,** *Science*, 307, 251-4

Guantes, R. and Poyatos, J. F. (2006). Dynamical principles of two-component genetic oscillators**,** *PLoS Comput Biol*, 2, e30

Wong, W. W. and Liao, J. C. (2006). The design of intracellular oscillators that interact with metabolism**,** *Cell Mol Life Sci*, 63, 1215-20

Slee, E. A.*, et al.* (2004). To die or not to die: how does p53 decide?**,** *Oncogene*, 23, 2809-18

Sharpless, N. E. and DePinho, R. A. (2002). p53: good cop/bad cop**,** *Cell*, 110, 9-12

Kohn, K. W. and Pommier, Y. (2005). Molecular interaction map of the p53 and Mdm2 logic elements, which control the Off-On switch of p53 in response to DNA damage**,** *Biochem Biophys Res Commun*, 331, 816-27

Lu, X. (2005). p53: a heavily dictated dictator of life and death**,** *Curr Opin Genet Dev*, 15, 27-33

Liu, G. and Chen, X. (2006). Regulation of the p53 transcriptional activity**,** *J Cell Biochem*, 97, 448-58

Matoba, S.*, et al.* (2006). p53 regulates mitochondrial respiration**,** *Science*, 312, 1650-3

Roger, L.*, et al.* (2006). Control of cell migration: a tumour suppressor function for p53?**,** *Biol Cell*, 98, 141-52

Scoumanne, A. and Chen, X. (2006). The epithelial cell transforming sequence 2, a guanine nucleotide exchange factor for Rho GTPases, is repressed by p53 via protein methyltransferases and is required for G1-S transition**,** *Cancer Res*, 66, 6271-9

Jung, E. J.*, et al.* (2006). Myosin VI is a mediator of the p53-dependent cell survival pathway**,** *Mol Cell Biol*, 26, 2175-86

Lengner, C. J.*, et al.* (2006). Osteoblast differentiation and skeletal development are regulated by Mdm2-p53 signaling**,** *J Cell Biol*, 172, 909-21

Yu, X.*, et al.* (2006). The regulation of exosome secretion: a novel function of the p53 protein**,** *Cancer Res*, 66, 4795-801

Momand, J.*, et al.* (1992). The mdm-2 oncogene product forms a complex with the p53 protein and inhibits p53-mediated transactivation**,** *Cell*, 69, 1237-45

Fuchs, S. Y.*, et al.* (1998). Mdm2 association with p53 targets its ubiquitination**,** *Oncogene*, 17, 2543-7

Fuchs, S. Y.*, et al.* (1998). JNK targets p53 ubiquitination and degradation in nonstressed cells**,** *Genes Dev*, 12, 2658-63

Ganguli, G. and Wasylyk, B. (2003). p53-independent functions of MDM2**,** *Mol Cancer Res*, 1, 1027-35

Meek, D. W. and Knippschild, U. (2003). Posttranslational modification of MDM2**,** *Mol Cancer Res*, 1, 1017-26

Leng, R. P.*, et al.* (2003). Pirh2, a p53-induced ubiquitin-protein ligase, promotes p53 degradation**,** *Cell*, 112, 779-91

Corcoran, C. A.*, et al.* (2004). The p53 paddy wagon: COP1, Pirh2 and MDM2 are found resisting apoptosis and growth arrest**,** *Cancer Biol Ther*, 3, 721-5

Dornan, D.*, et al.* (2004). The ubiquitin ligase COP1 is a critical negative regulator of p53**,** *Nature*, 429, 86-92

Bratsun, D.*, et al.* (2005). Delay-induced stochastic oscillations in gene regulation**,** *Proc Natl Acad Sci U S A*, 102, 14593-8

Perry, M. E.*, et al.* (1993). The mdm-2 gene is induced in response to UV light in a p53-dependent manner**,** *Proc Natl Acad Sci U S A*, 90, 11623-7

Knippschild, U.*, et al.* (1995). Cell-specific transcriptional activation of the mdm2-gene by ectopically expressed wild-type form of a temperature-sensitive mutant p53**,** *Oncogene*, 11, 683-90

Lahav, G.*, et al.* (2004). Dynamics of the p53-Mdm2 feedback loop in individual cells**,** *Nat Genet*, 36, 147-50

Geva-Zatorsky, N.*, et al.* (2006). Oscillations and variability in the p53 system**,** *Mol Syst Biol*, 2, 2006 0033

Gohler, T.*, et al.* (2002). Specific interaction of p53 with target binding sites is determined by DNA conformation and is regulated by the C-terminal domain**,** *J Biol Chem*, 277, 41192-203

Espinosa, J. M.*, et al.* (2003). p53 functions through stress- and promoter-specific recruitment of transcription initiation components before and after DNA damage**,** *Mol Cell*, 12, 1015-27

Nayak, B. K. and Das, B. R. (1999). Differential binding of NF1 transcription factor to P53 gene promoter and its depletion in human breast tumours**,** *Mol Biol Rep*, 26, 223-30

Reisman, D.*, et al.* (1993). c-Myc trans-activates the p53 promoter through a required downstream CACGTG motif**,** *Cell Growth Differ*, 4, 57-65

Boggs, K. and Reisman, D. (2006). Increased p53 transcription prior to DNA synthesis is regulated through a novel regulatory element within the p53 promoter**,** *Oncogene*, 25, 555-65

Oda, K.*, et al.* (2000). p53AIP1, a potential mediator of p53-dependent apoptosis, and its regulation by Ser-46-phosphorylated p53**,** *Cell*, 102, 849-62

Appella, A. a. (2003). Handbook of Cell Signaling**,** *Academic Press*,

Jones, S. N.*, et al.* (1995). Rescue of embryonic lethality in Mdm2-deficient mice by absence of p53**,** *Nature*, 378, 206-8

Montes de Oca Luna, R.*, et al.* (1995). Rescue of early embryonic lethality in mdm2-deficient mice by deletion of p53**,** *Nature*, 378, 203-6

Iwakuma, T. and Lozano, G. (2003). MDM2, an introduction**,** *Mol Cancer Res*, 1, 993-1000

Freedman, D. A. and Levine, A. J. (1998). Nuclear export is required for degradation of endogenous p53 by MDM2 and human papillomavirus E6**,** *Mol Cell Biol*, 18, 7288-93

Geyer, R. K.*, et al.* (2000). The MDM2 RING-finger domain is required to promote p53 nuclear export**,** *Nat Cell Biol*, 2, 569-73

Joseph, T. W., *et al.* (2003). Nuclear and cytoplasmic degradation of endogenous p53 and HDM2 occurs during down-regulation of the p53 response after multiple types of DNA damage, *Faseb J*, 17, 1622-30

Lohrum, M. A., *et al.* (2000). Identification of a cryptic nucleolar-localization signal in MDM2, *Nat Cell Biol*, 2, 179-81

Moll, U. M., *et al.* (2005). Transcription-independent pro-apoptotic functions of p53, *Curr Opin Cell Biol*, 17, 631-6

Li, M., *et al.* (2003). Mono- versus polyubiquitination: differential control of p53 fate by Mdm2, *Science*, 302, 1972-5

Liu, L., *et al.* (1999). p53 sites acetylated in vitro by PCAF and p300 are acetylated in vivo in response to DNA damage, *Mol Cell Biol*, 19, 1202-9

Zhu, Q., *et al.* (2001). Mdm2 mutant defective in binding p300 promotes ubiquitination but not degradation of p53: evidence for the role of p300 in integrating ubiquitination and proteolysis, *J Biol Chem*, 276, 29695-701

Grossman, S. R., *et al.* (2003). Polyubiquitination of p53 by a ubiquitin ligase activity of p300, *Science*, 300, 342-4

Feng, L., *et al.* (2005). Functional analysis of the roles of posttranslational modifications at the p53 C terminus in regulating p53 stability and activity, *Mol Cell Biol*, 25, 5389-95

Krummel, K. A., *et al.* (2005). The C-terminal lysines fine-tune P53 stress responses in a mouse model but are not required for stability control or transactivation, *Proc Natl Acad Sci U S A*, 102, 10188-93

Dai, M. S., *et al.* (2006). Balance of Yin and Yang: ubiquitylation-mediated regulation of p53 and c-Myc, *Neoplasia*, 8, 630-44

Chen, D., *et al.* (2005). ARF-BP1/Mule is a critical mediator of the ARF tumor suppressor, *Cell*, 121, 1071-83

Brooks, C. L. and Gu, W. (2006). p53 ubiquitination: Mdm2 and beyond, *Mol Cell*, 21, 307-15

Li, M., *et al.* (2004). A dynamic role of HAUSP in the p53-Mdm2 pathway, *Mol Cell*, 13, 879-86

Shvarts, A., *et al.* (1996). MDMX: a novel p53-binding protein with some functional properties of MDM2, *Embo J*, 15, 5349-57

Stad, R.*, et al.* (2001). Mdmx stabilizes p53 and Mdm2 via two distinct mechanisms**,** *EMBO Rep*, 2, 1029-34

Badciong, J. C. and Haas, A. L. (2002). MdmX is a RING finger ubiquitin ligase capable of synergistically enhancing Mdm2 ubiquitination**,** *J Biol Chem*, 277, 49668-75

Sherr, C. J.*, et al.* (2005). p53-Dependent and -independent functions of the Arf tumor suppressor**,** *Cold Spring Harb Symp Quant Biol*, 70, 129-37

Zhang, Y.*, et al.* (1998). ARF promotes MDM2 degradation and stabilizes p53: ARF-INK4a locus deletion impairs both the Rb and p53 tumor suppression pathways**,** *Cell*, 92, 725-34

Tao, W. and Levine, A. J. (1999). P19(ARF) stabilizes p53 by blocking nucleo-cytoplasmic shuttling of Mdm2**,** *Proc Natl Acad Sci U S A*, 96, 6937-41

Stott, F. J.*, et al.* (1998). The alternative product from the human CDKN2A locus, p14(ARF), participates in a regulatory feedback loop with p53 and MDM2**,** *Embo J*, 17, 5001-14

Dai, M. S. and Lu, H. (2004). Inhibition of MDM2-mediated p53 ubiquitination and degradation by ribosomal protein L5**,** *J Biol Chem*, 279, 44475-82

Dai, M. S.*, et al.* (2004). Ribosomal protein L23 activates p53 by inhibiting MDM2 function in response to ribosomal perturbation but not to translation inhibition**,** *Mol Cell Biol*, 24, 7654-68

Dai, M. S.*, et al.* (2006). Regulation of the MDM2-p53 pathway by ribosomal protein L11 involves a post-ubiquitination mechanism**,** *J Biol Chem*, 281, 24304-13

Argentini, M.*, et al.* (2001). The contribution of the acidic domain of MDM2 to p53 and MDM2 stability**,** *Oncogene*, 20, 1267-75

Kawai, H.*, et al.* (2003). Critical contribution of the MDM2 acidic domain to p53 ubiquitination**,** *Mol Cell Biol*, 23, 4939-47

Meulmeester, E.*, et al.* (2003). Critical role for a central part of Mdm2 in the ubiquitylation of p53**,** *Mol Cell Biol*, 23, 4929-38

Zhang, Y.*, et al.* (2003). Ribosomal protein L11 negatively regulates oncoprotein MDM2 and mediates a p53-dependent ribosomal-stress checkpoint pathway**,** *Mol Cell Biol*, 23, 8902-12

Takagi, M.*, et al.* (2005). Regulation of p53 translation and induction after DNA damage by ribosomal protein L26 and nucleolin**,** *Cell*, 123, 49-63

Gostissa, M.*, et al.* (1999). Activation of p53 by conjugation to the ubiquitin-like protein SUMO-1**,** *Embo J*, 18, 6462-71

Rodriguez, M. S.*, et al.* (1999). SUMO-1 modification activates the transcriptional response of p53**,** *Embo J*, 18, 6455-61

Watson, I. R. and Irwin, M. S. (2006). Ubiquitin and ubiquitin-like modifications of the p53 family**,** *Neoplasia*, 8, 655-66

Fogal, V.*, et al.* (2000). Regulation of p53 activity in nuclear bodies by a specific PML isoform**,** *Embo J*, 19, 6185-95

Kwek, S. S.*, et al.* (2001). Functional analysis and intracellular localization of p53 modified by SUMO-1**,** *Oncogene*, 20, 2587-99

Muller, S.*, et al.* (2001). SUMO, ubiquitin's mysterious cousin**,** *Nat Rev Mol Cell Biol*, 2, 202-10

Chen, L. and Chen, J. (2003). MDM2-ARF complex regulates p53 sumoylation**,** *Oncogene*, 22, 5348-57

Gostissa, M.*, et al.* (2003). Regulation of p53 functions: let's meet at the nuclear bodies**,** *Curr Opin Cell Biol*, 15, 351-7

Jackson, P. K. (2001). A new RING for SUMO: wrestling transcriptional responses into nuclear bodies with PIAS family E3 SUMO ligases**,** *Genes Dev*, 15, 3053-8

Seeler, J. S. and Dejean, A. (2001). SUMO: of branched proteins and nuclear bodies**,** *Oncogene*, 20, 7243-9

Minty, A.*, et al.* (2000). Covalent modification of p73alpha by SUMO-1. Two-hybrid screening with p73 identifies novel SUMO-1-interacting proteins and a SUMO-1 interaction motif**,** *J Biol Chem*, 275, 36316-23

Seet, B. T.*, et al.* (2006). Reading protein modifications with interaction domains**,** *Nat Rev Mol Cell Biol*, 7, 473-83

Krek, W. (1998). Proteolysis and the G1-S transition: the SCF connection**,** *Curr Opin Genet Dev*, 8, 36-42

Liu, Y. C. (2004). Ubiquitin ligases and the immune response**,** *Annu Rev Immunol*, 22, 81-127

Banerjee, A.*, et al.* (1993). The bacterially expressed yeast CDC34 gene product can undergo autoubiquitination to form a multiubiquitin chain-linked protein**,** *J Biol Chem*, 268, 5668-75

d'Azzo, A.*, et al.* (2005). E3 ubiquitin ligases as regulators of membrane protein trafficking and degradation**,** *Traffic*, 6, 429-41

Dhananjayan, S. C.*, et al.* (2005). Ubiquitin and control of transcription**,** *Essays Biochem*, 41, 69-80

Rotin, D.*, et al.* (2000). Ubiquitination and endocytosis of plasma membrane proteins: role of Nedd4/Rsp5p family of ubiquitin-protein ligases**,** *J Membr Biol*, 176, 1-17

Panasenko, O.*, et al.* (2006). The yeast CCR4-not complex controls ubiquitination of the nascent associated polypeptide complex**,** *J Biol Chem*,

Baarends, W. M.*, et al.* (2000). Specific aspects of the ubiquitin system in spermatogenesis**,** *J Endocrinol Invest*, 23, 597-604

Kikonyogo, A.*, et al.* (2001). Proteins related to the Nedd4 family of ubiquitin protein ligases interact with the L domain of Rous sarcoma virus and are required for gag budding from cells**,** *Proc Natl Acad Sci U S A*, 98, 11199-204

Thrower, J. S.*, et al.* (2000). Recognition of the polyubiquitin proteolytic signal**,** *Embo J*, 19, 94-102

Haglund, K. and Dikic, I. (2005). Ubiquitylation and cell signaling**,** *Embo J*, 24, 3353-9

Hochstrasser, M. (2006). Lingering mysteries of ubiquitin-chain assembly**,** *Cell*, 124, 27-34

Eletr, Z. M.*, et al.* (2005). E2 conjugating enzymes must disengage from their E1 enzymes before E3-dependent ubiquitin and ubiquitin-like transfer**,** *Nat Struct Mol Biol*, 12, 933-4

Reiss, Y.*, et al.* (1989). Binding sites of ubiquitin-protein ligase. Binding of ubiquitin-protein conjugates and of ubiquitin-carrier protein**,** *J Biol Chem*, 264, 10378-83

Rape, M.*, et al.* (2006). The processivity of multiubiquitination by the APC determines the order of substrate degradation**,** *Cell*, 124, 89-103

Pickart, C. M. (2001). Mechanisms underlying ubiquitination**,** *Annu Rev Biochem*, 70, 503-33

van Nocker, S. and Vierstra, R. D. (1993). Multiubiquitin chains linked through lysine 48 are abundant in vivo and are competent intermediates in the ubiquitin proteolytic pathway**,** *J Biol Chem*, 268, 24766-73

Gumbart, E. C.-C. a. J. (2006). http://www.ks.uiuc.edu/Training/CaseStudies/pdfs/ubq.pdf**,**

Begley, T. P.*, et al.* (1999). Thiamin biosynthesis in prokaryotes**,** *Arch Microbiol*, 171, 293-300

Unkles, S. E.*, et al.* (1999). Eukaryotic molybdopterin synthase. Biochemical and molecular studies of Aspergillus nidulans cnxG and cnxH mutants**,** *J Biol Chem*, 274, 19286-93

Huang, D. T.*, et al.* (2004). Ubiquitin-like protein activation**,** *Oncogene*, 23, 1958-71

Scheel, H. (2005). Comparative Analysis of the ubiquitin-proteasome system in *Homo sapiens* and *Saccharomyces cerevisiae***,** *dissertation*,

Szczepanowski, R. H.*, et al.* (2005). Crystal structure of a fragment of mouse ubiquitin-activating enzyme**,** *J Biol Chem*, 280, 22006-11

VanDemark, A. P. and Hill, C. P. (2002). Structural basis of ubiquitylation**,** *Curr Opin Struct Biol*, 12, 822-30

Jiang, Y. H. and Beaudet, A. L. (2004). Human disorders of ubiquitination and proteasomal degradation**,** *Curr Opin Pediatr*, 16, 419-26

Dominguez, C.*, et al.* (2004). Structural model of the UbcH5B/CNOT4 complex revealed by combining NMR, mutagenesis, and docking approaches**,** *Structure*, 12, 633-44

Saville, M. K.*, et al.* (2004). Regulation of p53 by the ubiquitin-conjugating enzymes UbcH5B/C in vivo**,** *J Biol Chem*, 279, 42169-81

Hoppe, T. (2005). Multiubiquitylation by E4 enzymes: 'one size' doesn't fit all**,** *Trends Biochem Sci*, 30, 183-7

Hochstrasser, M. (2001). SP-RING for SUMO: new functions bloom for a ubiquitin-like protein**,** *Cell*, 107, 5-8

Seeler, J. S. and Dejean, A. (2003). Nuclear and unclear functions of SUMO**,** *Nat Rev Mol Cell Biol*, 4, 690-9

Muller, S.*, et al.* (1998). Conjugation with the ubiquitin-related modifier SUMO-1 regulates the partitioning of PML within the nucleus**,** *Embo J*, 17, 61-70

Johnson, E. S. and Blobel, G. (1999). Cell cycle-regulated attachment of the ubiquitin-related protein SUMO to the yeast septins**,** *J Cell Biol*, 147, 981-94

Guet, C. C., *et al.* (2002). Combinatorial synthesis of genetic networks, *Science*, 296, 1466-70

Ronen, M., *et al.* (2002). Assigning numbers to the arrows: parameterizing a gene regulation network by using accurate expression kinetics, *Proc Natl Acad Sci U S A*, 99, 10555-60

Batt, G., *et al.* (2005). Validation of qualitative models of genetic regulatory networks by model checking: analysis of the nutritional stress response in Escherichia coli, *Bioinformatics*, 21 Suppl 1, i19-28

King, R. D., *et al.* (2005). On the use of qualitative reasoning to simulate and identify metabolic pathways, *Bioinformatics*, 21, 2017-26

Fall, C. P., *et al.* (2002). Computational Cell Biology, *Springer Verlag, 1st edition*, Hardcover: 488 pages

Liu, Q. and Jia, Y. (2004). Fluctuations-induced switch in the gene transcriptional regulatory system, *Phys Rev E Stat Nonlin Soft Matter Phys*, 70, 041907

Thattai, M. and van Oudenaarden, A. (2004). Stochastic gene expression in fluctuating environments, *Genetics*, 167, 523-30

Hanggi, P. (2002). Stochastic resonance in biology. How noise can enhance detection of weak signals and help improve biological information processing, *Chemphyschem*, 3, 285-90

Gillespie, D. T. (1976). General method for numerically simulating the stochastic time evolution of coupled chemical reactions, *Journal of Computational Physics*, 22,

Gillespie, D. T. (1977). Exact stochastic simulation of coupled chemical reactions., *J. Phys. Chem.*, 81,

Haseltine, E. L. and Rawlings, J. B. (2002). Approximate simulation of coupled fast and slow reactions for stochastic chemical kinetics, *J Chem Phys*, 117, 6959-6969

Rao, C. V. and Arkin, A. P. (2003). Stochastic chemical kinetics and the quasi-steady-state assumption: Application to the Gillespie algorithm, *J Chem Phys*, 118, 4999-5010

Rathinam, M., *et al.* (2003). Stiffness in stochastic chemically reaction systems: the implicit tau-leaping method, *J Chem Phys*, 119, 12784-12794

Stundzia, A. B., Lumsden, C.J. (1996). Stochastic simulation of coupled reaction-diffusion processes, *J. Comput. Phys.*, 196–207

Ander, M., P. Beltrao, B. Di Ventura, J. Ferkinghoff-Borg, M. Foglierini, A. Kaplan, C. Lemerle, I. Tomás-Oliveira and L. Serrano (2004). SmartCell, a framework to simulate cellular processes that combines stochastic approximation with diffusion and localisation: analysis of simple networks**,** *Syst. Biol.*, 1, 129-138

Alfonsi, A.*, et al.* (2005). Adaptive simulation of hybrid stochastic and deterministic models for biochemical systems**,** *CEMRACS 2004, ESAIM Proceedings 2005*,

Salis, H. and Kaznessis, Y. (2005). Accurate hybrid stochastic simulation of a system of coupled chemical or biochemical reactions**,** *J Chem Phys*, 122, 54103

Gitai, Z. (2005). The new bacterial cell biology: moving parts and subcellular architecture**,** *Cell*, 120, 577-86

Gorlich, D.*, et al.* (2003). Characterization of Ran-driven cargo transport and the RanGTPase system by kinetic measurements and computer simulation**,** *Embo J*, 22, 1088-100

Nedelec, F.*, et al.* (2003). Self-organisation and forces in the microtubule cytoskeleton**,** *Curr Opin Cell Biol*, 15, 118-24

Sawai, S.*, et al.* (2005). An autoregulatory circuit for long-range self-organization in Dictyostelium cell populations**,** *Nature*, 433, 323-6

Collier, J. R.*, et al.* (1996). Pattern formation by lateral inhibition with feedback: a mathematical model of delta-notch intercellular signalling**,** *J Theor Biol*, 183, 429-46

Dens, E. J.*, et al.* (2005). Cell division theory and individual-based modeling of microbial lag Part I. The theory of cell division**,** *Int J Food Microbiol*, 101, 303-18

Wu, D.*, et al.* (2005). Phase synchronization and coherence resonance of stochastic calcium oscillations in coupled hepatocytes**,** *Biophys Chem*, 115, 37-47

Lemerle, C.*, et al.* (2005). Space as the final frontier in stochastic simulations of biological systems**,** *FEBS Lett*, 579, 1789-94

Oliner, J. D.*, et al.* (1993). Oncoprotein MDM2 conceals the activation domain of tumour suppressor p53**,** *Nature*, 362, 857-60

Emmerich, B.*, et al.* (1975). [Proceedings: Susceptibility of endogenous mRNA translation to emetine and cycloheximide in cell free systems from plasma cell tumors, reticulocytes and liver]**,** *Hoppe Seylers Z Physiol Chem*, 356, 228

Liang, S. H. and Clarke, M. F. (2001). Regulation of p53 localization**,** *Eur J Biochem*, 268, 2779-83

Belle, A.*, et al.* (2006). Quantification of protein half-lives in the budding yeast proteome**,** *Proc Natl Acad Sci U S A*, 103, 13004-9

Honda, R. and Yasuda, H. (2000). Activity of MDM2, a ubiquitin ligase, toward p53 or itself is dependent on the RING finger domain of the ligase**,** *Oncogene*, 19, 1473-6

Brooks, C. L. and Gu, W. (2004). Dynamics in the p53-Mdm2 ubiquitination pathway**,** *Cell Cycle*, 3, 895-9

Heinemeyer, W.*, et al.* (1993). PRE2, highly homologous to the human major histocompatibility complex-linked RING10 gene, codes for a yeast proteasome subunit necessary for chrymotryptic activity and degradation of ubiquitinated proteins**,** *J Biol Chem*, 268, 5115-20

Inoue, T.*, et al.* (2001). MDM2 can promote the ubiquitination, nuclear export, and degradation of p53 in the absence of direct binding**,** *J Biol Chem*, 276, 45255-60

Tsien, R. Y. (1998). The green fluorescent protein**,** *Annu Rev Biochem*, 67, 509-44

Shimizu, H.*, et al.* (2002). The conformationally flexible S9-S10 linker region in the core domain of p53 contains a novel MDM2 binding site whose mutation increases ubiquitination of p53 in vivo**,** *J Biol Chem*, 277, 28446-58

Huh, W. K.*, et al.* (2003). Global analysis of protein localization in budding yeast**,** *Nature*, 425, 686-91

Nakamura, S.*, et al.* (2000). Multiple lysine mutations in the C-terminal domain of p53 interfere with MDM2-dependent protein degradation and ubiquitination**,** *Mol Cell Biol*, 20, 9391-8

Rodriguez, M. S.*, et al.* (2000). Multiple C-terminal lysine residues target p53 for ubiquitin-proteasome-mediated degradation**,** *Mol Cell Biol*, 20, 8458-67

Kim, Y. H.*, et al.* (1999). Covalent modification of the homeodomain-interacting protein kinase 2 (HIPK2) by the ubiquitin-like protein SUMO-1**,** *Proc Natl Acad Sci U S A*, 96, 12350-5

Corboy, M. J.*, et al.* (2005). Aggresome formation**,** *Methods Mol Biol*, 301, 305-27

Haslbeck, M.*, et al.* (2005). Disassembling protein aggregates in the yeast cytosol. The cooperation of Hsp26 with Ssa1 and Hsp104**,** *J Biol Chem*, 280, 23861-8

Weis, K.*, et al.* (1994). Retinoic acid regulates aberrant nuclear localization of PML-RAR alpha in acute promyelocytic leukemia cells**,** *Cell*, 76, 345-56

Xirodimas, D. P.*, et al.* (2001). Cocompartmentalization of p53 and Mdm2 is a major determinant for Mdm2-mediated degradation of p53**,** *Exp Cell Res*, 270, 66-77

Fu, L.*, et al.* (2005). Nuclear aggresomes form by fusion of PML-associated aggregates**,** *Mol Biol Cell*, 16, 4905-17

Markossian, K. A. and Kurganov, B. I. (2004). Protein folding, misfolding, and aggregation. Formation of inclusion bodies and aggresomes**,** *Biochemistry (Mosc)*, 69, 971-84

Pearson, M.*, et al.* (2000). PML regulates p53 acetylation and premature senescence induced by oncogenic Ras**,** *Nature*, 406, 207-10

Kurki, S.*, et al.* (2003). Cellular stress and DNA damage invoke temporally distinct Mdm2, p53 and PML complexes and damage-specific nuclear relocalization**,** *J Cell Sci*, 116, 3917-25

Johnston, J. A.*, et al.* (1998). Aggresomes: a cellular response to misfolded proteins**,** *J Cell Biol*, 143, 1883-98

Li, M.*, et al.* (2002). Acetylation of p53 inhibits its ubiquitination by Mdm2**,** *J Biol Chem*, 277, 50607-11

Bossis, G.*, et al.* (2005). Down-regulation of c-Fos/c-Jun AP-1 dimer activity by sumoylation**,** *Mol Cell Biol*, 25, 6964-79

Sharp, D. A.*, et al.* (1999). Stabilization of the MDM2 oncoprotein by interaction with the structurally related MDMX protein**,** *J Biol Chem*, 274, 38189-96

Zeng, S. X.*, et al.* (2003). The acetylase activity of p300 is dispensable for MDM2 stabilization**,** *J Biol Chem*, 278, 7453-8

Feng, J.*, et al.* (2004). Stabilization of Mdm2 via decreased ubiquitination is mediated by protein kinase B/Akt-dependent phosphorylation**,** *J Biol Chem*, 279, 35510-7

Buschmann, T.*, et al.* (2000). SUMO-1 modification of Mdm2 prevents its self-ubiquitination and increases Mdm2 ability to ubiquitinate p53**,** *Cell*, 101, 753-62

Fuchs, S. Y.*, et al.* (2002). SUMO-1 modification of Mdm2 prevents its self-ubiquitination and increases Mdm2 ability to ubiquitinate p53**,** *Cell*, 110, 531

Chernov, M. V.*, et al.* (2001). Regulation of ubiquitination and degradation of p53 in unstressed cells through C-terminal phosphorylation**,** *J Biol Chem*, 276, 31819-24

Zhou, B. P.*, et al.* (2001). HER-2/neu induces p53 ubiquitination via Akt-mediated MDM2 phosphorylation**,** *Nat Cell Biol*, 3, 973-82

Gu, J.*, et al.* (2002). Mutual dependence of MDM2 and MDMX in their functional inactivation of p53**,** *J Biol Chem*, 277, 19251-4

Gronroos, E.*, et al.* (2004). YY1 inhibits the activation of the p53 tumor suppressor in response to genotoxic stress**,** *Proc Natl Acad Sci U S A*, 101, 12165-70

Hochstrasser, M. (1996). Ubiquitin-dependent protein degradation**,** *Annu Rev Genet*, 30, 405-39

Rajapurohitam, V.*, et al.* (2002). Control of ubiquitination of proteins in rat tissues by ubiquitin conjugating enzymes and isopeptidases**,** *Am J Physiol Endocrinol Metab*, 282, E739-45

Desterro, J. M.*, et al.* (1998). SUMO-1 modification of IkappaBalpha inhibits NF-kappaB activation**,** *Mol Cell*, 2, 233-9

Tong, H.*, et al.* (1997). Crystal structure of murine/human Ubc9 provides insight into the variability of the ubiquitin-conjugating system**,** *J Biol Chem*, 272, 21381-7

Schmidt, D. and Muller, S. (2002). Members of the PIAS family act as SUMO ligases for c-Jun and p53 and repress p53 activity**,** *Proc Natl Acad Sci U S A*, 99, 2872-7

Goodson, M. L.*, et al.* (2001). Sumo-1 modification regulates the DNA binding activity of heat shock transcription factor 2, a promyelocytic leukemia nuclear body associated transcription factor**,** *J Biol Chem*, 276, 18513-8

Liang, S. H.*, et al.* (1998). Cooperation of a single lysine mutation and a C-terminal domain in the cytoplasmic sequestration of the p53 protein**,** *J Biol Chem*, 273, 19817-21

Wansink, D. G.*, et al.* (1993). Fluorescent labeling of nascent RNA reveals transcription by RNA polymerase II in domains scattered throughout the nucleus**,** *J Cell Biol*, 122, 283-93

Rubbi, C. P. and Milner, J. (2000). Non-activated p53 co-localizes with sites of transcription within both the nucleoplasm and the nucleolus**,** *Oncogene*, 19, 85-96

Bernardi, R.*, et al.* (2004). PML regulates p53 stability by sequestering Mdm2 to the nucleolus**,** *Nat Cell Biol*, 6, 665-72

Borden, K. L. (2002). Pondering the promyelocytic leukemia protein (PML) puzzle: possible functions for PML nuclear bodies**,** *Mol Cell Biol*, 22, 5259-69

Gall, J. G. (2000). Cajal bodies: the first 100 years**,** *Annu Rev Cell Dev Biol*, 16, 273-300

Laroche, T.*, et al.* (2000). The dynamics of yeast telomeres and silencing proteins through the cell cycle**,** *J Struct Biol*, 129, 159-74

Zhao, J.*, et al.* (2005). MDM2 negatively regulates the human telomerase RNA gene promoter**,** *BMC Cancer*, 5, 6

Elenbaas, B.*, et al.* (1996). The MDM2 oncoprotein binds specifically to RNA through its RING finger domain**,** *Mol Med*, 2, 439-51

White, D. E.*, et al.* (2006). Mouse double minute 2 associates with chromatin in the presence of p53 and is released to facilitate activation of transcription**,** *Cancer Res*, 66, 3463-70

Gotta, M.*, et al.* (1997). Localization of Sir2p: the nucleolus as a compartment for silent information regulators**,** *Embo J*, 16, 3243-55

Original publications

From *in vivo* to *in silico* biology and back

Barbara Di Ventura*, Caroline Lemerle*, Konstantinos Michalodimitrakis and Luis Serrano, *Nature* **443**, 527-533(5 October 2006)

* these authors contributed equally to this work

Adaptive simulation of hybrid stochastic and deterministic models for biochemical systems

Aurélien Alfonsi, Eric Cancès, Gabriel Turinici, Barbara Di Ventura and Wilhelm Huisinga, *ESAIM Proceedings* **2005** Sept; 14:1-13

Space as the final frontier in stochastic simulations of biological systems

Lemerle, C., Di Ventura, B. & Serrano, L., *FEBS Lett* **2005** Mar 21;579(8):1789-94

SmartCell: a framework to simulate cellular processes that combines stochastic approximation with diffusion and localisation: analysis of simple gene networks

Ander, M., Beltrao, P., Di Ventura, B., Ferkinghoff-Borg, J., Foglierini, M., Kaplan, A., Lemerle, C., Tomas-Oliveira, I. & Serrano, L., *Systems Biology* **2004** 1 129-139

p53 sumoylation is conserved in budding yeast and correlates with its localization to nuclear bodies reminiscent of human PML bodies, manuscript in preparation